The International Journal of Advanced Manufacturing Technology
https://doi.org/10.1007/s00170-024-14984-9

CRITICAL REVIEW

Application of drill bit coatings for fiber/metal stack drilling in aircraft manufacturing: a comprehensive review

Joy Mathavan Jebaratnam[1]

Received: 4 June 2024 / Accepted: 26 December 2024

Abstract
The integration of hybrid composite/metal stack panels in aircraft manufacturing introduces significant advancements by combining the strengths of both materials. This review paper examines the critical role of coated drill bits in addressing the challenges associated with drilling these advanced materials. Coatings, such as Ti-based and diamond coatings, are shown to enhance drill bit performance by increasing wear resistance, reducing friction, and improving heat management. These improvements lead to better drilling outcomes, including reduced temperatures, minimized delamination, lower burr formation, and superior surface roughness and circularity. The review highlights the effectiveness of various coatings and their impact on drilling parameters like thrust force and torque, while also addressing the complexities of managing wear and maintaining diameter consistency. Ultimately, the strategic use of drill bit coatings and careful optimization of drilling conditions are essential for achieving high-quality results and advancing efficiency and sustainability in aircraft manufacturing.

Keywords Aerospace engineering · Drill bit · Tungsten carbide · Microscopic characterization and microanalysis · Wear · Surface coating

Abbreviations

AlTiN	Aluminum titanium nitride coating
AlTiCrN	Aluminum titanium chromium nitride coating
ANOVA	Analysis of variance
ASME	American Standard of Mechanical Engineers
BUE	Build-up edge
BUL	Build-up layer
CFRP	Carbon fiber reinforced polymer
CFRP/Al	Carbon fiber reinforced polymer/aluminum
CrN	Chromium nitride
CVD	Chemical vapor deposition
C7	Nano-crystalline AlTiN grains embedded in an amorphous matrix of silicon nitride (Si_3N_4)
DF	Delamination factor
DLC	Diamond like carbon
FMC	Fiber metal composite
HSS	High speed steel
IFTC	Infra-red thermography camera
LWQ	Local wear quantity
MCD	Microcrystalline diamond
MD CFRP	Multi directional Carbon fiber reinforced plastic
MoS_2	Molybdenum disulfide
MQL	Minimum quantity lubrication
NCD	Nanocrystalline diamond
PCBN	Polycrystalline cubic boron nitride
PCR	Partial correlation regression
PVD	Physical vapor deposition
ta-C	Tetrahedral amorphous carbon
ta-C + Cr	Chromium dopant added tetrahedral amorphous carbon

Highlights

- Effective coatings exhibit small grain size, high hardness, and good toughness.
- Coatings reduce friction and thereby drilling temperatures, and improve hole quality.
- In CFRP, wear mechanisms include abrasion, edge rounding, and localized chipping.
- In metal panel, wear progression include adhesion, crater wear, chipping, and fracture.
- Diamond, DLC, and TiAlN based coatings are mostly analyzed by researchers so far.

✉ Joy Mathavan Jebaratnam
joymathavan2013@gmail.com

[1] Department of Engineering Technology, Faculty of Technology, University of Jaffna, Kilinochchi Premises, Ariviyal Nagar, Kilinochchi 44000, Sri Lanka

Published online: 18 January 2025

ta-C + Ti	Titanium dopant added tetrahedral amorphous carbon
Ti	Titanium alloy
TiN	Titanium nitride coating
TiAlCr	Titanium aluminum chromium coating
TiAlCrN	Titanium aluminum chromium nitride coating
TiAlN	Titanium aluminum nitride coating
TiAlZrN	Titanium aluminum zirconium nitride coating
TiSi	Titanium silica coating
TiSiN	Titanium silica nitride coating
UD CFRP	Unidirectional carbon fiber reinforced plastic
WC	Tungsten carbide

1 Introduction

Aircraft industries have recently concentrated on creating hybrid composite/metal stack panels to improve the characteristics of next-generation aircrafts. Hybrid stacks often consist of materials comprised of multilayer fiber reinforced polymers (FRP) and metal alloys (titanium alloy or aluminum alloy). The ability to improve some notable characteristics without considerably raising total weight is one of the key advantages of stack design [1–4]. The use of composite and metal solves the shortcomings of metal in terms of corrosion resistance and fatigue strength as well as the shortcomings of composites in terms of bearing strength, repairability and impact strength [5]. The analysis of the use of titanium, aluminum, and composite materials in various commercial aircrafts are shown in Fig. 1. It reveals a rise in composite and a decline in aluminum in the aviation industry. The data of Fig. 1 are obtained from Starke and Staley and Giasin [6, 7]. The usual configuration of CFRP/metal stacks are CFRP/Ti6Al4V and CFRP/Al (Al2024, Al7050, Al7075) that are broadly used by aerospace industries these days [4, 8]. Major aircraft manufacturers, such as Airbus and Boeing, are extensively employing this multi-panel material in new generation passenger airplanes with the aim to fabricate structural elements such as skin segments, fuselages, and wing connections which support energy conservation and help system's performance enhancement [9]. Thin layers of composite material and alloy panels can be used to make these stack panels, and they can be joined together by using adhesives like epoxy [10, 11]. Additionally, the staking reduces defects such as hole surface roughness, diameter error [12], exit delamination [13], and entrance burr height compared to individual CFRP or metal panel drilling [8]. Contradictorily, Xu et al. mentioned that there are still a number of problems related with drilling composite CFRP/Ti stacks in a single pass, including severe hole damage, and poor hole precision [9]. Various actions are being taken in aircraft industry such as improving drill bit geometry, optimizing drilling parameters, introduction of coolant, and application of coating to minimize those damages. This review article deals with the actions taken through application of coatings to reduce the hole damage and increase the tool durability.

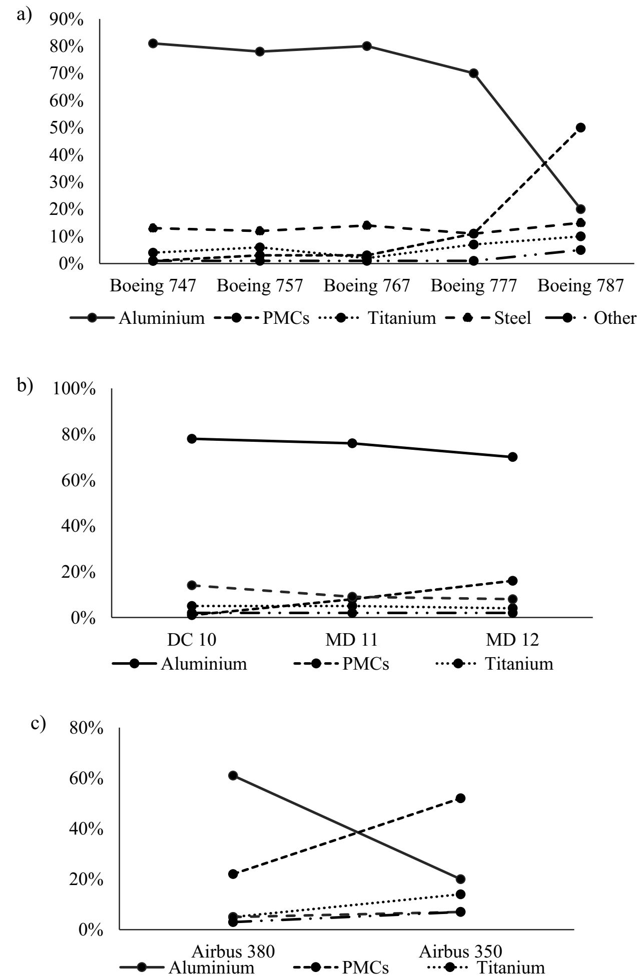

Fig. 1 The percentage usage of materials in (**a**) Boeing, (**b**) McDonnell Douglas, and (**c**) Airbus aircrafts (PMC—polymer matrix composite)

In general, the composite-metal system provides improved features such as CFRP's superior corrosion resistance, high specific stiffness, excellent fatigue strength [14, 15], light weight, and shape adaptability [16–21], while the metal shows favorable strength-to-weight ratio, isotropic behavior, strong fracture resistance, superior repairability [22, 23], low density, and high hardness [24–26]. In CFRP composites, the strength of the composite material is mainly governed by the fiber. Despite the fact that CFRP parts are frequently produced in ready-to-use shapes, machining procedures (such as drilling, pocket milling, or edge milling) are frequently necessary to meet functional and dimensional requirements [27].

CFRPs give huge challenges and difficulties for machining [20, 28] since it comprises extremely abrasive carbon fibers that create abrasive drill bit wear and drill bit edge chipping [29–32]. Mechanistic and numerical modeling of machining CFRPs continue to be challenging tasks in both academia and industry because of its anisotropic behavior and heterogeneous structure [33–35]. The most challenging aspects of commercial cutting of CFRP materials remain the active management of the in-process reactions, including drill bit wear, machining temperatures, acoustic emission (AE), and cutting forces [36–38]. Because of the limited thermal conductivity of CFRP, the cutting temperature is exceptionally high, which results in lowering the quality of the drilled hole by loss of epoxy on CFRP surfaces, and the softened matrix being smeared at the tool–work boundary [39].

Ti alloy, on the other hand, due to its intrinsic characteristics, such as low modulus of elasticity, low heat conductivity, and high chemical affinity to drill bit materials, is still recognized in the modern manufacturing community as an incredibly challenging material to cut. Ti6Al4V is the alloy form of Ti which is vastly used in the aerospace industry and it has great strength and little thermal conductivity. When adjusting the drilling speed to 75 m/min from 25 m/min in dry conditions, drilling temperatures can reach from 500 to 1000 °C in Ti6Al4V alloy [40]. This causes a number of drill bit wear issues, including cracking, chipping, and non-uniform flank wear [41]. Due to the high chemical affinity of the drill bit material with workpiece and the high cutting temperatures, built-up edge (BUE) and diffusion issues might occur while drilling titanium alloys [42]. Poor surface integrity, quick drill bit wear, and high force and temperature generation can all cause unique problems. Additionally, the composite-panel drilling has a substantial interrelated influence on the Ti-drilling operation, making the cutting processes more complex than in cases of single Ti alloy drilling [4].

In aircraft constructions, drilling is a common machining technique used to produce round holes of various sizes and depths. Three hundred thousand to three million holes may be present in commercial aircraft [7, 43–49]. Drilling these holes can provide significant challenges due to the vast differences in the characteristics of FRP and metal panels. Matrix distortion, delamination, fiber shrinkage, hole size, hole circularity, exit burr effect, and other phenomena of a like kind are some of these [4, 14, 15, 20, 22, 50–52]. These issues are the reason for around 60% of all part rejections [11, 43, 53–55].

The main goal of this study is to present an in-depth analysis of drill bit coating application which may result in less friction in tool work interface and thereby reduce the drilling temperature to provide solutions for problems in stack drilling of the aircraft components. There are not any review papers in regard to the application of drill bit coating while performing FRP/metal stack drilling for the aircraft applications and this review paper is expected to fill this gap to give a detailed idea to help the aircraft industries. First, the key challenges of material usage in aircraft industry are discussed in terms of metal and composite stacks. The different types of coatings used and their merits and demerits will be briefed in the next section. Then, the performance indicators of the manufacturing defects in terms of drilling forces, tool wear, and temperature generation will be discussed. The key findings of experimental studies conducted regarding the application of coating for drill bit over the past few years while performing FRP/metal stack-up drilling process and their impact on hole quality will then be outlined. By emphasizing relevant findings from the literature, this review paper strives to bring forth the benefits of coating drill bit and comparing the outcomes of different coatings.

2 Introduction to coating

Coating is a thin layer of a protective material, applied to the drill bit's surface. By increasing the drill bit's lifespan and enhancing its chemical and physical stability at high temperatures, the coating enhances the drill bit's performance and permits faster cutting rates [56]. These coatings have been tested for increasing drill bit wear resistance and life as well as lowering production and setup costs [57]. In comparison to uncoated bits, coated bits are stronger, more lubricated, sharp, heat resistant, and durable [58]. While machining, coatings prevent drill bit overheating and adhesion of lump chips [57]. In manufacturing, drill bits are typically coated with either physical vapor deposition (PVD) or chemical vapor deposition (CVD) methods [59]. Drill bits with PVD-TiAlN coatings are frequently utilized in metal drilling processes due to their excellent chemical stability, wear resistance, and hardness. Typically, the PVD laborious coating will increase the life of the drill bit and improve machining performance [60, 61]. Kwon et al. followed the CVD procedure to diamond coat the step drill and discovered that the grains are initially quite coarse, but when the coating duration is increased, the grains become fine and the surface becomes smoother [62]. Table 1 summarizes the research works carried out on drill bit coating application in CFRP/metal drilling process in aircraft manufacturing sector. The detailed specification of workpiece and tool, the cutting environment, the coating type and method, and the machining parameters used—all are concisely briefed in the table.

Table 1 Summary of details regarding the coated tools used for stack material drilling

Workpiece specifications	Tool specifications	Drilling Parameters and environment	Author
CFRP/Al7075/CFRP Thickness of Al 26.1 mm and CFRP 2.8 mm Weight fraction of fiber and resin were 64% and 36% A 0.25-mm-thick layer of epoxy glue was used to join the aluminum and composite	DLC-coated drill bit of diameter = 6.8 mm, flute length = 45 mm, point angle = 118° TiAlN-coated drill bit of diameter = 6.8 mm, flute length = 43 mm, point angle = 140°	Coating: DLC / TiAlN Cutting speed: 170.8 m/min / 128.0 m/min Spindle speed: 8000 rev/min / 6000 rev/min Feed rate: 1300 mm/min / 1200 mm/min Feed: 0.200 mm/rev / 0.163 mm/rev	[63]
CFRP/Al7010-T7451 Multidirectional composite Thickness is 7 mm and an average ply thickness of 0.19 mm Al 7010 thickness 14 mm	Double margin drill Flute length (mm) = 25 Web thickness (mm) = 1.36 Diameter (mm) = 6 Helix angle = 30° Point angle = 124° Coating—uncoated, diamond, TiAlCrN and AlTiSiN-G coated	Spindle speed = 3000 rev/min Cutting speed = 55 m/min Feed rate = 120 mm/min Feed = 0.04 mm/rev MQL = 16 ml/min	[64]
Ti6Al4V/CFRP/AA7050 (Each panel is 10 mm thick) CFRP consisting of 36 unidirectional prepregs with a volume percentage of carbon fibers equal to 56.5% Ply sequence [45°/0°/135°/90°/45°/0°]3 s	Coating—uncoated and TiAlN/TiN-coated WC twist drills Relief angle = 14° Helix angle = 30° Point angle = 140° Diameter = 6.35 mm	Feed (mm/rev) = 0.05, 0.08 With and without pecking Cutting fluid—water-based emulsion delivered internally at a flow rate of 30 l/min and a pressure of 70 bar, containing 7–8% soluble mineral oil	[65]
Ti-6Al-4 V/CFRP/Al 7050 T7451 (each panel is 10 mm thick) CFRP—unidirectional, 0.125 mm thick carbon fiber prepregs (Cytec 977–2/HTS) Fiber orientation—45°/0°/135°/90°/45°/0° The Ti, CFRP, and Al were joined together using a robust adhesive film (3 M AF163)	Coating—uncoated, CVD diamond coated and C7 coated WC drills Diameter (mm) = 6.35 Cutting length (mm) = 40 and corresponding shank is = 8 mm Helix angle = 30° Point angle = 130°	Cooling—wet and spray mist Cutting speed—Ti/CFRP and Al = 1000/2000 rev/min (20/40 m/min), 2000/4000 rev/min (40/80 m/min), 3000/6000 rev/min (60/120 m/min) Feed rate = 0.05 0.1 0.15 mm/rev Cutting fluid—water/oil emulsion supplied at a flow rate of around 15 l/min and pump pressure of 70 bar that contains 7–8% of soluble oil (Hocut 3380)	[66]

Table 1 (continued)

Workpiece specifications	Tool specifications	Drilling Parameters and environment	Author
T800/X850 CFRP and 7075-T651 Al Thickness of CFRP = 8.74 mm Thickness of Al = 6 mm CFRP Volume fraction = 65%. CFRP composite laminate is made of 46 unidirectional-plies and laying-up Sequence—[±45/0/−45/0/+45/0/+45/90/−45/0/−45/0/+45/0/+45/90/−45/90/−45/0/+45/0] s	Cutting edge length (mm) = 5.8 Diameter (mm) = 9.53 Helix angle = 30° First drill point angle = 130° Second drill point angle = 60° Diamond coating = 4 µm thick	Spindle speed = 1000, 2000, 3000 rev/min Feed rate = 0.02, 0.04, 0.06, 0.08 mm/rev	[67]
Ti-6Al-4 V/CFRP/Al 7050 T7451 (each panel is 10 mm thick) CFRP—unidirectional, 0.125 mm thick carbon fiber prepregs (Cytec 977–2/HTS) Fiber orientation—45°/0°/135°/90°/45°/0° The Ti, CFRP, and Al were joined together using a robust adhesive film (3 M AF163)	Drill coating—uncoated, CVD diamond-coated and C7-coated WC diameter (mm) = 6.35 Cutting length (mm) = 40 Corresponding shank size (mm) = 8 Helix angle = 30° Point angle = 130°	Environment—wet and spray mist Cutting speed—Ti/CFRP and Al = 1000/2000 rev/min (20/40 m/min), 2000/4000 rev/min (40/80 m/min), 3000/6000 rev/min (60/120 m/min) Feed rate = 0.05 0.1 0.15 mm/rev Cutting fluid—water/oil emulsion supplied at a flow rate of around 15 l/min and pump pressure of 70 bar that contains 7–8% of soluble oil (Hocut 3380)	[68]
CFRP/Al2024/CFRP CFRP thickness = 2.5 mm Al thickness = 5 mm The stacking sequence of T700/Qy8911 CFRP is [+45/−45/0/+45/0/0/−45/90/45/0/−45/0/+45/90/+45/0] s	Uncoated and TiAlN coated Helix angle = 20° Point angle = 135°	Cutting speed = 15, 30, 45, 60 m/min Spindle speed = 752, 1504, 2256, 3009 rev/min Feed rate = 0.025, 0.05, 0.075, 0.1 mm/rev	[69]
CFRP/Al2024 The composite plate is made of unidirectional prepreg with 16 plies CFRP thickness = 4.25 mm Fiber volume fraction is 58% Al 2024 thickness = 3 mm	Uncoated and nc-CrAlN/a-Si_3N_4 (Tripple Alwin) coated Coating thickness = 2.32 µm Diameter = 6 mm Point angle = 136°	Spindle speed = 1050, 2020, 2750 rev/min Feed (mm/rev) = 0.05, 0.1, and 0.15	[70]

Table 1 (continued)

Workpiece specifications	Tool specifications	Drilling Parameters and environment	Author
CFRP/Ti6Al4V annealed Ti6Al4V alloy and T300/914 CFRP laminate Stacking sequence of [45/ − 45/0/90] s Each stack has 4 mm thickness Fiber volume fraction = 60%	Diameter = 6.35 mm 1. Uncoated carbide twist drill Chisel edge = 0.11 mm Helix angle = 20° Point angle = 135° 2. PVD TiAlN-coated carbide twist drill Chisel edge = 0.22 mm Helix angle = 27.2° Point angle = 140°	Feed rate, f = 0.03, 0.06, 0.09, 0.12, 0.15 mm/rev Cutting speed = 15, 30, 45, 60 m/min Cutting sequence—Ti to CFRP, CFRP to Ti	[9]
Ti-6Al-4 V thickness = 6.73 mm CFRP laminate thickness = 7.54 mm with a 0.1885-mm average ply thickness The CFRP with epoxy matrix Lay-up sequence [(0/45/90/ − 451)$_4$(0/90/0/90)] s Volume fraction = 60%	Nanocrystalline AlTiN grains surrounded by Si_3N_4 matrix–coated, uncoated, and AlTiN-coated drills made of WC-9% Co Coating thickness = 3 µm Diameter (mm) = 9.525 Flute length (mm) = 38.1 (2 flutes) Helix angle = 25° Point angle = 135°	Drilling CFRP panel was done at 6000 rev/min and 0.0762 mm/rev feed rate When drilling Ti panel, 500 rev/min and 0.0508 mm/rev of feed rate were employed A coolant that dissolves in water and has a steady flow rate of 16 ml/min	[71]
CFRP/Al6013-T651 0°/90° woven fiber orientation	Diameter = 8 mm Uncoated, TiAlN and TiN-coated HSS drills Coating thickness = 1.5–4 µm Helix angle = 30° Point angles = 90°, 118, 135°	Cutting speed (m/min) = 100, 125, and 150 Corresponding spindle speeds (rev/min) = 4000, 5000, and 6000, respectively	[72]
CFRP/Ti6Al4V The CFRP laminate was an epoxy based (FRD-YZR-03) thermosetting plastic reinforced by the T700 carbon fibers subjected to the lay-up sequence [(0°/ − 45°/45°/90°)$_4$] s Fiber volume fraction = 60% CFRP thickness = 6.60 mm Ti6Al4V thickness = 6.28 mm	PVD TiAlN-coated (t = 3 ~ 4 µm) and CVD diamond-coated (t = 10 µm) WC drills Diameter = 6 mm Helix angle = 30° Point angle = 140° Cutting edge length = 25 mm Chisel edge length = 0.22 mm Rake angle = 10° 1st clearance angle = 12° 2nd clearance angle = 20°	Feed rates (mm/rev) = 0.025, 0.050, 0.075, and 0.100 Cutting speeds (m/min) = 15, 30, 45, and 60 Micro-cutting oil made from vegetables (MICROLUBE 2000) with a 15-ml/h flow rate and 0.6 MPa of compressed air pressure	[41]
T700/7901 CFRP and Ti6Al4V plate UD CFRP	TiAlN-coated carbide twist drills	Speed = 1000, 1500, 2000 rev/min Feed = 50 mm/min	[73]

Table 1 (continued)

Workpiece specifications	Tool specifications	Drilling Parameters and environment	Author
CFRP thickness = 9.16 mm Ti6Al4V thickness = 6.8 mm multilayer CFRP UD T800 carbon fibers and X850 thermoset epoxy resin, fiber volume fraction = 65% Sequence = [(45°/90°/ − 45°/0°)$_6$] s	Uncoated and diamond-coated WC drills with two cutting lips Diameter = 6.35 mm Helix angle = 30° Point angle = 140°	Speed (m/min) = 20, 35, 50, 65 Feed (mm/rev) = 0.015, 0.03, 0.045, 0.06 Drilling sequence = Ti → CFRP, CFRP → Ti	[74]
The CFRP (T700) panel with an epoxy-based (FRD-YZR-03) CFRP thickness = 6.60 mm Fiber volume fraction = 60% Ti6Al4V thickness = 6.28 mm	TiAlN-coated drill bit and diamond-coated drill bit Diameter = 6 mm Helix angle = 30° Point angle = 140°	Feed rate (mm/rev) = 0.025, 0.050, 0.075, and 0.100 Cutting speed (m/min) = 15, 30, 45, and 60 Coolant flow rate = 15 ml/h, at compressed air pressure of 0.6 MPa	[75]
CFRP thickness = 3 mm Ti thickness = 9.5 mm	TiAlCr/TiSi and TiAlN coated cemented carbide drills diameter (mm) = 6	Feed rate (mm/rev) = 0.1, 0.2 Cutting speed (m/min) = 9.4, 18.8 Cutting method = Water-mist-cooling (100 ml/h), Dry	[76]
Composite material M21E and titanium T16AL/4 V (BstA56)	Diameter = 6 mm C7-coated carbide drills of 90% carbide and 10% cobalt Coating thickness = 2.5 µm	CFRP / Ti Cutting speed (rev/min): 4500 / 1400 Feed rate (mm/min): 457.2 / 119	[12]
CFRP and aluminum 7010-T651	Diameter = 15 mm WC/Co drill bit Point angle = 140° 6-facet Coating—TiAlCrN	CFRP / Al Feed rate: 0.038 mm/rev / 0.16 mm/rev Cutting speed: 56.6 m/min / 95.0 m/min Cooling strategy—dry, coolant flow (1 l/h), coolant is Accu-Lube LB-4000	[77]
Ti6Al4V/CFRP/Al7050-T7651 stack The CFRP was composed of 30 UD prepregs, each with a 0.30-mm individual ply thickness Orientation – [45°/0°/135°/90°/45°/0°] Volume fraction = 56% Single fiber diameter = 6–8 µm	Twin-fluted WC drill Diameter = 6.38 mm 1. 0.5 µm PVD DLC coated Point angle = 140° Helix angle = 30° 2. 5–6 µm CVD diamond coated Point angle = 120° and 180° (two-stage point design) Helix angle = 30°	Coolant—15 l/min flow rate For the Ti layer, the cutting speed is 30 m/min, while for the CFRP and Al portions, it may reach up to 120 m/min	[78]

2.1 Ti-based coatings

Various Ti based coatings such as TiAlN, AlTiN, TiN, TiAlZrN, TiAlCrN, and TiAlCr are being tested as drill bit coatings for stack-up drilling. TiN coating has good adhesion property and effectively protects the bit from adhesive and abrasive wear [79]. Additionally, TiN has a low frictional coefficient compared to AlTiN and TiAlN coatings which results in reduction of hole surface roughness [80]. When cutting CFRP/Al2024-T3 alloy, Kurt et al. and Shunmugesh and Kavan mentioned that TiN-coated drill bits produced workpiece roughness that was comparable to that of TiAlN-coated drill bits [81, 82]. It is because titanium has a unique affinity for aluminum, which causes pressure and heat to specifically activate chemical and physical diffusion processes near the cutting edges. As a result, aluminum chips adhere to the coating, aluminizing the drill's surface and creating friction between the drill bit and the material, making drilled holes more uneven. Also, good thermal stability of TiN helps to prevent built-up edges and enhance heat transfer away from the cutting drill bit. The TiAlN coating, which has better oxidation resistance and hardness than TiN, is appropriate for dry machining applications [79, 83, 84]. Danisman et al. expressed that PVD TiAlN coated drill has sensible performance in terms of damage resistance, warmth corrosion resistance, oxidation resistance, and chemical stability when compared to TiN and TiAlN hard coatings [85]. Puneeth and Smitha had demonstrated that, compared to TiN-coated HSS and untreated HSS twist drill bits, TiAlN-coated HSS twist drill bits had a longer tool life [86]. Prajapati et al. compared TiAlN, TiN, and TiAlN + CrN coatings and found that, in addition to adherence of thin coating to substrate, TiAlN + CrN coating has good mechanical properties [87]. Furthermore, Giasin et al. mentioned that AlTiN/TiAlN coating with a microlayer structure is preferable for applications involving materials with a hardness above 45 HRC [56].

When considering monolayer and multilayer coatings, TiN monolayer coating outperformed TiN-surface multilayer coating and TiCN coating films when evaluating thrust force and torque [20, 88]. The cross-section view of nc-CrAlN/a-Si_3N_4 (Tripple Alwin) multilayer nano-coating is shown in Fig. 2 as an example of multilayer coating. These are nanocrystalline forms of coatings composed of very hard nanocrystalline crystals that are 10 nm in size and produce high hardness. The machining performance of TiAlN/TiAlZrN multilayer coatings has improved due to its wear behavior, similar to the TiAlZrN monolayer with comparable mechanical properties, despite a reduced bilayer period [89].

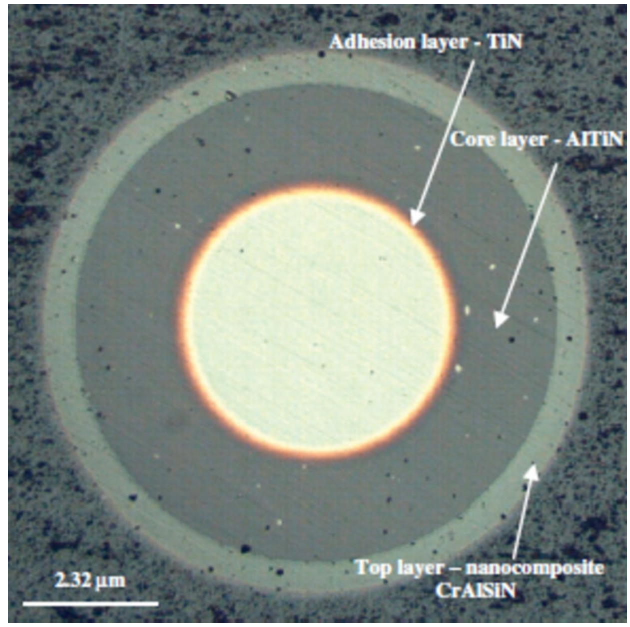

Fig. 2 Cross-section view of nc-CrAlN/a-Si_3N_4 (Tripple Alwin) nano-coating [70]

2.2 Diamond coating

Cemented tungsten carbide is widely utilized as drill bit material for CFRP/metal stack drilling; however, it exhibits quick wear in machining it, demanding research into the substrate and coating of carbide drill bits [90–93]. It was found by a few researchers that diamond-coated low-Co added carbide drill bit has shown to be the most effective drill bit material for stack-up machining [94–96]. To reduce drill bit wear and extend drill bit life, many firms also apply diamond coatings [62]. Drill bits have been covered in diamond coatings of various microstructures and thicknesses because they offer great qualities like high hardness, high thermal conductivity, low friction coefficients, high wear resistance, and chemical stability [64, 95–104]. To prevent excessive drill bit wear under high-speed machining and for cutting hard materials like CFRP, diamond-coated drill bits are extremely essential. In CVD diamond coating procedure, which employs gaseous CH_4 with a lot of carbon [62], a coating of diamond will be deposited that is several microns thick on the surface of tungsten carbide (WC). In this method, Co is removed from the WC drill bit surface by a pre-treatment procedure that strengthens the adherence of the diamond covering. The CH_4 gas is then heated by a hot filament to a temperature of between 700 and 1000 °C and deposited on the drill's surface. Compared to polycrystalline diamond (PCD), CVD diamond is more robust and harder [62].

The drill bit performance can be tailored by taking into account the qualities of the coating layer and the diamond grain size. While microcrystalline diamond (MCD) coatings offer high adhesion and wear resistance, nanocrystalline diamond (NCD) coatings' hardness is comparatively low because of the development of non-diamond phases, such as *sp2* graphitic carbon [105]. Nevertheless, the lubricating effect of graphitic phases can lower the machining resistance. Additionally, grain refining can be used to reduce workpiece surface roughness [106–109]. Dual- and multilayer diamond coatings have been created that combine the benefits of MCD and NCD coatings thanks to advancements in the fabrication of monolayer drill bit coatings of MCD or NCD [101, 106, 107, 110–117]. When compared with single-layer coated drill bits, dual and multilayer coated drill bits display exceptional machining performance because of the wear resistance and adhesion given by MCD near to the substrate and the lubrication effect from the action of NCD on the coating surface [105]. However, dual- and multilayer diamond coatings are limited in real-world applications because of the variation in residual stress between the layers and the loss of adhesion caused by the high graphitic carbon content at the MCD-NCD interface layer contact. Research was done on gradient diamond coatings, in which the grain size continuously declines from MCD of the substrate interface to NCD of the coating surface to address these problems. The adherence of a coating with such a microstructural transition may be superior to layers of MCD and NCD that alternate [105].

2.3 Diamond-like carbon coating

Carbon atoms exhibit three primary hybridized states: graphite, diamond, and diamond-like carbon (DLC). Graphite is characterized by 100% *sp2* hybridization, while diamond is categorized as 100% *sp3* hybridization. Graphite possesses a hexagonal plane construction with strong covalent in-plane bonds and weak Van der Waals out-of-plane bonds, resulting in a low coefficient of friction (COF). Contradictorily, diamond features a tetrahedral structure in which each atom is bonded with three others covalently, resulting in electrical insulation, highest natural hardness, and exceptional thermal conductivity. DLC exhibits a hybrid structure of *sp2* and *sp3* carbon atoms, and its properties depend on the ratio of these hybridizations [118]. The term diamond-like carbon (DLC) was first introduced by Aisenberg and Chabot [119]. They used the ion beam deposition method with carbon (C) and argon (Ar) particles and a graphite electrode to create DLC layers at room temperature. These films exhibited optical transparency, wear resistance, and electrical conductivity, with a somewhat crystalline structure reminiscent of diamond lattices. Aisenberg and Chabot observed that the use of DLC coatings enhanced the cutting performance of paper-cutting blades and reduced frictional coefficients [120].

Four different DLC coatings such as hydrogen-free amorphous carbon (a-C), hydrogen-free tetrahedral amorphous carbon (ta-C), hydrogenated amorphous carbon (a-C:H), and hydrogenated tetrahedral amorphous carbon (ta-C:H) are being used in industrial applications these days. They typically have great wear resistance and little friction. On the other hand, based on the *sp2/sp3* hybridization ratio and microstructure of DLC coatings, different tribological behaviors might be observed in different friction circumstances [121–124]. a-C:H coatings deliver ultra-low friction in vacuum or inert environments [125, 126], whereas ta-C coatings offer high wear resistance and ultra-low friction in the presence of hydrogen, oxygen, or water molecules [127, 128]. Under oil-based boundary lubrication, the wear was substantially higher in the ta-C/steel system in comparison with the a-C:H/steel system [129]. ta-C possesses several desirable properties such as low COF, excellent protection against adhesive wear, and tribo-oxidation that make it suitable for stack-up drilling applications. Its high-stress endurance is improved by this feature, even in dry and poorly lubricated operating environments. ta-C's high hardness provides exceptional resistance to wear from abrasives. Its inert surface chemistry guarantees seamless functioning, minimizes sticking, and gets rid of deposit-related demolding problems [130]. Moreover, ta-C exhibits improved corrosion resistance and optical transparency [131]. Furthermore, a 2-µm-thick ta-C coating significantly increased the resistance of stainless steel to abrasive wear, extending its lifetime to 85 years from 1 week [132]. These enhanced qualities result in reduced wear on highly stressed surfaces, extended component service life, and increased manufacturing process productivity.

Researchers have explored the effects of alloying DLC with transition metals such as Ti [133–135] and Cr [118, 135]. DLC is inherently brittle, and the formation of nanoscale carbide inclusions is induced by alloying it with stable metals that generate carbides, increasing the material's hardness [132]. Figure 3a shows a PVD coating set up of ta-C coating with alloying element in the coating machine. The PVD coating method is capable of producing highly pure and high-performance coatings because it transfers the coating material at the atomic or molecular level. In Fig. 3b, the coating layer referred to ta-C, seed layer referred to Ti layer, and substrate material is the tool material. Alloying with group IIB, IIIB, and IVB transition elements is often employed to improve the mechanical characteristics of ta-C films by improving the bond strength between the substrate and ta-C [136]. This approach can reduce stress on the film and promote good adhesion with intermediate layers [137]. Few studies have found that ta-C coatings under varied loads ranging from 10 to 70 mN have a hardness range of 20 to 29.1 GPa [136, 138, 139] and ta-C + Ti coating

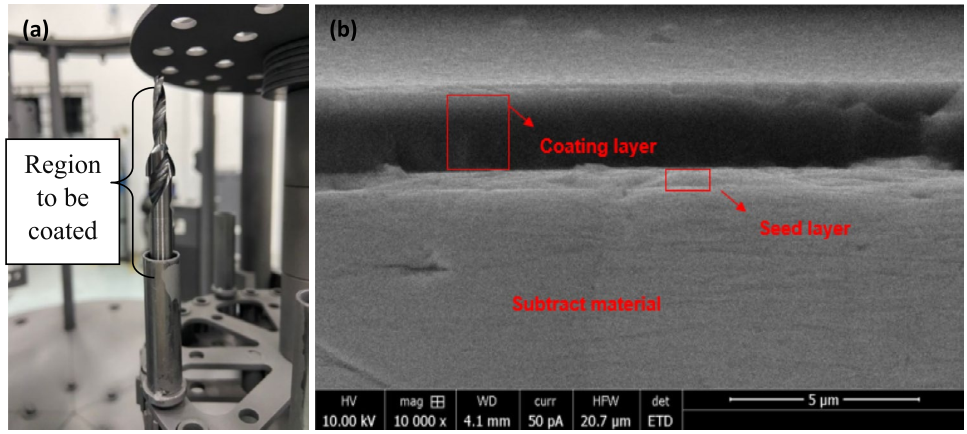

Fig. 3 (**a**) Drill bit setup for PVD coating process. (**b**) SEM image after applying coating [143]

at lower critical load (10 mN) have a hardness range of 16.8–28.1 GPa [140, 141]. ta-C + Cr coating's hardness was measured by Fiaschi et al. to be between 2.5 and 3.5 GPa at 100 mN load, and the reason for this low value is the low amount of (around 50%) sp^3 atoms [118]. Zhang et al. found that ta-C + Ti coatings exhibited adhesive strength values in the range of 359–381 mN [141]. When considering the coefficient of friction of ta-C coatings, Konca et al. obtained it between 0.07 and 0.20 in ambient air for tungsten molybdenum high-speed steel tools (M2 tool steel) coated with 2.2 ± 0.2 µm ta-C against Al and Ti counterparts [142]. Fiaschi et al. applied 1–1.5-µm-thick ta-C + Cr coating on pure iron and AISI 304 stainless steel substrates and obtained a COF of 0.2–0.5 and 0.17–0.25, respectively [118]. Guo et al. obtained a COF of 0.07 for $Ti_{4\%}$-ta-C coating with the thickness of 520 ± 20 nm [140] and Zhang et al. obtained a COF of 0.14–0.22 for taC + Ti with 100Cr6 steel counterpart [141]. Based on these findings regarding hardness, bond strength, and COF, it can be decided that the addition of seed layer/alloying element to DLC can further improve the drilling quality.

3 Influence of tool coating on performance indicators of stack material drilling

3.1 Impact of tool coating on drill bit wear

One of the crucial aspects in drilling processes is drill bit wear, which has a direct effect on drill bit life, hole surface quality, and production costs. When cutting CFRP/Ti or CFRP/Al stacks, drill-bit wear happens as the consequence of rubbing of the cutting edge against the tough carbon fibers and the attrition, abrasion, and adhesion brought on by the aluminum or titanium alloy [74]. Because of the abrasive character of the reinforcing carbon fibers in CFRP panels, abrasion acts as the major wear method for drill bit edges, leading to cutting-edge rounding or edge dulling. On the other hand, titanium alloys cause rapid drill bit wear growth with serious diffusion, crater wear, adhesion, as well as catastrophic failures like fracture or edge chipping because of their low thermal conductivity leading to elevated cutting temperatures and inherent high strength sustained at higher temperatures [74].

D'Orazio et al. mentioned that abrasion, edge rounding, and localized chipping at the cutting edge are the primary wear modes when using a drill bit coated in DLC (Fig. 4), whereas abrasion and aluminum particle adhesion on the rake surface are the main wear mechanisms when using a drill bit coated in nanocomposite TiAlN (Fig. 5) while drilling CFRP/Al stack [63]. The SEM images of the rake and flank faces of the DLC-coated tool after drilling 170 holes are displayed in Fig. 4. As seen in Fig. 4a–c, it is evident that chipping is occurring, mostly in the vicinity of the cutting edge. This is due to an excess of mechanical stresses brought on by the high cutting speed in that area. Figure 4c and d depicts flank wear and edge rounding. Figure 5c shows the adhesion of AA7075 particles (diameter lower than 50 µm) observed on the rake face, far from cutting edge, and Fig. 5d shows the fracture of the TiAlN coating in the area surrounding Al particles. According to Montoya et al., abrasion was the major wear type on the uncoated drill bit [64]. The corner, chisel edge, primary, and secondary cutting edges exhibited abrasion. TiAlCrN and AlTiSiN-G coated drills showed abrasion, coating failure, and adhesion wear, with aluminum forming a build-up edge (BUE) on the failed coating [64]. The rough surface from grinding operations, not fully covered by a 4-µm coating, caused aluminum to adhere to the rake face. Both TiAlCrN and AlTiSiN-G coatings retained the same surface profile as uncoated drills due to similar material adhesion. In contrast, a thicker 6-µm diamond coating provided a smooth surface, only experiencing abrasion and minimal aluminum adhesion wear [64]. Fujiwara et al. found that TiAlCr/TiSi coatings offered superior wear resistance and reduced chip adherence compared to TiAlN and TiSiN when drilling CFRP/Ti6Al4V stacks [144].

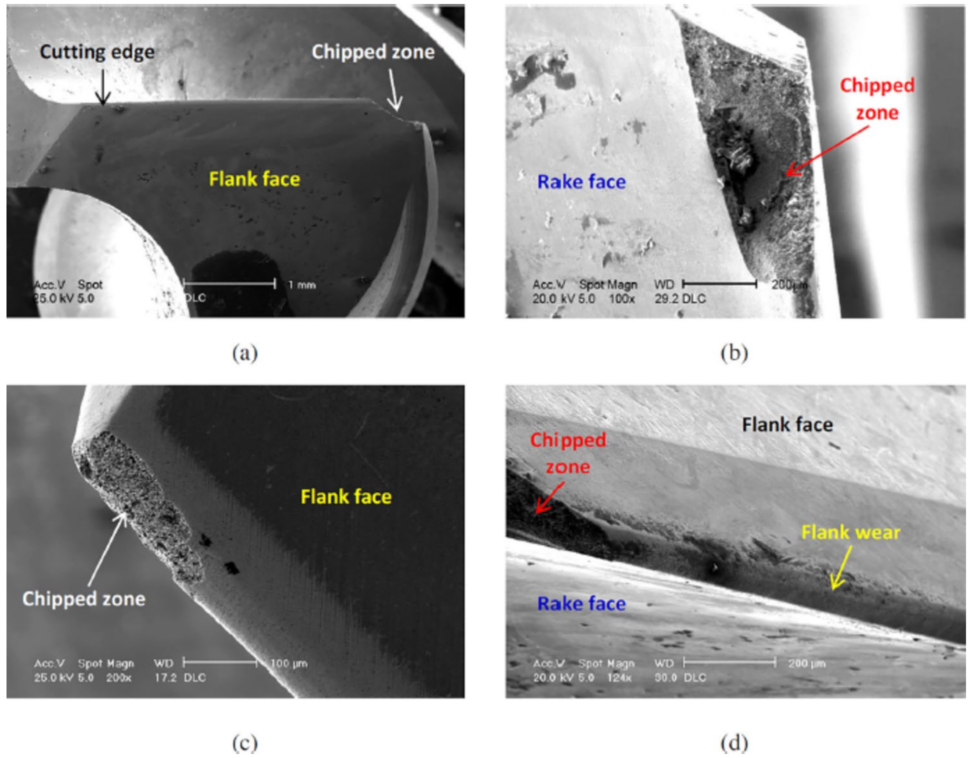

Fig. 4 SEM images of the DLC coated drill after a number of holes equal to 170: (**a**) flank face showing edge chipping, (**b**) chipped zone from the rake face, (**c**) chipped zone from the flank face, and (**d**) flank wear and edge rounding [63]

Contradictorily, when drilling CFRP/Al2024 stacks, Zitoune et al. observed that the primary wear mode is aluminum adhesion due to interlocking of alloy asperities on the cutting edge under high contact pressure, without diffusion or oxidation. SEM analysis showed that coated drills have a superior surface finish compared to uncoated drills, mainly due to the polishing process before PVD coating, which enhances surface quality in both composite and aluminum panel. However, drill coatings do not prevent aluminum fusion on the cutting edges [70]. Shyha et al. conducted experiments on Ti/CFRP/Al stacks using a CVD diamond-coated WC drill bit, choosing reverse sequence to avoid the damage caused by sharp Ti chips while excavating. They found that the most frequent failure mode was coating peeling/flaking after a few holes. Other failure mechanisms included chip clogging at the flutes, cutting lip breakage due to BUE development, and serious corner rounding of the cutting edge caused by abrasion from CFRP also lead to coating failure for a notable extent [66].

Xu et al. noted that when drilling CFRP/Ti6Al4V in dry conditions, TiAlN-coated drills retain their corner edge topography better than diamond-coated drills, which suffer from severe edge fracture. The TiAlN coating's low thermal conductivity helps transfer heat to the chips, softening them and reducing adhesive wear. Conversely, the diamond coating's high thermal conductivity causes heat to be conducted through the drill body, raising the edge temperature [41]. When subjected to temperatures greater than 600–700 °C, the diamond probably experiences oxidation and graphitization, and brittle graphite is prone to breaking while undergoing drilling [145, 146].

When it comes to flank wear, it is defined in ISO 8688:1 that the flank wear is measured in a parallel direction to the wear facet and in a perpendicular direction to the initial cutting edge, for example, from the initial cutting edge to the wear facet limit which cuts the initial flank face. According to D'Orazio et al., while drilling a CFRP/AA7075/CFRP stack, the DLC-coated drill experiences significantly less flank wear than the TiAlN-coated one as shown in Fig. 6 [63]. Flank wear on DLC-coated drill bits increases monotonically with the number of holes drilled due to chipping around the perimeter. However, the flank wear was consistently lower than that of TiAlN-coated drill bits, with TiAlN showing 2.25 times more wear than DLC after 170 holes, as shown in Fig. 6 [63]. Montoya et al. mentioned that good hole quality and lower thrust forces can be attained if the flank wear is low. They further mentioned that AlTiSiN-G and TiAlCrN coatings were ineffective since the flank wear was extremely similar to that of the drill bit without a coating. However, the diamond coating was effective since the flank wear measured with the uncoated drill was 50% more than that measured with the diamond-coated drill [64]. Xu et al. found that under dry conditions, TiAlN-coated drills show a flank wear width of about 31 μm with titanium particles adhering to the cutting edges, while diamond-coated drills exhibit a flank wear width of around 23 μm

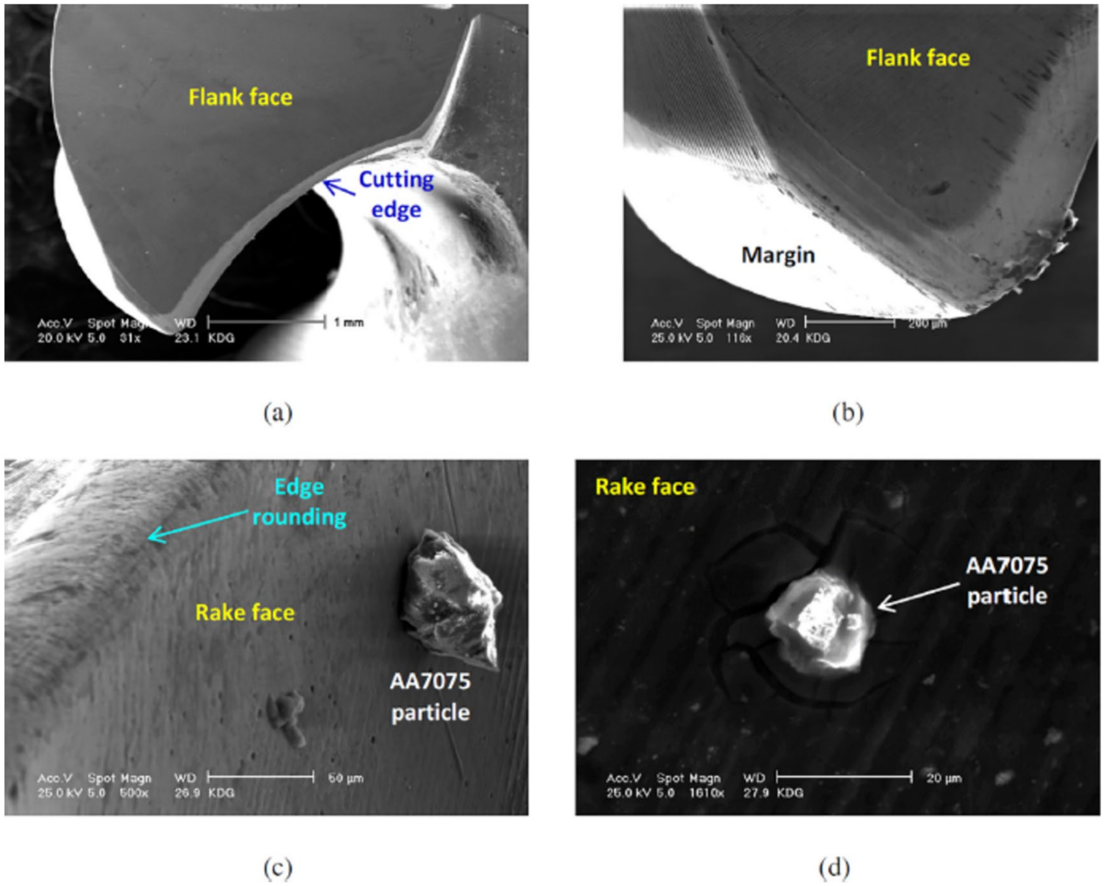

Fig. 5 SEM images of the nanocomposite TiAlN coated drill after a number of holes equal to 170: (**a**) flank face, (**b**) flank wear, (**c**) edge rounding and rake face, and (**d**) fractured coating in the area surrounding Al particles stuck to the rake surface [63]

with significant edge chipping [41]. The diamond coating's low COF and high thermal conductivity result in minimal

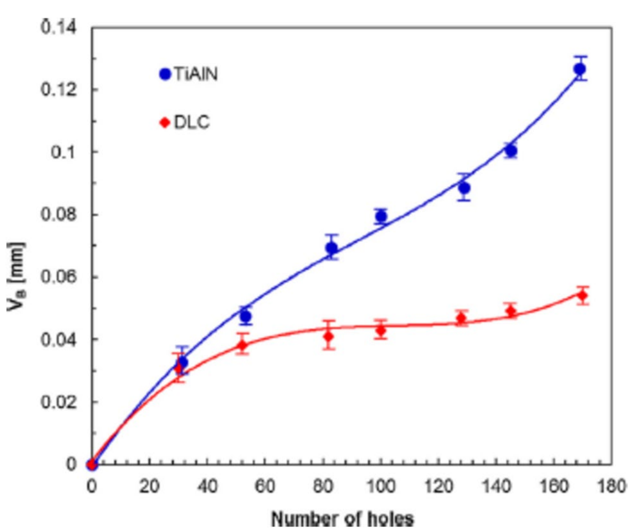

Fig. 6 Flank wear progression during drilling of CFRP/AA7075 stacks [63]

titanium fusion on the edges. Under minimum quantity lubrication (MQL), TiAlN-coated drills have a reduced flank wear width of 25 µm, whereas diamond-coated drills experience significantly greater wear, with a maximum flank wear width of 57 µm due to titanium chip accumulation and CFRP chip abrasion [41]. Kuo et al. reported that when drilling Al/CFRP/Ti panels, uncoated drill bits have a longer lifespan than PVD TiAlN/TiN-coated WC drills. Uncoated drills generated 180 holes with a flank wear of no more than 0.23 mm, while coated drills met the 0.30 mm flank wear requirement after 90–148 holes. ANOVA calculations showed that both feed rate and drill bit coating significantly influenced drill wear, with feed rate having a higher partial correlation regression (PCR) at 78.4%. [65]. Tashiro et al. found that the TiAlCr/TiSi-coated drill had a longer lifespan than the TiAlN-coated drill since the TiAlCr/TiSi coating had a 40% greater coating strength than the TiAlN coating. Additionally, they found that tool life under water mist drilling was shorter than that in dry drilling as the life of drill was 90 holes in water-mist cooling and 140 holes in the dry process. They believed that 0.2 mm of flank wear represented the maximum drill bit life [76].

Wang et al. said that the drill bit wear is a combination of edge rounding wear and flank wear [71]. For the purpose of comparison, Fig. 7 displays the LWQ in CFRP-only and Ti-only while drilling the 40th hole, together with the flank wear and edge rounding wear (assessed in LWQ) of the coated drills in drilling of CFRP/Ti stack. The total flank wear land from drilling CFRP and Ti individually is greater than that from drilling the CFRP/Ti stack for both coated drills. The edge rounding wear measurements from drilling CFRP-only, combined with those from Ti-only, differ by less than 10% from those obtained from the CFRP/Ti stack. This small discrepancy is likely due to variations in drill geometry. Thus, with LWQ applied, tool wear from drilling the CFRP/Ti stack equals the sum of the wear from drilling CFRP on the edge and Ti on the flank. They further mentioned that, to the overall drill bit wear, the involvement of the Ti layer is quite minimal in comparison to CFRP [71]. Montoya et al. mentioned that if the rate of wear on the rake face accelerates faster than the wear on the flank face, it would result in a higher local wear quantity (LWQ) but a smaller flank wear measurement [64]. In this way the value of flank wear is directly impacted by the rake face's wear.

Wang et al. mentioned that when drilling CFRP/Ti stack using AlTiN-coated, nanocomposite-coated, and uncoated drills, the flank wear was 145, 135, and 104 μm, respectively, and edge rounding wear was 1650, 1500, and 1450 μm^2, respectively [71]. This shows that the uncoated drills outperformed the coated carbide drills. They added that drilling a CFRP/Ti stack prevented edge chipping because the carbon fibers in the upper plate brush off any Ti fusion when drilling the bottom plate as shown in Fig. 8b and d and increase drill life. The Ti fusion left behind from drilling the Ti plate was completely gone after drilling around 1 mm into the top of the CFRP plate (Fig. 8b), and also the cutting edge is rounded and smoothed (Fig. 8d) [71]. Figure 8a and c displays the drills with the Ti adhesion after drilling the bottom Ti plate of the CFRP/Ti stack. The hardness of carbon fiber, roughly twice that of titanium, efficiently removes Ti fusion from the drill's cutting edge according to abrasive wear theory. Initially, rounding the edge while cutting the CFRP layer prevents edge chipping, but as the drill becomes dull over time, the likelihood of edge chipping decreases while Ti fusion near the cutting edge increases. At this stage, removing Ti adhesion becomes crucial to minimize chipping [71].

Cao et al. noted that thrust force and temperature increased as more holes were drilled in a CFRP/Ti stack using a TiAlN-coated drill bit. This led to adhesive wear, increased chip–drill contact area, and higher frictional wear. Initially, edge rounding wear occurred due to abrasive carbon fibers. As cutting temperature rose, Ti chips chemically adhered to the drill margin, which was eventually damaged by abrasive carbon fibers and WC–Co grains, leading to the removal of Ti fusion and TiAlN coating with increased spindle speed and drilling [73].

Drill bit wear significantly impacts drill bit life, hole quality, and production costs in drilling processes. In cutting CFRP/Ti or CFRP/Al stacks, wear occurs due to the tough carbon fibers causing abrasion and the aluminum or titanium alloys causing attrition, abrasion, and adhesion. Carbon fibers mainly cause abrasion leading to edge rounding or dulling, while titanium alloys cause rapid wear with diffusion, crater wear, adhesion, and catastrophic failures due to high cutting temperatures. Various coatings on drill bits, such as DLC, TiAlN, TiAlCrN, AlTiSiN-G, and diamond, affect wear differently. DLC coatings exhibit abrasion, edge rounding, and localized chipping. TiAlN coatings show abrasion and aluminum particle adhesion, while TiAlCr/TiSi coatings perform better due to higher wear resistance and reduced chip adherence. Uncoated drills often face severe abrasion, while diamond-coated drills face coating failure but minimal adhesion wear. Flank wear is a key indicator of drill bit wear. Studies indicate that DLC coatings experience less

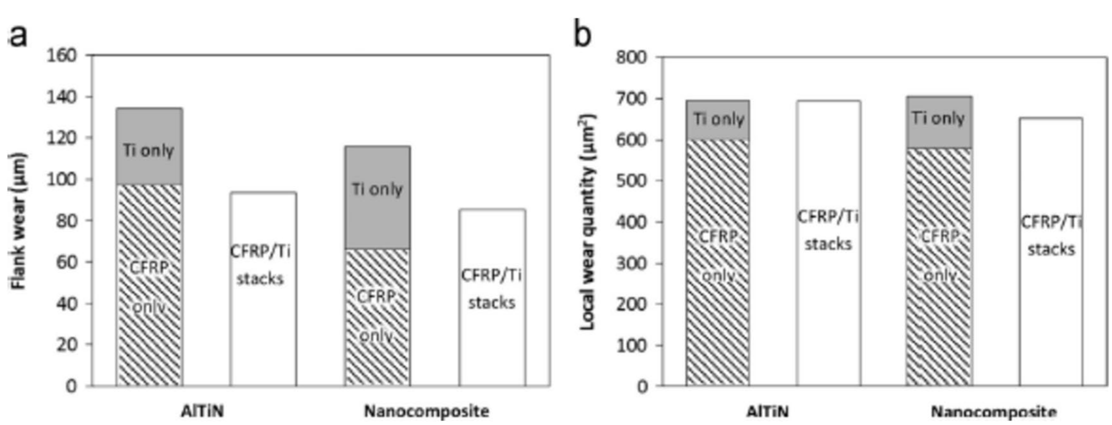

Fig. 7 Comparison of flank wear and edge rounding wear (LWQ) of the AlTiN and nanocomposite coated drills at hole 40. (**a**) Flank wear and (**b**) edge rounding wear [71]

flank wear than TiAlN, and diamond coatings effectively reduce wear. However, under certain conditions like MQL, diamond coatings show greater wear due to titanium chip accumulation. Uncoated drills sometimes outperform coated drills in certain conditions. The interaction between CFRP and Ti, such as CFRP brushing off Ti fusion, significantly affects wear and drill life. Overall, factors like feed rate, drill bit coating, and cutting conditions (dry or MQL) play crucial roles in determining drill bit wear and performance, and the quantitative data of this section is summarized in Table 2.

3.2 Effect of tool coating on thrust force

Since it affects the quality of the drilled holes and the resulting drill bit wear, thrust force during drilling is one of the primary parameters used to assess the machinability and power consumption of various composite/metal stacks in drilling operations [29, 64, 147–149]. Drill bit geometry, cutting parameters, drill bit material, drill bit coating, workpiece material, lubrication-cooling process etc. all have an impact on thrust force [63].

The cutting force required to remove the material from the workpiece is produced during the machining process by the drill bit moving against the workpiece. Regardless of the drill bits used, machining the Ti6Al4V panel often involves substantially larger thrust force than machining the CFRP panel [9, 41, 76]. This is attributable to the different chip removal processes used by metallic and composite materials. The titanium alloy chips are split according to elastoplastic deformation and have serrated and continuous shapes, which results in significantly larger mechanical resistance and consequently larger force magnitudes [150, 151]. In contrast, the CFRP panel is managed by the brittle fracture chip removal mode, which produces powdery chips and produce thrust forces of much lower magnitudes. When drilling CFRP/Al/CFRP stacks, Zhong et al. also agreed that, regardless of coated or uncoated drill bit, the maximum thrust force in the drilling of CFRP panel is smaller than that of Al panel [69]. According to Shyha et al., drilling Ti/CFRP/Al with an uncoated drill bit showed the force required for Ti (2200 N) was about three times higher than for CFRP and Al (700 N each). With worn drill bits, thrust forces increased by 5, 7, and 16 times in Al, Ti, and CFRP, respectively. Further, feed rate and cooling were crucial for CFRP and Al, while drill coating significantly affected thrust force in Ti, with a PCR of 23%. For the first hole drilled with an unworn bit, a diamond-coated drill had higher thrust forces than an uncoated drill in Ti and CFRP, but the reverse was true for Al [66]. Wang et al. observed that the thrust force recorded during drilling of Al (150-350N) was about two times greater than that recorded during drilling of CFRP (80–180 N) when utilizing a diamond-coated drill to drill CFRP/Al [67]. Montoya et al. obtained a thrust force value of 40–100 N in CFRP panel and 120–180 N in Al panel on the first hole regardless of coated or uncoated tools

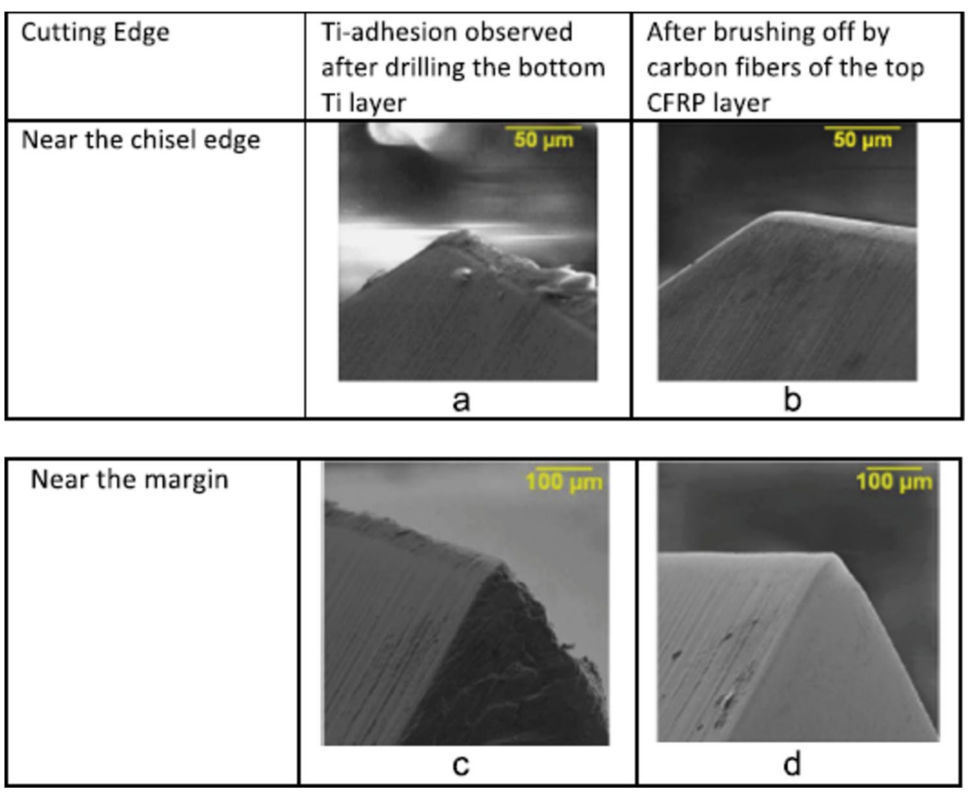

Fig. 8 The SEM pictures of the drill cutting edges (**a**, **c**) before and (**b**, **d**) after drilling into the top CFRP layer when drilling CFRP/Ti stack [71]

[64]. D'Orazio et al. showed that the thrust force in Al panel with either DLC-coated or TiAlN-coated drill varies between 600 and 800 N, while in CFRP panel, it varies between 150 and 300 N as shown in Fig. 9 [63]. It can also be seen from Fig. 9 that, after 170 holes, the value of thrust force in Al (F_{AA7075}) increases by around 8.7% when using the DLC coated drill and by around 27.9% while using the nanocomposite TiAlN coated tool. Similarly, the value of thrust force in CFRP (F_{CFRP}) with the DLC-coated drill increases by around 52% of the starting value, compared to 57.3% with the TiAlN-coated tool. These disparities can be explained by the fact that the DLC coated tool experiences less severe tool wear than the TiAlN tool. However, Brinksmeier et al. detected the opposite patterns when using a bigger drill diameter (16 mm), CFRP panel shows higher thrust forces than Al panel [152]. Kuo et al., when drilling a Ti/CFRP/Al stack panel, discovered that the variance in thrust force was Ti > CFRP > Al, regardless of coating [65]. The variation in the cutting forces produced by the drill and the various workpiece materials can account for this disparity in forces [153]. Kuo et al. obtained the thrust forces in Ti panel to be almost twofold higher than that in CFRP and Al panels when drilling with PVD DLC and CVD diamond-coated drill bits. The thrust force magnitudes were in the order of Ti > Al > CFRP for both the coatings irrespective of feed rate [78]. Tashiro et al. observed that drilling CFRP/Ti6Al4V with TiAlCr/TiSi and TiAlN drill bits showed higher thrust force at the CFRP entrance, which gradually decreased. In contrast, the titanium alloy section experienced significant thrust force at both the entrance and exit due to its resistance to cutting. As the drill bit progressed through both layers, the thrust force decreased [76]. Furthermore, TiAlN-coated drills produced higher thrust forces in Ti panels and lower in CFRP panels compared to TiAlCr/TiSi-coated drills. Mist cooling and TiAlCr/TiSi coating further reduced thrust force in both panels [76].

Montoya et al. found that uncoated drills produced 30 to 50% lower average thrust force for the initial hole compared to diamond-, TiAlCrN-, and AlTiSiN-G-coated tools when drilling CFRP/Al stacks. This difference is due to the coating thickness affecting cutting-edge sharpness, with uncoated drills having a radius increase of 9 µm, compared to 11 µm for TiAlCrN and AlTiSiN-G, and 15 µm for diamond-coated drills [64]. Kuo et al. observed that TiAlN/TiN-coated drills increased thrust forces by 12–18% compared to uncoated drills when drilling Ti/CFRP/Al panels. This increase is due to the coating's larger cutting-edge radius of 33 µm versus 22 µm for uncoated drills as shown in Fig. 10. ANOVA results indicated that both feed rate and drill bit coating significantly affected torque and thrust force in the Ti layer, while only feed rate influenced these parameters in the Al layer. For the CFRP layer, neither factor was significant [65].

Zhong et al. mentioned that the maximum thrust force with a TiAlN-coated drill is less than that of an uncoated drill because of the high hardness of the TiAlN coating [69]. The existence of TiAlN coating reduces the tendency of the drill to adhere with the aluminum chips when drilling the aluminum stack, resulting in a lower thrust force when using a TiAlN-coated drill bit [69]. Kuo et al. found that while drilling at a feed rate of 0.08 mm/rev, CVD diamond-coated drill, generated slightly lesser thrust forces (Ti—524 N; CFRP—187 N; Al—243 N) compared to using a DLC-coated drill (Ti—526 N; CFRP—222 N; Al—265 N) [78]. The reduced thrust forces were due to the drill's design, featuring a sharper 120° primary point angle and a 180° secondary angle, which shortened the cutting lips and lowered torque requirements. Wang et al. found that while drilling CFRP/Ti stacks with AlTiN-coated, nanocomposite-coated, and uncoated drill bits, no significant variation in thrust force was observed across 80 holes. However, the nanocomposite and AlTiN-coated drill bits produced slightly higher thrust forces in the titanium and CFRP panels [71]. According to Xu et al., the thrust forces created by the TiAlN-coated drills (75–150 N in CFRP panel and 300–550 N in Ti panel) under the MQL condition are significantly lower than those obtained by the diamond-coated drills (75–300 N in CFRP panel and 550–1200 N in Ti panel) in CFRP/Ti drilling as shown in Fig. 11 [41]. This phenomenon is brought about by the application of MQL, which raises the humidity in the drilling region. Because the tribological characteristics of diamond coatings is highly sensitive to humidity, the COF of the coatings tends to be boosted when the humidity rises, resulting in a larger cutting force [154]. On the one hand, the brittle characteristics of the carbon/epoxy system are retained in the composite polymer matrix due to the cooling effects caused by the MQL oil supply. The greater thrust forces that are achieved when applying the MQL condition indicate that the CFRP phase does not soften and, as a result, resists a greater mechanical resistance to the chisel and drill cutting edges [41]. Figure 11 further shows that the thrust forces created by the TiAlN-coated drills (60–150 N in CFRP panel and 280–550 N in Ti panel) under dry condition are slightly higher than those obtained by the diamond-coated drills (40–125 N in CFRP panel and 230–550 N in Ti panel) [41]. Zitoune et al. reported that when using an uncoated drill bit to drill composites, the thrust forces obtained are 20–25% higher than when using a coated drill bit [70]. This variation increased to a value of 47% when drilling the aluminum component, and which can be explained by the coated drill bits' significant reduction in friction between the machined surface and the drill's body as well as between the drill bit's flutes and the chips [70]. However, according to Montoya et al. the usual thrust force in the aluminum plate

Table 2 Quantitative comparison of the effect of coatings on tool damage

Workpiece	Tool	Parameters	Thrust on first hole	Thrust on last hole	Torque on first hole	Torque on last hole	Tool wear on last hole	Temperature	Reference
CFRP/Al7075/CFRP; thickness of Al = 26.1 mm and CFRP = 2.8 mm	DLC = 6.8 mm, flute length = 45, point angle = 118 (1–170 holes)	Cutting speed [m/min] = 170.8 Feed rate [mm/min] = 1300	CFRP = 125 N; Al7075 = 680 N	CFRP = 225N; Al7075 = 780N	–	–	Vb = 0.06 mm	–	[63]
	TiAlN = 6.8 mm, flute length = 43, point angle = 140 (1–170 holes)	Cutting speed [m/min] = 128.0 Spindle speed [rpm] = 1200	CFRP = 175 N; Al7075 = 610 N	CFRP = 300 N; Al7075 = 800 N	–	–	Vb = 0.13 mm	–	
CFRP/Al7010; thickness of CFRP = 7 mm and Al = 14 mm	Uncoated, 6 mm (1–250 holes)	Cutting speed (m/min) = 55; feed rate (mm/min) = 120; MQL = 16 ml/min	CFRP = 45 N; Al7075 = 125 N	CFRP = 350 N; Al7075 = 325 N	–	–	Vb = 70 µm (75 holes)	–	[64]
	Diamond coated, 6 mm diameter (1–250 holes)		CFRP = 95 N; Al7075 = 175 N	CFRP = 210 N; Al7075 = 150 N	–	–	Vb = 50 µm (75 holes)	–	
	TiAlCrN coated, 6 mm diameter (1–75 holes)		CFRP = 65 N; Al7075 = 145 N	CFRP = 225 N; Al7075 = 275 N	–	–	Vb = 77 µm (75 holes)	–	
	AlTiSiN-G coated, 6 mm diameter (1–75 holes)		CFRP = 70 N; Al7075 = 145 N	CFRP = 235 N; Al7075 = 280 N	–	–	Vb = 70 µm (75 holes)	–	
Ti-6Al-4 V/CFRP/Al 7050 T7451; each panel is 10 mm thick	Uncoated, 6.35 mm diameter (wet) (holes 1 and 310)	20/40 m/min; 0.05 rev/min	–	–	–	–	Vb = 0.3 mm (310 holes)	–	[68]
	CVD diamond coated, 6.35 mm diameter (wet) (holes 1 and 156)	20/40 m/min; 0.05 rev/min	–	–	–	–	Vb = 0.3 mm (197 holes)	–	
	C7 coated, 6.35 mm diameter (wet) (holes 1 and 268)	20/40 m/min; 0.1 rev/min	–	–	–	–	Vb = 0.3 mm (268 holes)	–	
	Uncoated, 6.35 mm diameter (spray mist) (holes 1 and 64)	20/40 m/min; 0.15 rev/min	–	–	–	–	Vb = 0.3 mm (92 holes)	–	

Table 2 (continued)

Workpiece	Tool	Parameters	Thrust on first hole	Thrust on last hole	Torque on first hole	Torque on last hole	Tool wear on last hole	Temperature	Reference
CFRP/Al; thickness of CFRP = 4.25 mm and Al = 3 mm	Uncoated; 6 mm diameter (1–70 holes)	Spindle speed—1050, 2020, and 2750 rpm Feed: 0.05, 0.1, and 0.15 mm/rev	CFRP = 142 N; Al = 485 N	CFRP = 280 N; Al = 510 N	–	–	–	–	[70]
	nc-CrAlN/a-Si_3N_4 coated, 6 mm diameter (1–70 holes)		CFRP = 115 N; Al = 375 N	CFRP = 198N; Al = 422N	–	–	–	–	
Ti-6Al-4 V/CFRP; Ti 6.73 mm, CFRP 7.54 mm	Uncoated	6000 rpm and 0.0762 mm/rev feed rate were used in CFRP panel 500 rpm and 0.0508 mm/rev feed rate were used in Ti. Coolant with a flow rate of 16 ml/min	Ti = 410 N; CFRP = 120 N	Ti = 1320 N; CFRP = 470 N	Ti = 310 Nm; CFRP = 50 Nm	Ti = 750 Nm; CFRP = 180 Nm	Vb = 104 µm (120 holes) LWQ 1450 µm^2	–	[71]
	AlTiN coated		Ti = 430 N; CFRP = 200 N	Ti = 1260 N; CFRP = 530 N	Ti = 360Nm; CFRP = 45Nm	Ti = 760Nm; CFRP = 190Nm	Vb = 135 µm (120 holes) LWQ 1650 µm^2	–	
	nc-AlTiN surrounded by Si_3N_4 matrix coated		Ti = 420 N; CFRP = 120 N	Ti = 1400 N; CFRP = 510 N	Ti = 450 Nm; CFRP = 60 Nm	Ti = 800 Nm; CFRP = 200 Nm	Vb = 145 µm (120 holes) LWQ 1500 µm^2	–	
CFRP/Ti6Al4V; thickness CFRP = 6.6 mm and Ti6Al4V = 6.28 mm	TiAlN coated; 6 mm diameter (1–16 holes)	Speeds (Vc)—15, 30, 45, and 60 m/min Feed (*f*) of 0.025, 0.050, 0.075, and 0.100 mm/rev. Vegetable-based micro-cutting oil with a flow rate of 15 ml/h	CFRP = 65 N; Ti = 180 N	CFRP = 140 N; Ti = 550 N	–	–	–	–	[41]
	TiAlN coated (MQL); 6 mm diameter (1–16 holes)		CFRP = 70 N; Ti = 300 N	CFRP = 130 N; Ti = 500 N	–	–	–	–	
	Diamond coated; 6 mm diameter (1–16 holes)		CFRP = 45 N; Ti = 250 N	CFRP = 125 N; Ti = 550 N	–	–	–	–	
	Diamond coated (MQL); 6 mm diameter (1–16 holes)		CFRP = 87 N; Ti = 550 N	CFRP = 285 N; Ti = 1200 N	–	–	–	–	

Table 2 (continued)

Workpiece	Tool	Parameters	Thrust on first hole	Thrust on last hole	Torque on first hole	Torque on last hole	Tool wear on last hole	Temperature	Reference
CFRP/Ti6Al4V Thickness of CFRP = 9.16 mm and Ti6Al4V = 6.8 mm	Uncoated (CFRP to Ti); 6.35 mm (1–16 holes)	Speed—20, 35, 50, 65 m/min Feed—0.015, 0.03, 0.045, 0.06 mm/rev Sequence CFRP → Ti, Ti → CFRP	CFRP = 76–132 N; Ti = 280–630 N	–	–	–	–	CFRP = 205–230 °C Ti = 370–515 °C	[74]
	Uncoated (Ti to CFRP); 6.35 mm (1–16 holes)		CFRP = 68–110 N; Ti = 255–440 N	–	–	–	–	CFRP = 215–255 °C Ti = 350–500 °C	
	Diamond coated (CFRP to Ti); 6.35 mm (1 – 16 holes)		CFRP = 58 – 120N; Ti = 240 – 500N	–	–	–	–	CFRP = 175–210 °C Ti = 323–500 °C	
	Diamond coated (Ti to CFRP); 6.35 mm (1 – 16 holes)		CFRP = 49 – 104N; Ti = 250 – 380N	–	–	–	–	CFRP = 190–230 °C Ti = 280–450 °C	
CFRP/Ti6Al4V	TiAlN coated (1–50 holes)	Speed—1000, rev/min Feed 50 mm/min	CFRP = 63–90 N; Ti = 240–380N	–	–	–	Vb = 10–63 µm	–	[73]
CFRP/Ti6Al4V Thickness of CFRP = 6.60 mm and Ti6Al4V = 6.28 mm	TiAlN coated; 6 mm diameter (1–16 holes)	Cutting speed (Vc)—15, 30, 45, and 60 m/min Feed rate (*f*)—0.025, 0.050, 0.075, and 0.100 mm/rev Coolant flow rate of 15 ml/h	–	–	CFRP = 0.6–1.4 Nm Ti = 1–3.5 Nm	–	–	–	[75]
	TiAlN coated (MQL); 6 mm diameter (1–16 holes)		–	–	CFRP 0.3–1.3 Nm Ti 0.5–2.2 Nm	–	–	–	
	Diamond coated; 6 mm diameter (1–16 holes)		–	–	CFRP 0.5–1.3 Nm Ti 0.9–2.2 Nm	–	–	–	
	Diamond coated (MQL); 6 mm diameter (1–16 holes)		–	–	CFRP 0.4–1.2 Nm Ti 0.8–3.9 Nm	–	–	–	

Table 2 (continued)

Workpiece	Tool	Parameters	Thrust on first hole	Thrust on last hole	Torque on first hole	Torque on last hole	Tool wear on last hole	Temperature	Reference
CFRP/Ti6Al4V Thickness of CFRP = 3 mm and Ti alloy = 9.5 mm	TiAlCr/TiSi (mist); 6 mm diameter (90 holes)	Speed—18.8 m/min, feed—0.02 mm/rev	CFRP = 450 Ti = 1500	CFRP = 550 Ti = 1820	CFRP = 0.2 Nm Ti = 2.26 Nm	CFRP = 0.4 Nm; Ti = 4.5Nm	0.2 mm (140 holes)	–	[76]
	TiAlCr/TiSi (dry); 6 mm diameter (1–140 holes)		CFRP = 250 Ti = 1300	CFRP = 500 Ti = 1500	CFRP = 0.01 Nm Ti = 2.24 Nm	CFRP = 0.3 Nm Ti = 4.4 Nm	0.2 mm (90 holes)	–	
	TiAlN (dry); 6 mm diameter (1–100 holes)		CFRP = 430 Ti = 1681	CFRP = 530 Ti = 1850	CFRP = 0.2 Nm Ti = 2.25 Nm	CFRP = 0.4 Nm Ti = 2.95 Nm	0.23 mm (100 holes)	–	
CFRP/Ti6Al4V	C7 coated; 6 mm diameter (1–24 holes)	CFRP—4500 rpm and 457.2 mm/min; Ti—1400 rpm and 119 mm/min	CFRP = 150–270 Ti = 700–850	–	CFRP = 0.6–1.1 Nm; Ti = 2.4–3.9 Nm	–	–	–	[12]

Table 2 (continued)

Workpiece	Tool	Parameters	Thrust on first hole	Thrust on last hole	Torque on first hole	Torque on last hole	Tool wear on last hole	Temperature	Reference
CFRP/Ti6Al4V; each stack is 4 mm thick	6.35 mm diameter uncoated tool, 0.11 mm chisel edge, helix angle 20° and point angle 135°; CFRP to Ti (1–20 holes)	Cutting speed, vc (m/min) 15, 30, 45, 60 Feed rate, *f* (mm/rev) 0.03, 0.06, 0.09, 0.12, 0.15 Cutting sequence CFRP → Ti, Ti → CFRP	CFRP = 80–200 N; Ti = 220–650 N	–	CFRP = 5 – 40Nm; Ti = 50 – 300Nm	–	–	–	[9]
	6.35 mm diameter PVD TiAlN-coated twist drill, 0.22 mm-chisel edge, helix angle = 27.2° and point angle = 140°; CFRP to Ti sequence (1–20 holes)		CFRP = 170–350 N Ti = 500–950 N	–	CFRP = 7–37 Nm Ti = 50–240 Nm	–	–	–	
	6.35 mm diameter PVD TiAlN-coated twist drill with 0.22-mm chisel edge, helix angle of 27.2° and point angle = 140°; sequence Ti to CFRP (1–20 holes)		CFRP = 140–320 N Ti = 500–920 N	–	CFRP = 2–90 Nm Ti = 60–260 Nm	–	–	–	
Ti-6Al4V/CFRP/AA7050 Each layer 10 mm thick	Uncoated; 6.35 mm diameter (1–180 holes, 0.05 and 0.08 mm/rev)	Feed rate—0.05 and 0.08 mm/rev at 90th hole	Ti = 1800 N CFRP = 750 N Al = 510 N	Ti = 1620 N; CFRP = 680 N; Al = 550 N	Ti = 1550 Nm CFRP = 560 Nm Al = 690 Nm	Ti = 1870 Nm; CFRP = 620 Nm; Al = 900Nm	0.17 mm (180 holes)	–	[65]
	TiAlN/TiN coated; 6.35 mm diameter (1–160 holes, 0.05 and 0.08 mm/rev)		Ti = 2050 N; CFRP = 810N; Al = 530 N	Ti = 1860 N; CFRP = 770 N; Al = 580 N	Ti = 1450 Nm; CFRP = 510 Nm; Al = 620 Nm	Ti = 1700 Nm; CFRP = 640 Nm; Al = 1060 Nm	0.34 mm (160 holes)	–	

Table 2 (continued)

Workpiece	Tool	Parameters	Thrust on first hole	Thrust on last hole	Torque on first hole	Torque on last hole	Tool wear on last hole	Temperature	Reference
CFRP/Al2024/CFRP; thickness of CFRP = 2.5 mm, and Al = 5 mm	Uncoated (1–16 holes)	Cutting speed (m/min) 15, 30, 45, 60 Feed rate (mm/rev) 0.025, 0.05, 0.075, 0.1	Upper CFRP = 80–227 N; Al = 200–465 N; Lower CFRP = 100–257 N	–	–	–	–	–	[69]
	TiAlN coated (1–16 holes)		Upper CFRP = 86–187 N; Al = 130–425 N; Lower CFRP = 80–180 N	–	–	–	–	–	
CFRP/Al7075-T651; thickness of CFRP = 8.74 mm, and Al = 6 mm	Diamond coated; 9.53 mm diameter	Spindle speed, *n* (rpm) 1000, 2000, 3000; Feed rate, *f* (mm/rev) 0.02, 0.04, 0.06, 0.08	CFRP = 90–165 N; Al = 160–340 N	–	–	–	–	–	[67]

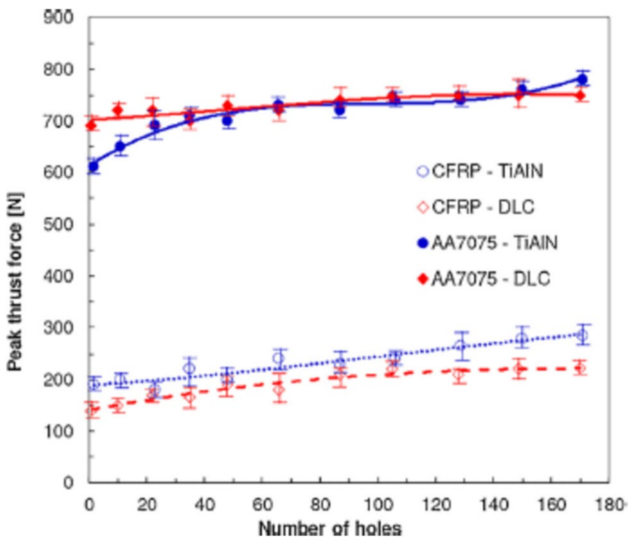

Fig. 9 Evolution of thrust force with number of holes using TiAlN and DLC-coated tools [63]

exhibits a nearly asymptotic tendency when the diamond coating breaks [64]. The application of a diamond coating reduced the force when drilling CFRP by 65% and when drilling Al by 35% for the same cutting circumstances by reducing drill bit wear. The material softening brought on by high temperatures and the drill bit geometry's automatic optimization could both account for this pattern [64].

When considering the hole number against thrust force, Kuo et al. observed 56%, 52%, and 30% increase in thrust force in the 10th hole compared to first hole when drilling Ti, CFRP, and Al panels, respectively, with DLC-coated drill bit [78]. The premature chipping and strong adherence of workpiece on the cutting edge of the drill were identified as the causes of the sudden increase in thrust force. Montoya et al. mentioned that the thrust forces produced by both uncoated and diamond-coated drills steadily rise with an increase in the number of drilled holes in both CFRP and Al components, primarily because of drill bit wear [64]. Tashiro et al. also mentioned that when drilling CFRP/Ti6Al4V using TiAlCr/TiSi and TiAlN-coated cemented carbide drills, the thrust force rises with the number of holes [76]. Ghassemieh et al. found that drilling CFRP/Ti6Al4V with C7 (nano-crystalline AlTiN grains in Si_3N_4)-coated drills saw thrust forces increase with the number of holes. Specifically, wear increased thrust forces by about 20% in Ti and 87% in CFRP [12].

Therefore, it can be decided that thrust force is influenced by factors like drill bit geometry, cutting parameters, drill bit material, workpiece material, and lubrication-cooling processes, and the quantitative data of this section is summarized in Table 2. Drilling Ti6Al4V panels typically requires significantly higher thrust force compared to CFRP panels due to differences in chip removal processes. Worn drill bits further increase thrust forces significantly. Coatings on drill bits affect thrust forces differently based on the workpiece material. For example, TiAlN-coated drills tend to produce lower thrust forces than uncoated drills due to their high hardness and reduced adhesion with aluminum chips. However, some studies have reported higher thrust forces with coated drills, attributed to cutting-edge sharpness. Uncoated drills often generate lower thrust forces initially compared to coated drills, as coatings can increase the cutting-edge radius, reducing sharpness. Cooling conditions such as MQL also impact thrust forces, particularly in composite drilling. MQL can increase humidity in the drilling area, affecting the tribological properties of coatings and subsequently the cutting forces. Thrust forces generally increase with the number of drilled holes, primarily due to drill bit wear. The rate of increase varies among different materials and coatings. For instance, diamond-coated drills show a significant reduction in thrust forces for both CFRP and aluminum, attributed to reduced wear. In contrast, the thrust forces produced by TiAlN-coated drills tend to be higher, especially in titanium panels. Drill bit coatings and cooling conditions are critical in managing thrust forces, with specific coatings and lubrication methods showing significant effects on thrust force magnitudes.

Fig. 10 Cutting edge radius of the (**a**) uncoated and (**b**) TiAlN/TiN-coated drills [65]

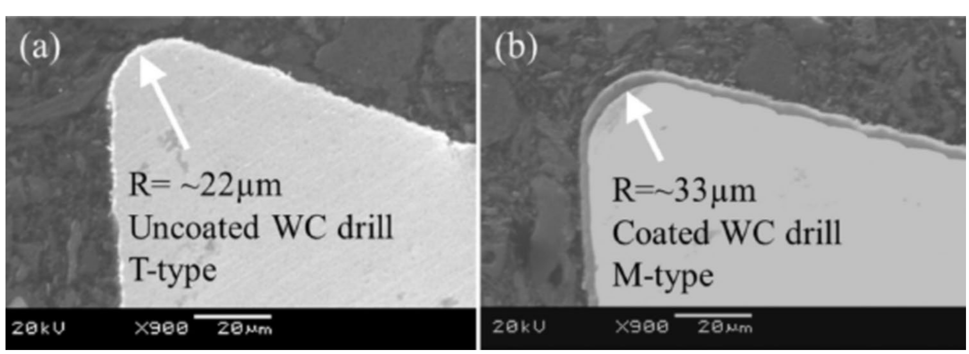

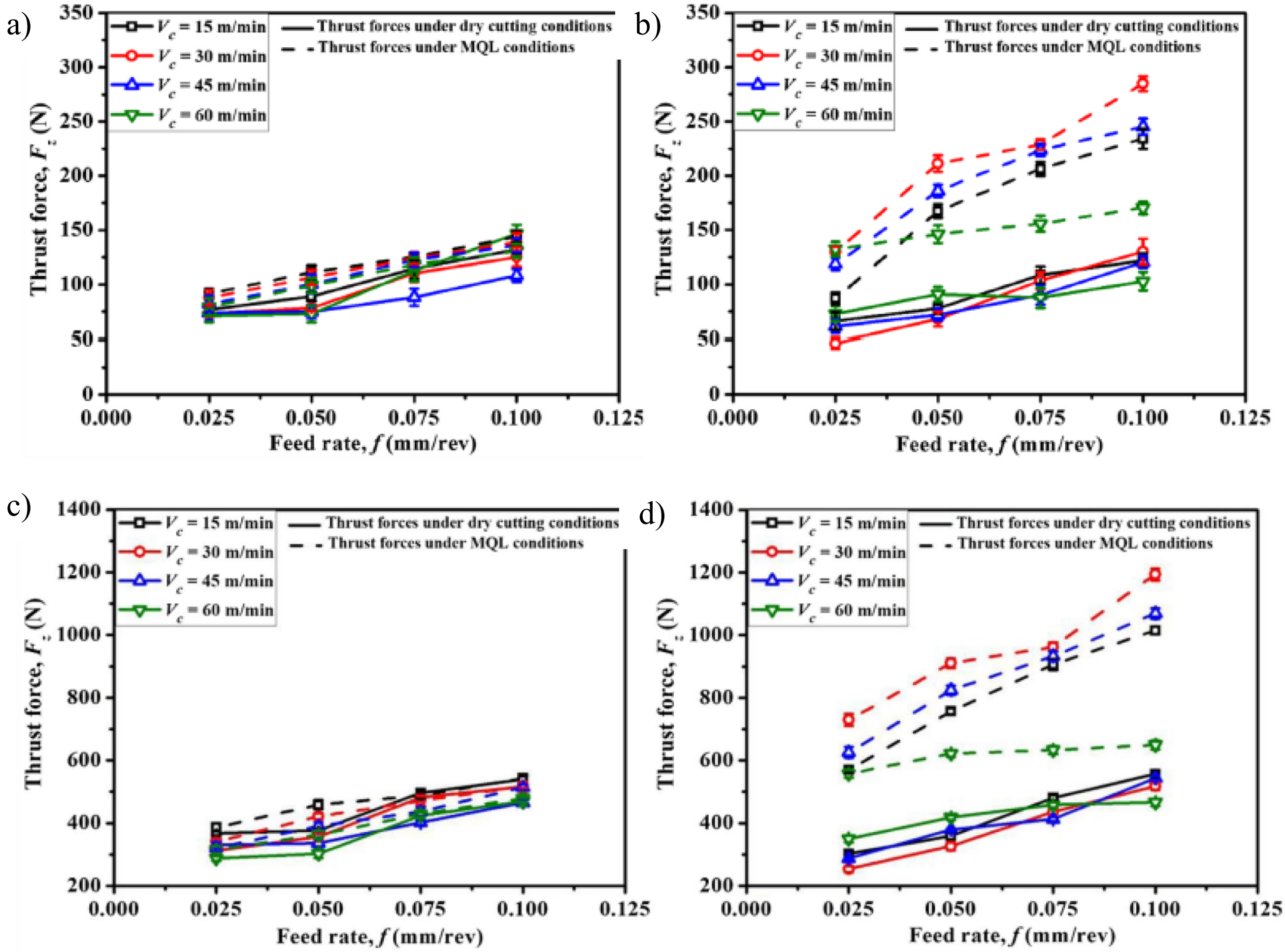

Fig. 11 Comparison of the thrust forces under two cutting environments for the CFRP panel with (**a**) TiAlN-coated and (**b**) diamond-coated drills and for the titanium phase with (**c**) TiAlN-coated and (**d**) diamond-coated drills [41]

3.3 Influence of tool coating on torque

According to Xu and Mansori, drilling CFRP/Ti stacks with a PVD TiAlN-coated drill resulted in slightly larger torque magnitudes in CFRP panels than with an uncoated drill, but significantly lower torque magnitudes in Ti panels. They added that the application of coating has less impact on torque than feed and speed [9]. Drilling CFRP/Ti stacks using AlTiN-coated, nanocomposite-coated, and uncoated drill bits were compared by Wang et al. [71]. Uncoated drill bit produced somewhat less torque in Ti panel than AlTiN and nanocomposite coated drill bits, despite there being no appreciable variation in torque throughout the testing (80 holes). When drilling Ti/CFRP/Al panel, Kuo et al. reported that TiAlN/TiN-coated drills generated up to 10% less torque, which was consistent with the enhanced wear resistance offered by the TiAlN/TiN coating at the corners [65].

According to Shyha et al., the lowest torque when drilling Ti/CFRP/Al was recorded in CFRP followed by Al and Ti with an uncoated drill [66]. This result can be attributed to the propensity of both aluminum and titanium chips to attach to drill edges and lips. Furthermore, as the test came to an end, the torque levels in Al, Ti, and CFRP, respectively, rose by a factor of 3, 4, and 5 with the used drill bits. According to Kuo et al., when drilling Ti/CFRP/Al with PVD DLC-coated and CVD diamond-coated drill, the lowest torque is recorded in CFRP followed by Al and Ti irrespective of feed rate [78]. Furthermore, after 10 holes, torque in the Ti, CFRP, and Al sections rose by two to three times its starting levels and then did not show any significant increment until 70 holes. According to Tashiro et al., drilling CFRP/Ti6Al4V with a drill bit coated in TiAlCr/TiSi and TiAlN resulted in significantly less torque in CFRP part compared to titanium alloy part [76]. The torque nearly doubled in size in the 140th hole when the drill bit is advanced through the hole. The friction between the titanium alloy and the drill may have risen due to the drill's high wear at the 140th hole [76]. Additionally, in dry and mist-cooled environment, drill with TiAlN coating produced less torque in titanium panel than the drill with TiAlCr/TiSi coating. Ghassemieh concurred that, between the first and last (21st) holes, the torque of the CFRP portion increased by 50% while drilling CFRP/Ti6Al4V using a C7-coated drill [12].

Xu et al. found that TiAlN-coated drills had lower torque under MQL conditions compared to dry cutting, but diamond-coated drills showed the same torque under both conditions due to the diamond coating's low friction coefficient. Under MQL at cutting speeds of 30 and 45 m/min, diamond-coated drills generated higher torque on titanium alloy due to severe chip congestion, which increased friction during chip removal [75].

Therefore, it can be said that the presence of coatings on drill bits, such as PVD TiAlN, AlTiN, and nanocomposite coatings, can influence torque in drilling operations, but the effect of coatings on torque appears to be less pronounced than other factors like feed rate and speed. The quantitative data of this section is summarized in Table 2. Torque levels tend to increase as drill bits wear down. The accumulation of swarf on drill edges and lips can contribute to increased torque. The frictional interaction between drill bits and workpiece plays a crucial role in torque generation. The choice of coating can affect friction coefficients and subsequently impact torque levels. Additionally, the use of minimum quantity lubrication (MQL) can influence torque, with diamond-coated drills exhibiting stable torque levels due to their low friction coefficient.

3.4 Impact of tool coating on temperature

To understand drilling quality of CFRP/metal stacks, it is crucial to recognize the thermal properties of CFRP resins. CFRP's matrix resin, typically an amorphous polymer, transitions through glassy, elastic, and viscous states depending on temperature, with the glass-transition temperature around 200 °C. At this point, epoxy resin deteriorates and debonds from carbon fibers [67]. Wang et al. found that drilling CFRP/Al stacks with diamond-coated drills resulted in a peak temperature of 232 °C in the CFRP layer, which dropped to 115 °C in the Al layer. This is due to CFRP's low heat conductivity causing heat buildup, while aluminum's high thermal conductivity allows for rapid heat dissipation [67].

According to Xu et al., while drilling CFRP/Ti with both uncoated and diamond-coated drills [74], it is seen that the diamond-coated drills generate comparatively lesser cutting temperatures than the uncoated ones, as shown in Fig. 12, demonstrating enhanced heat conduction at the workpiece–tool interface [74]. This phenomenon can be explained by the diamond coating's better thermal conductivity (1600–2000 W/mK), which is approximately 54–68 times higher than that of WC (29.2 W/mK) and allows for rapid discharge of heat at the workpiece–tool interface. Its lower COF also improves tribological interaction at the tool–chip and workpiece–tool interface [74].

When Cao et al. used a TiAlN-coated drill bit to drill CFRP/Ti stack, they found that as the cutting-edge worn and degraded, the shearing plastic temperature of the Ti significantly rose. Because of the frictional action between the fracture edge and fibers, the cutting temperature during the interface drilling stage exceeded the glass transition temperature (T_g) at the 20th hole, with friction heat and plastic heat increased continuously as the number of drilled holes increased [73].

Therefore, it can be said that exceeding glass-transition temperature (T_g) can lead to resin deterioration and potential debonding of carbon fibers from the matrix. To prevent such issues, it is essential to carefully control the drilling process to avoid surpassing T_g. Drilling CFRP layers can generate significant heat due to the material's poor heat conductivity. However, the excellent thermal conductivity of metal allows for effective heat dissipation once the drilling process transitions to metal panel. Diamond-coated drills generally produce lower cutting temperatures compared to uncoated drills. The diamond coating's lower friction coefficient and higher thermal conductivity contribute to improved heat management at the tool-to-workpiece interface.

4 Effect of tool coating on improving hole quality parameters

The application of the coating boosts the drill bit's corrosion and oxidation resistance while extending its lifespan. Researches have shown that the use of the coating greatly affects the drilled hole dimensions of composite/metal stacked panels in terms of geometry, linearity, delamination damage, and surface roughness [41, 68, 70, 74, 75, 155–157]. The drill bit coating is anticipated to have small grains that can generate a sharp cutting edge [24, 70], good toughness to prevent deformation [155], high hardness to provide excellent wear resistance [68, 74], and reduction in heat generation. Each of these characteristics is essential for desired drill bit life, machinability, and hole quality [158]. The quantitative data of Sect. 4 is summarized in Table 3.

4.1 Delamination on composite panel

Delamination in the composite panel is often a particularly severe failure condition in hybrid CFRP/metal stack drilling because of its irreversible nature, which accounts for a significant percentage of component rejections in actual production [9]. Delamination is defined as the interlaminar debonding across adjacent layers of a composite. Since it adversely affects the fatigue life and assembly performance

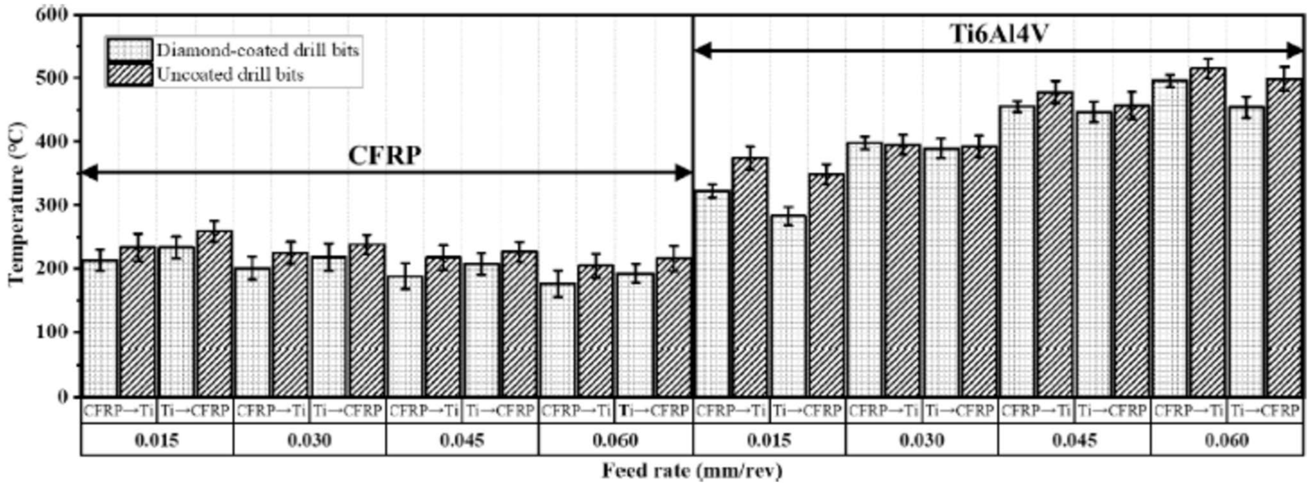

Fig. 12 Comparison of the maximum cutting temperatures obtained by the IFTC with the temperature compensations for different drill bits and cutting sequences under varying feed rates (*Vc* = 20 m/min) [74]

of composite laminates, it is thought to be the most serious damage [160]. Delamination results from bending strains between the material contact point and the drill bit [161]. Furthermore, under alternating loading situations, delamination will spread further, eventually leading to the premature end of the life span of the composite components [41]. Peeling up and pushing down are the mechanisms by which drilling-induced delamination happens at the edge of both entrance and exit holes. Delamination of the CFRP layer can occur even with a wear-free drill due to the drill flute peeling off the CFRP top layer [63, 162] and AA7075 chip evacuation through the hole [63, 64].

D'Orazio et al. found that the delamination factor (DF) increased with the number of drilled holes. For the first hole in a CFRP/Al7075/CFRP stack, DLC-coated drills had a DF value about 55.5% lower and TiAlN-coated drills about 50% lower than the last hole. A wear-free TiAlN-coated drill had nearly double the DF of a DLC-coated drill. This difference is likely due to the DLC coating's high hardness, which reduces thrust forces and enhances wear resistance [63]. A reduction in thrust force can significantly contribute to minimizing the DF, thereby enhancing the overall quality of hole during drilling [69]. Conflictingly, the delamination factor produced by diamond coated drill bit (0.17–0.3 in MQL condition and 0.03–0.07 in dry condition) is more than that produced by TiAlN-coated drill bit (0.1–0.15 in MQL condition and 0.03–0.05 in dry condition), according to Xu et al. [41]. This also demonstrates that the MQL environment promotes CFRP delamination. According to Montoya et al., delamination does not occur all the way around the hole entry, but rather in regions where a 45° angle is formed by the direction of the chip movement (caused by the drill's rotation) and the fiber orientation [64].

Zhong et al. found that the exit delamination produced by an uncoated drill bit when drilling a CFRP/Al/CFRP stack was approximately 4 to 8 times larger than that achieved with a TiAlN-coated drill bit as shown in Fig. 13 [69]. This significant difference is due to the increased hardness of the TiAlN-coated drill bit. Additionally, Zhong et al. noted that the DF at the hole exit was greater for the uncoated drill bit compared to the entrance, and this variation was less pronounced when using the TiAlN-coated drill bit. A study by Bayraktar and Turgut contradicts these findings, indicating that uncoated drills outperformed TiN and TiAlN-coated HSS drills in terms of minimizing the DF [72]. Furthermore, in terms of delamination, the TiN and TiAlN-coated drills performed similar to each other. This discrepancy is explained by the coating's ability to dull the cutting edge, making it more challenging for the drill to penetrate the material [72]. Similarly, Xu and Mansori concurred that an uncoated drill with a DF value of 1.15 produced slightly better delamination quality in comparison to a TiAlN-coated drill with a DF value of 1.206 when drilling CFRP/Ti [9]. Jebaratnam et al. found that drilling CFRP/Al7075-T6 with uncoated WC tools consistently exceeded the industry delamination factor (DF) limit of 1.206. In contrast, ta-C coated tools drilled up to 90 holes with exit delamination below this threshold, thanks to the coating's high hardness and strong bond strength, which reduce delamination [163]. However, ta-C + Cr coated tools reached a DF below 1.206 for only 40 holes before surpassing the tolerance limit. The lower hardness and bond strength of ta-C + Cr coating led to faster wear and higher DF due to increased thrust force [163].

Xu and Mansori found that drilling CFRP → Ti with a TiAlN-coated drill bit resulted in more precise CFRP hole shapes and less fiber/matrix damage compared to the

Table 3 Quantitative comparison of the effect of coatings on hole damage

Workpiece	Tool	Hole diameter (mm)	Hole circularity (µm)	Surface roughness (µm)	Delamination	Entry burr height (µm)	Reference
CFRP/Al7075/CFRP; thickness of Al = 26.1 mm and CFRP = 2.8 mm	DLC = 6.8 mm, flute length = 45, point angle = 118 (1–170 holes)	CFRP in = 6.81–6.77 Al7075 = 6.8–6.76 CFRP out = 6.78–6.74	–	–	DF = 6–14%	–	[63]
	TiAlN = 6.8 mm flute length = 43, point angle = 140 (1–170 holes)	CFRP in = 6.81–6.79 Al7075 = 6.81–6.79 CFRP out = 6.79–6.73	–	–	DF = 11–21%	–	
CFRP/Al7010; thickness of CFRP = 7 mm and Al = 14 mm	Uncoated, 6 mm (1–250 holes)	CFRP in = 5.965–5.972 Mid = 5.965–5.979 Al out = 5.968–5.974	–	CFRP = 1–7; Al = 0.2–1.3	–	–	[64]
	Diamond coated, 6 mm diameter (1–250 holes)	CFRP in = 5.978–5.972 Mid = 5.980–5.970 Al out = 5.977–5.965	–	CFRP = 1–2.8; Al = 0.1–0.6	–	–	
	TiAlCrN coated, 6 mm diameter (1–75 holes)	CFRP in = 5.962–5.980 Mid = 5.973–5.993 Al out = 5.964–5.993	–	–	–	–	
	AlTiSiN-G coated, 6 mm diameter (1–75 holes)	CFRP in = 5.973–5.956 Mid = 5.975–5.964 Al out = 5.980–5.960	–	–	–	–	
Ti-6Al-4 V/CFRP/Al 7050 T7451; each panel is 10 mm thick	Uncoated, 6.35 mm diameter (wet) (holes 1 and 310)	Ti = 6.357–6.34 CFRP = 6.349–6.33 Al = 6.349–6.335	Ti = 78–18 CFRP = 33–23 Al = 54–12	Ti = 0.3–0.9 CFRP = 0.6–5 Al = 0.19–0.21	–	Entry Ti = 27–225; Al = 21–90; Exit Ti = 30–255; Al = 61–283	[68]
	CVD diamond coated, 6.35 mm diameter (wet) (holes 1 and 156)	Ti = 6.351–6.345 CFRP = 6.35–6.341 Al = 6.353–6.345	Ti = 48–7; CFRP = 38–9; Al = 9–2	Ti = 0.36–0.9; CFRP = 0.6–27; Al = 0.23–0.15	–	Entry Ti = 32–135; Al = 15–50; Exit Ti = 51–140; Al = 21–961	
	C7 coated, 6.35 mm diameter (wet) (holes 1 and 268)	Ti = 6.356–6.336 CFRP = 6.351–6.339 Al = 6.361–6.34	Ti = 28–9; CFRP = 10–17; Al = 4–18	Ti = 0.48–0.97; CFRP = 0.5–9; Al = 0.3–0.1	–	Entry Ti = 23–212; Al = 22–110; Exit Ti = 25–301; Al = 90–430	
	Uncoated, 6.35 mm diameter (spray mist) (holes 1 and 64)	Ti = 6.358–6.357 CFRP = 6.429–6.471 Al = 6.379–6.35	Ti = 27–28; CFRP = 16–13; Al = 11–10	Ti = 0.53–0.63; CFRP = 1.7–9; Al = 0.75–1.45	–	Entry Ti = 28–57; Al = 25–60; Exit Ti = 30–110; Al = 120–165	
CFRP/Al; thickness of CFRP = 4.25 mm and Al = 3 mm	Uncoated; 6 mm diameter (1–70 holes)	–	–	CFRP = 3–6.8; Al = 0.8–3.6	–	–	[70]
	nc-CrAlN/a-Si_3N_4 coated, 6 mm diameter (1–70 holes)	–	–	CFRP = 1.8–6.7; Al = 0.7–2.8	–	–	

Table 3 (continued)

Workpiece	Tool	Hole diameter (mm)	Hole circularity (µm)	Surface roughness (µm)	Delamination	Entry burr height (µm)	Reference
CFRP/Al7075-T651; thickness of CFRP = 8.74 mm and Al = 6 mm	Diamond coated; 9.53 mm diameter	CFRP in = 9.541–9.564 CFRP out = 9.54–9.593 Al = 9.535–9.547	–	CFRP = 2.2–2.8; Al = 0.4–0.7	–	–	[67]
CFRP/Al2024/CFRP; thickness of CFRP = 2.5 mm and Al = 5 mm	Uncoated (1–16 holes)	–	–	–	DF% entry = 0.01–0.9 DF% exit = 1.7–5.6	–	[69]
	TiAlN coated (1–16 holes)	–	–	–	DF% entry = 0.04–0.5 DF% exit = 0.3–1.8	–	
CFRP/Ti6Al4V; thickness CFRP = 6.6 mm and Ti6Al4V = 6.28 mm	TiAlN coated; 6 mm diameter (1–16 holes)	–	–	–	DF% = 0.02–0.05	–	[41]
	TiAlN coated (MQL); 6 mm diameter (1–16 holes)	–	–	–	DF% = 0.11–0.14	–	
	Diamond coated; 6 mm diameter (1–16 holes)	–	–	–	DF% = 0.025–0.06	–	
	Diamond coated (MQL); 6 mm diameter (1–16 holes)	–	–	–	DF% = 0.175–0.31	–	
CFRP/Ti6Al4V; thickness of CFRP = 9.16 mm and Ti6Al4V = 6.8 mm	Uncoated (CFRP to Ti); 6.35 mm (1–16 holes)	–	–	–	–	Exit Ti = 420–720	[74]
	Uncoated (Ti to CFRP); 6.35 mm (1–16 holes)	–	–	–	–	Exit Ti = 210–370	
	Diamond coated (CFRP to Ti); 6.35 mm (1–16 holes)	–	–	–	–	Exit Ti = 360–430	
	Diamond coated (Ti to CFRP); 6.35 mm (1–16 holes)	–	–	–	–	Exit Ti = 180–240	
CFRP/Ti6Al4V	TiAlN coated (1–50 holes)	–	–	–	100–263 µm; DF = 1.53%		[73]
CFRP/Ti6Al4V; thickness of CFRP = 6.60 mm and Ti6Al4V = 6.28 mm	TiAlN coated; 6 mm diameter (1–16 holes)	CFRP = 6.0–6.57; Ti = 6.02–6.11	CFRP = 130; Ti = 20	–	–	Exit Ti = 65–164	[75]
	TiAlN coated (MQL); 6 mm diameter (1–16 holes)	CFRP = 5.96–6.38; Ti = 5.97–6.0	CFRP = 150; Ti = 25	–	–	Exit Ti = 40–75	
	Diamond coated; 6 mm diameter (1–16 holes)	CFRP = 6.04–6.53; Ti = 6.01–6.04	CFRP = 115; Ti = 15	–	–	Exit Ti = 33–125	
	Diamond coated (MQL); 6 mm diameter (1–16 holes)	CFRP = 5.95–6.32; Ti = 5.95–6.0	CFRP = 90; Ti = 25	–	–	Exit Ti = 80–184	

Table 3 (continued)

Workpiece	Tool	Hole diameter (mm)	Hole circularity (µm)	Surface roughness (µm)	Delamination	Entry burr height (µm)	Reference
CFRP/Ti6Al4V; thickness of CFRP = 3 mm and Ti alloy = 9.5 mm	TiAlCr/TiSi (mist); 6 mm diameter (90 holes)	CFRP = 6.05–6.1; Ti = 6.01–6.02	–	–	–		[76]
	TiAlCr/TiSi (dry); 6 mm diameter (1–140 holes)	CFRP = 6.1–6.15; Ti = 6.01–6.025	–	–	–		
	TiAlN (dry); 6 mm diameter (1–100 holes)	CFRP = 6.13–6.47; Ti = 6–6.01	–	–	–		
CFRP/Ti6Al4V	C7 coated; 6 mm diameter (1–24 holes)	–	–	CFRP = 2.2 –0.8; Ti = 0.25–0.39	DF% = 0.5–2.8	–	[12]
Ti6Al4V/CFRP/Al7050-T7651	PVD DLC coated 6.38 mm diameter, point angle = 140° and helix angle = 30° (1–70 holes)	Ti = 6.403; CFRP = 6.381; Al = 6.379	Ti = 120; CFRP = 65; Al = 42	–	–	Entry Ti = 60; Al = 35; Exit Ti = 100; Al = 380	[159]
	CVD diamond coated 6.38 mm diameter, 120° and 180° two-stage point design, helix angle = 30° (1–70 holes)	Ti = 6.377; CFRP = 6.370; Al = 6.369	Ti = 20; CFRP = 31; Al = 33	–	–	Entry Ti = 80 Al = 20 Exit Ti = 80 Al = 90	

Table 3 (continued)

Workpiece	Tool	Hole diameter (mm)	Hole circularity (µm)	Surface roughness (µm)	Delamination	Entry burr height (µm)	Reference
CFRP/Ti6Al4V; each stack is 4 mm thick	6.35 mm diameter uncoated carbide tool with 0.11 mm chisel edge, helix angle 20° and point angle 135° CFRP to Ti (1–20 holes)	CFRP in = 6.38–6.47; CFRP out = 6.38–6.55; Ti in = 6.365–6.385; Ti out = 6.37–6.385	CFRP = 4.8–6; Ti 5–7.5	CFRP = 2–5; Ti = 0.4–1.1	DF% = 1.02–1.15	Exit Ti = 80–185	[9]
	6.35 mm diameter PVD TiAlN-coated carbide twist drill, 0.22-mm chisel edge, helix angle = 27.2° and a point angle = 140° CFRP to Ti sequence (1–20 holes)	CFRP in = 6.375–6.391; CFRP out = 6.373–6.408; Ti in = 6.372–6.389; Ti out = 6.386–6.392	CFRP = 5.5–18; Ti = 6–13	CFRP = 1–3.5; Ti = 0.35–1.15	DF% = 1.03–1.21	Exit Ti = 120–265	
	6.35 mm diameter PVD TiAlN-coated carbide twist drill with 0.22-mm chisel edge, helix angle of 27.2° and a point angle of 140° Sequence Ti to CFRP (1–20 holes)	CFRP in = 6.27–6.39; CFRP out = 6.13–6.388; Ti in = 6.21–6.375; Ti out = 6.26–6.368	CFRP = 8.5–22; Ti 9–27	CFRP = 0.3–2.1; Ti = 0.2–1.4	DF% = 1.06–1.28	Exit Ti = 95–220	
Ti-6Al4V/CFRP/AA7050 (each 10 mm thick)	Uncoated; 6.35 mm diameter (1–180 holes, 0.05 mm/rev)	Ti = 6.355; CFRP = 6.343; Al = 6.335	Ti = 155, CFRP = 137, Al = 95	T = 0.55, CFRP = 0.73, Al = 0.25	–	Entry Ti = 200; Exit Al = 300	[65]
	Uncoated; 6.35 mm diameter (1–180 holes, 0.08 mm/rev)	Ti = 6.362; CFRP = 6.357; Al = 6.354	Ti = 80, CFRP = 57, Al = 46	Ti = 0.66, CFRP = 0.59, Al = 0.28	–	Entry Ti = 220; Exit Al = 200	
	TiAlN/TiN coated; 6.35 mm diameter (0.05 mm/rev)	Ti = 6.347; CFRP = 6.338; Al = 6.344 (90th hole)	Ti = 93, CFRP = 78, Al = 49 (1–90 holes)	Ti = 0.59, CFRP = 0.64, Al = 0.26 (1–90 holes)	–	Entry Ti = 130; Exit Al = 130 (1–90 holes)	
	TiAlN/TiN coated; 6.35 mm diameter (0.08 mm/rev)	Ti = 6.347; CFRP = 6.342; Al = 6.336 (1–145 holes)	Ti = 73, CFRP = 55, Al = 41 (1–145 holes)	Ti = 0.61, CFRP = 0.65, Al = 0.23 (1–180 holes)	–	Entry Ti = 160; Exit Al = 160 (1–160 holes)	

Ti → CFRP order. The maximum delamination factor was 1.2 for CFRP → Ti and 1.3 for Ti → CFRP [9]. Because of the underlying Ti alloy's support, which reduces workpiece dynamics and laminate deflection, the exit CFRP delamination is effectively controlled, preventing it from getting worse as drill bit wear progresses [73, 74]. Meanwhile, the continual presence of high-temperature Ti alloy chips caused by the worn cutting edge close to the hole's edge causes thermal–mechanical erosion of the CFRP layers at the interface [73, 164, 165].

On the whole, delamination is a critical concern in the drilling of hybrid FRP/metal stack-up panels, as it represents a severe and often irreversible failure mode. The type of drill bit coating plays a significant role in mitigating delamination. Diamond-like carbon (DLC) coatings and TiAlN coatings have demonstrated their ability to reduce delamination, primarily due to their high hardness, which can spread and reduce thrust forces, thereby minimizing the delamination factor. Some studies report that uncoated drills perform better, and this discrepancy may be attributed to cutting-edge sharpness. The sequence in which drilling occurs, whether from CFRP to metal or vice versa, can also influence the extent of delamination.

4.2 Burr formation on metal panel

The occurrence of the burr defect in the Ti panel poses a significant challenge, particularly when compared to other forms of surface damage in metallic materials. This issue often necessitates additional steps such as disassembly, deburring, and re-assembly of the stacks, as pointed out by Xu et al. [9]. The deburring process alone can consume up to 40% of the total cutting time and contribute to roughly 30% of the overall assembly cost if burrs are formed at the exit of the drilled hole, as highlighted by Sui et al. [166]. Niknam et al. state that the ductility, hardness, and tensile yield strength of the material are the primary mechanical parameters that impact the burr's shape [167].

Hassan and Razali reported that drilling CFRP/Al stacks using a TiAlN-coated drill bit delivered superior drilling performance in comparison to an uncoated drill bit, particularly in terms of burr height, which was maintained below 80 μm, thus obviating the need for a deburring process [168]. This finding was corroborated by Kuo et al. when they drill Ti/CFRP/Al stack with a TiAlN/TiN-coated drill bit [65]. They additionally noted that the maximum entrance burr height produced by uncoated and TiAlN/TiN-coated drill bits was 0.2 and 0.15 mm, respectively, while the exit burr height was 0.3 mm for the uncoated drill bit and 0.15 mm for the TiAlN/TiN-coated drill bit at the end of the test. Hassan and Razali found that burr height increased for both uncoated and TiAlN-coated drills from the first to the sixtieth hole. However, burr height for uncoated drills surged from 128 to 327 μm after the 70th hole, while TiAlN-coated drills maintained a maximum burr height of under 100 μm until the 81st hole. The TiAlN coating reduced aluminum adhesion at the cutting edge, preventing build-up layers (BUL) or build-up edges (BUE) [168]. Xu et al. found that uncoated carbide drills produced higher drilling temperatures and larger burrs when machining CFRP/Ti stacks due to poor frictional contact and low thermal conductivity. This led to reduced rigidity in the exit titanium layers. In contrast, diamond-coated drills consistently generated lower burr heights in the titanium layers due to their high wear resistance, better heat dissipation, and lower mechanical loads, regardless of the process parameters [74].

Xu et al. also made note of the impact of friction coefficient and thermal conductivity in relation to the diamond

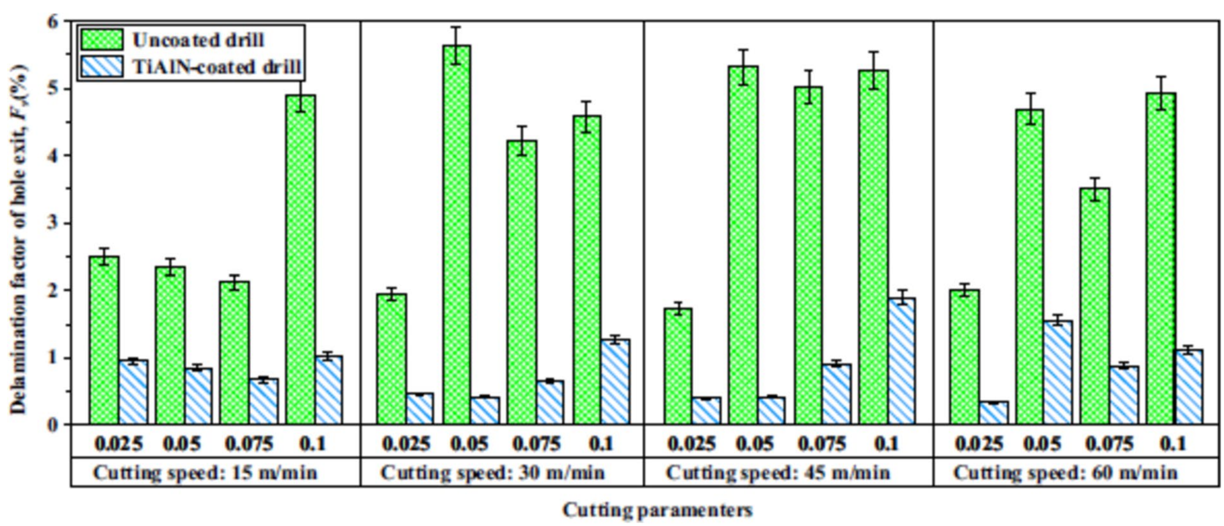

Fig. 13 Delamination factor results for holes exit [69]

and TiAlN coating when drilling CFRP/Ti stacks. According to Fig. 14, the burr height produced by TiAlN and diamond coated drill varies from 65 to 164 μm and 33–130 μm under dry condition. They found that the diamond coating, with its lower friction coefficient and higher thermal conductivity, played a role in reducing the temperature growth during drilling [75]. Furthermore, TiAlN-coated drills, with their poor thermal conductivity, accumulated heat at the drill bit–work interface, causing titanium expansion and burr formation [75]. Under MQL conditions, vegetable oil reduced drilling temperatures making titanium chips harder and more brittle, leading to lower burr heights (40–75 μm) and less sensitivity to feed rate changes. In contrast, diamond-coated drills produced higher burr heights (80–184 μm) under MQL due to titanium chip congestion, which increased local cutting temperatures and friction, exacerbating burr formation. [75]. Jebaratnam et al. mentioned that ta-C + Cr-coated tool produced a minimal burr height of 96.4 μm during drilling of CFRP/Al7075-T6 compared to uncoated and ta-C coated tools. The findings indicate that the ta-C + Cr-coated tool's lower coefficient of friction (COF) is what led to the tool's reduced burr height development [163]. Reduced COF causes the tool to rub against the workpiece surface less, which lowers temperature generation and reduces ductility at the hole edge, which in turn reduces the burr formation. The tool coated with ta-C has the highest coefficient of friction and generated the highest average burr height of 126.75 μm [163].

In their drilling experiments on a Ti/CFRP/Al stack, Shyha et al. measured entrance and exit burr heights. Their findings indicated that the CVD diamond-coated drill bit formed the best burr height results, followed by the uncoated drill bit, while the C7-coated drill bit produced the largest burr height among all [68]. They also noted that the entrance and exit burr heights of the top Ti panel did not show significant differences regardless of the drill bits used. This is because the burr height tends to be higher in more ductile materials [169]. Furthermore, the entrance burr height in Al panel was smaller than the exit burr height of that panel, regardless of the drill bits. This phenomenon was explained by the compaction of the CFRP layer above, which led to lower entrance burr heights, and the unsupported condition of the bottom Al panel, which resulted in higher exit burr heights [68]. Xu et al. mentioned in their study on CFRP/Ti6Al4V stacks that maximum temperatures were typically found at the exit side of the titanium panel, leading to more severe drilling-induced burrs at the exit side compared to the entry side [74].

Xu and Mansori explored the influence of cutting sequence on burr formation [9]. They observed that a TiAlN-coated drill typically resulted in higher burr widths (320 μm) compared to an uncoated drill (210 μm) when operating in the CFRP → Ti cutting sequence, especially under high-cutting-speed conditions. Additionally, they found that Ti → CFRP drilling produced fewer defects when high feed rates were applied. This difference was because of the supportive role of the bottom CFRP panel, which increased the stiffness of the exit Ti layer making it easier to shear the bottom surface layers and contributed to reducing the exit Ti burr defect. Xu et al. also agreed with it while drilling from Ti → CFRP which normally resulted in far lesser burr heights compared to the CFRP → Ti drilling order [74].

Considering all these things, burr formation is a significant challenge in the drilling of hybrid CFRP/metal stacks, often requiring additional post-processing steps and increasing both machining time and assembly costs. Burr height and formation are influenced by various factors, including material properties, drill bit coatings, cutting conditions, and

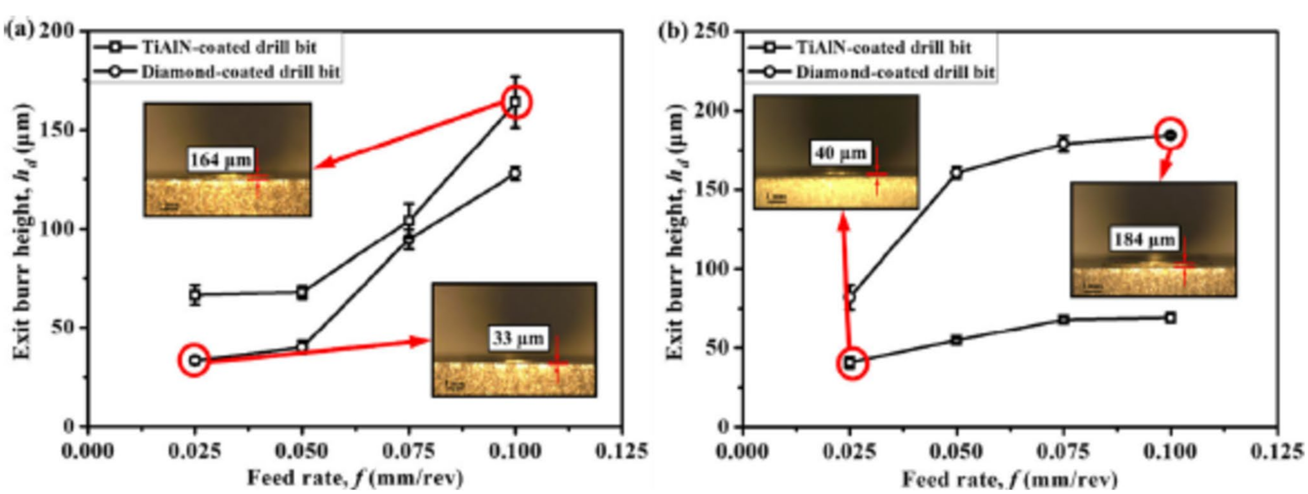

Fig. 14 The burr heights produced by the TiAlN-coated and diamond-coated drills at the fixed cutting speed of 30 m/min. (**a**) The dry cutting condition. (**b**) The MQL condition [75]

drilling sequences. Temperature distribution during drilling can contribute to burr formation, with maximum temperatures often observed at the exit side of the metallic phase, leading to more severe exit burrs. Material properties such as ductility, hardness, and tensile yield strength play a significant role in determining the shape and height of burrs. Coated drill bits, such as TiAlN and diamond-like carbon (DLC), have been shown to reduce burr height compared to uncoated drills. Coatings with higher hardness and better thermal conductivity can contribute to minimized burr formation. Drilling from metallic layer toward FRP produces better burr results due to the supportive role of the underlying FRP layer. The choice of cutting environment, such as minimum quantity lubrication (MQL), can affect burr height. The application of appropriate cooling and lubricating agents can reduce burr height by altering chip characteristics. High thermal conductivity and low friction coefficients, often associated with diamond coatings, can help reduce burr height.

4.3 Hole wall roughness

According to Batzer et al., the material being drilled, the machining conditions, and the type of drill used all have a major influence on the hole surface roughness [170]. Furthermore, the inhomogeneous properties of the composite part in comparison to the metal piece make it tough to minimize the hole surface roughness [171, 172].

According to Zitoune et al., the usage of nc-CrAlN/a-Si_3N_4 nano-coated drill bits resulted in an improved surface quality on Al and CFRP holes [70]. They obtained a roughness of 0.43–0.94 µm with an uncoated drill bit and 0.35–0.68 µm with a nc-CrAlN/a-Si_3N_4 nano-coated drill bit at a constant speed of 2750 rpm. This difference is mostly due to drill bit polishing, particularly prior to coating (PVD) for increased nanocrystalline layer bonding [70]. Montoya et al. observed that the roughness of hole walls in the initial 50 holes remained consistent for uncoated and diamond-coated drill bits as shown in Fig. 15. Uncoated drills showed increased hole roughness with more drilled holes, reaching 1.4 µm for aluminum and 6.5 µm for CFRP. Diamond-coated drills, however, maintained lower roughness, under 0.6 µm for aluminum and 2.8 µm for CFRP. This disparity is due to uncoated drills' wear and sharp edge deterioration, which initially resulted in smoother holes but became less effective over time, leading to higher roughness [64]. Kuo et al. corroborated this statement and added that flank wear does not directly impact the surface roughness of metal panels, whether they are aluminum (Al) or titanium (Ti) [65]. Additionally, Zitoune et al. obtained similar roughness values ranging from 1.6 to 4.6 µm when using nc-CrAlN/a-Si_3N_4 nano-coated drill bit, but observed higher roughness levels between 3.2 and 6.9 µm with uncoated drill bits when drilling CFRP panel of CFRP/Al stacks [70]. This discrepancy in roughness is attributed to the non-uniform composition and layer-by-layer stacking arrangement inherent to CFRP, which results in a larger standard deviation in hole surface roughness compared to Al7075-T6 panels [70]. This high deviation is also due to the presence of projecting fibers, fractures, and epoxy debris during drilling [173]. The deterioration of the CFRP hole surface may also be due to the scratches that occurred during the evacuation of chips produced while drilling Al7075-T6 panel [170, 174]. However, Shyha et al. have noted that the damage caused on CFRP hole surfaces by Al chips during drill bit feed/retraction can be mitigated by wet cutting [68]. Achieving minimal surface roughness in composites requires the dust generated during drilling to be fine, as this leads to improved surface roughness outcomes. Increased temperature in cutting zone also causes CFRP roughness. As the temperature increases during drilling, the bond between the fiber and matrix weakens, resulting in interfacial debonding of the fiber and resin. Consequently, the fiber is more easily separated from the matrix, leaving non-integrated fibers on the machined surface. This, in turn, contributes to an increase in hole surface roughness [67]. This scenario is not concentrated throughout the surface, but mostly at 135° between fiber alignment and the direction of drill bit movement. The occurrence of pitting phenomenon at the stacking sequence of 135° (−45°) is attributed to the negative cutting direction angle. In this context, instead of being cut, the uncut fibers are pulled out [64, 175]. This phenomenon can be elucidated by considering that fibers oriented in the −45° direction tend to experience significant elastic bending rather than shearing due to the pressure exerted by the drill cutting edge [176].

Shyha et al. when drilling Ti/CFRP/Al found that the hole surface roughness of the aluminum panel remained below 0.2 µm for 310 holes, unaffected by drill wear or coating loss when using C7 and CVD diamond-coated drills in wet conditions. In contrast, the titanium panel's roughness increased from 0.3 to 0.9 µm over the same number of holes, while the surface roughness of CFRP with uncoated drills rose to 5 µm from 0.5 µm [68]. Chip redeposition on titanium increased roughness due to material trapping and pressure-welding, whereas aluminum, being less prone to adhesion and positioned at the bottom of the stack, showed minimal chip adhesion. Surface roughness for CFRP remained at 3 µm for CVD diamond-coated, 9 µm for C7-coated, and 4.5 µm for uncoated drills for the first 200 holes. Furthermore, the surface quality deteriorated quickly under spray mist conditions [68]. In a study by Ghassemieh, it was mentioned that C7-coated drills achieved a surface roughness of less than 2 µm in CFRP and less than 0.4 µm in titanium panels for all 15 holes under dry conditions [12].

When working with CFRP/Al/CFRP stacks, Zhong et al. found that the surface roughness of holes machined

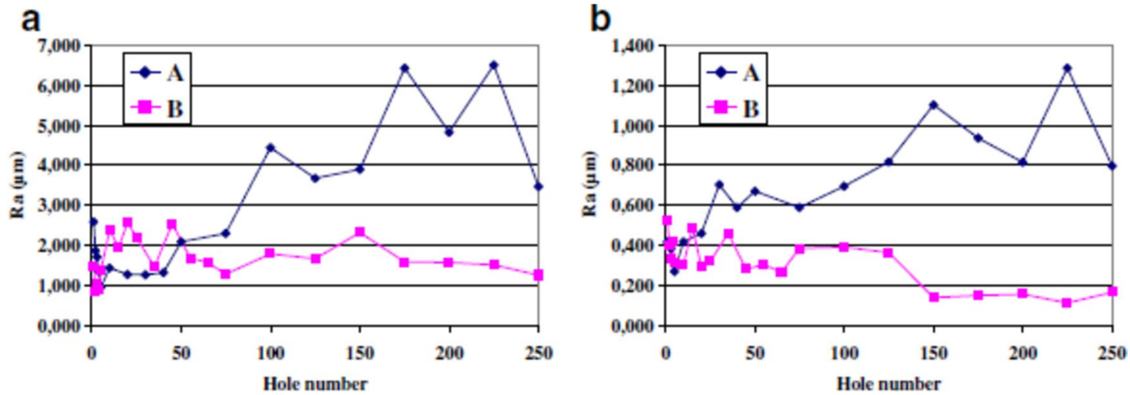

Fig. 15 Roughness Ra for the (**a**) CFRP part and (**b**) Al part using (**A**) uncoated and (**B**) diamond coated drill bits [64]

by TiAlN coated drills was superior to those drilled with uncoated drills [69]. This improvement is explained by the fact that, in comparison to uncoated drills, coated drills create less surface cavities on the CFRP hole walls. A similar finding was corroborated by Xu and Mansori when drilling CFRP/Ti6Al4V using TiAlN-coated drill bits [9]. The TiAlN coating exhibited a high level of hardness, resulting in reduced thrust forces and enhanced drill durability, ultimately contributing to a smoother hole surface finish [69]. Mathavan et al. mentioned that the average hole surface roughness of 100 holes drilled on CFRP panel while drilling CFRP/Al7075-T6 stack by uncoated, ta-C-coated, ta-C + Cr-coated, and ta-C + Ti-coated drills were 2.91, 2.4, 2.31, and 2.15 µm, respectively, which is below the industrial accepted limit of 3.2 µm [135]. The low roughness compared to uncoated tool is because of the lubrication effect of the coatings. Reduced heat production due to high lubrication leads to reduced fiber matrix debonding and reduced surface roughness in composite panels [135].

However, as indicated by Brinksmier and Janssen, the use of coated drill bits does not seem to have a discernible impact compared to uncoated drill bits on the damage inflicted on CFRP due to the erosion phenomenon caused by sharp chips interacting with the material [2]. Similarly, Kuo et al. reported that drilling Ti/CFRP/Al with a TiAlN/TiN-coated drill bit did not result in a discernible improvement in hole surface roughness in comparison to an uncoated WC drill bit [65]. In both cases, the surface roughness values for the Ti, CFRP, and Al layers fell within the respective ranges of 0.35–0.95 µm, 0.53–1.4 µm, and 0.11–0.5 µm for both types of drill bits. Moreover, the surface roughness of the holes made in the aluminum section did not appear to be affected by the application of coatings, such as TiAlN, TiAlN/AlN, and MoS_2, as demonstrated by Kalidas et al. [177]. Mathavan et al. also determined that the average hole surface roughness of holes drilled on aluminum alloy panels using ta-C-, ta-C + Cr-, and ta-C + Ti-coated drills was around 1.76 µm, while holes drilled using uncoated drills had an average of 1.43 µm [135]. It not only shows the ineffectiveness of coating on the hole surface roughness while drilling Al panel, but also, it produced a higher hole surface roughness value which is above the industrially accepted limit of 1.6 µm in Al panel.

The use of diamond-coated drills results in far better hole surface characteristics with less damage caused by drilling. This improvement is primarily attributable to the lower drilling forces and temperatures generated by diamond-coated drills, which effectively mitigate the mechanical and thermal impacts during stack drilling. As Fig. 16a illustrates, in the CFRP → Ti drilling order, very slight erosion damage is seen on the CFRP hole surfaces because of the diamond coating's improved performance, which lessens the negative impacts of titanium chip ejection [74]. The badly cut CFRP surfaces with cavities are mostly localized at the − 45° plies, as Fig. 16a indicates. Moreover, when drilling in the opposite order (Ti → CFRP) as shown in Fig. 16b, only small amounts of thermally induced damage are found on the composite hole surfaces. This phenomenon may be explained by the intrinsic qualities of the diamond coating, such as its high heat conductivity, low friction coefficient, and high hardness, which all work together to limit drill bit wear and lessen the mechanical and thermal consequences of the chip removal process [74]. Figure 16b further shows that the extremely heated drill edges that come into contact with the composite during drilling are the cause of the signs of pyrolysis, fuzzing, degradation, and matrix softening that are found within the drilled composite holes.

In general, coated drill bits, such as nc-CrAlN/a-Si_3N_4 nano-coated, ta-C-coated, or diamond-coated drills, yield superior surface quality compared to uncoated drills. Coatings contribute to reduced wear and better hole wall finish. Diamond-coated drills exhibit low friction coefficient, high hardness, and high thermal conductivity to improve the surface finish. The sequence in which the stack is drilled can impact surface roughness. Drilling from metallic to composite materials tends to cause more damage to the composite hole surfaces due to chip evacuation issues. Efficient evacuation of chips, especially in metallic-to-composite drilling sequences, plays a crucial role in minimizing surface damage. Inadequate chip removal can lead to abrasion and increased surface roughness. Elevated temperatures generated during drilling, particularly in composite materials, can lead to thermal degradation, microcracks, and matrix softening, contributing to increased roughness. It is worth noting that the application of cooling can have a significant impact on surface quality.

4.4 Hole diameter error

The main challenge encountered when drilling stack-up materials is the varying diameters between the materials [178]. Since various materials have varying moduli of elasticity, which can cause different kinds of elastic deformation, it is challenging to maintain consistent diameters between the stacked materials [179]. Misalignment between hole and drill bit sizes can necessitate costly repairs and affect assembly quality, with oversized holes risking looseness and undersized holes causing component failure due to concentrated pressures [180].

When drilling CFRP/AA7075/CFRP stack, D'Orazio et al. mentioned that, though both DLC- and TiAlN-coated drills showed increasing variation in diameter between entry and exit holes, TiAlN-coated drills had the trend with more pronounced difference as shown in Fig. 17 [63]. They further mentioned that the hole diameter decreased through the layers, with the exit diameter being significantly smaller than the entry diameter and the size of AA7075 hole diameter was between the CFRP layers. Aluminum chips' rotation causes greater entry diameter due to abrasion, while improved drill guiding reduces exit diameter [63]. Drilling temperature which is lower in the bottom CFRP layer due to better heat transfer and different elastic moduli of AA7075 (70.6 GPa) and CFRP (53 GPa) also contributed to the diameter discrepancy [63]. A similar incident of decrease in hole diameter with depth was reported by Kuo et al. while drilling Ti6Al4V/CFRP/AA7050 stack panel with uncoated

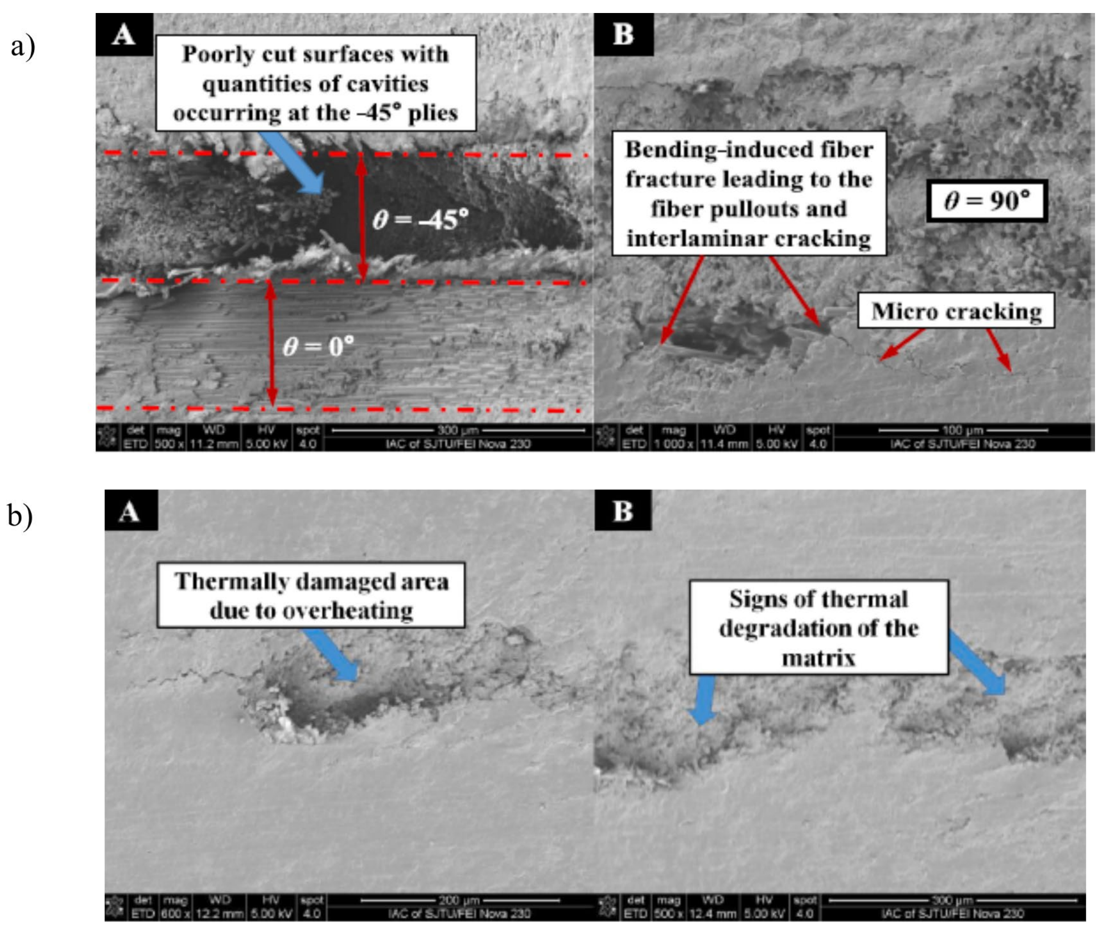

Fig. 16 SEM morphologies of the drilled composite hole walls when using the diamond-coated drill under the (**a**) CFRP→Ti sequence ($Vc=65$ m/min and $f=0.06$ mm/rev) and (**b**) Ti→CFRP sequence ($Vc=65$ m/min and $f=0.06$ mm/rev) [74]

and TiAlN/TiN-coated WC twist drills [65]. Contradictorily, Shyha et al. discovered that while drilling a Ti/CFRP/Al stack using diamond- and C7-coated drill bits under wet conditions, the diameter of the entry Ti panel and exit Al panel are bigger than that of the mid CFRP layer [68]. This situation might be caused by the fact that fibers tend to shrink when exposed to moist conditions. Conflictingly, Pardo et al. discovered that when cutting a CFRP/Al stack panel with AlTiCrN-coated drill bit, the interface diameters of the aluminum and CFRP holes were consistently bigger than the entry CFRP and exit Al holes [77]. Additionally, it was discovered that the interface diameters of the holes made in aluminum were consistently marginally larger than those made in CFRP. There are two potential causes for this. First off, the two materials' distinct elastic moduli result in varying degrees of elastic recovery [2, 68, 181]. Second, when the tool contacts with the lower Al layer, there's a chance of tool skidding, which causes the aluminum to have a little bigger entry diameter and the CFRP to have a somewhat larger exit diameter [77]. Conflictingly, Xu et al. pointed out that while using both TiAlN- and diamond-coated drill bits, the exit diameters of the CFRP panel are significantly bigger than those recorded in the entrance and middle areas [75]. Under the MQL condition, the disparity between the entrance and exit CFRP hole diameters is diminished and both diameters approach the nominal hole [75].

According to Pardo et al. and Perez et al., the sizes of the holes drilled in Al7075-T6 are usually greater than those drilled in CFRP because of the thermal expansion that occurs during the drilling process, irrespective of whether coated or uncoated drill bits are used [77, 182]. It is because, when drilling the Al7075-T6 panel, aluminum chips have a propensity to jam at the flute, increasing drilling temperature. As a result, the large diameter in aluminum panel is more likely to occur in a dry environment [77, 183]. Dry cutting of Ti6Al4V panel also encourages oversized hole diameters than the nominal one because of the titanium alloy's thermal expansion. The MQL condition creates holes with diameters, which are smaller than the nominal diameter. It is because, when drilling composite plates under cooling, the fibers have a tendency to contract, resulting in a smaller hole in the composite plate than the corresponding hole in the metal section [75]. However, there are some instances where the diameter of the hole in CFRP is bigger than that in Al7075-T6 either with coated or uncoated drill bits [64, 67, 184]. Zitoune et al. speculate that this may be because of more drill bit stability while drilling through the bottom Al layer [70]. Additionally, it was noticed by Montoya et al. that continuous chip production during the drilling of metal can lead to the chip twisting along the drill body and obstruct the chip evacuation [64]. This causes hot, sharp chips to form in the hole that cannot be removed smoothly, increasing the size of the CFRP holes and lowering the quality of the surface of the CFRP holes [152, 185].

According to Montoya et al., the relationship between the number of holes and the dimension of the holes is mostly steady while drilling CFRP/Al stacks with a drill bit of 6-mm diameter [64]. This stability is observed in the range of 5.965 to 5.98 mm for uncoated and diamond-coated drill bits, as well as in the range of 5.96 to 5.995 mm for TiAlCrN-coated drill bits and 5.955 to 5.98 mm for AlTiSiN-G-coated drill bits. Tashiro et al. noted that when drilling CFRP/Ti panels using TiAlN and TiAlCr/TiSi-coated drills, the hole size remained stable in the Ti panel but increased in the CFRP panel as the number of holes increased [76]. In contrast, Shyha et al. discovered that, regardless of whether

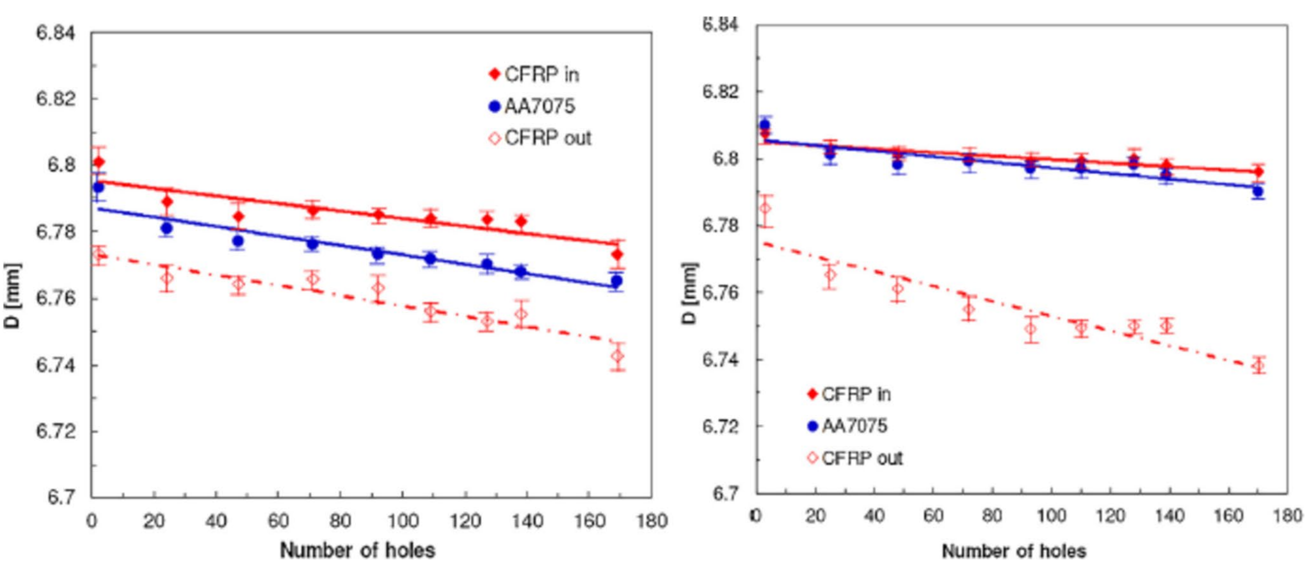

Fig. 17 Evolution of hole diameter with number of holes using (**a**) DLC-coated drill and (**b**) TiAlN-coated drill [63]

coated or uncoated drill bit is used, the hole diameter decreased with an increase in the number of holes when performing wet cutting of Ti/CFRP/Al stacks [68]. This pattern is attributed to the material loss caused by drill bit wear evolution as the number of holes increases. They also stated that the first hole made by uncoated drill bit was less than the nominal diameter, whereas the first hole made by diamond- and C7-coated drill was larger than the nominal diameter. According to D'Orazio et al., the DLC-coated drill bit created undersized holes in both CFRP and AA7075 panels, but TiAlN-coated drill bit initially created large holes, which eventually reduced to generate undersized holes after midway in both CFRP and AA7075 panels due to drill bit wear [63]. Conversely, Wang et al. observed that the holes created by the diamond-coated cemented carbide drill bit in both CFRP and Al7075-T651 were large throughout the trial [67]. Similarly, Tashiro et al. discovered that holes drilled with both TiAlCr/TiSi- and TiAlN-coated drills are large in both CFRP and Ti panels [76]. They added that, in CFRP panels, the deviation with TiAlN-coated drill is greater than that with TiAlCr/TiSi-coated drill, but in Ti panels, the deviation with TiAlN-coated drill is slightly lower than that with TiAlCr/TiSi-coated drill. Additionally, the holes drilled in Ti panels by both drills are smaller than those drilled in CFRP panels [76]. Xu and Mansori found that hole sizes in both CFRP and Ti panels were oversized (nominal diameter = 6.35 mm) in CFRP/Ti drilling, regardless of whether uncoated or TiAlN coated drill bit is used [9]. The TiAlN-coated drill bit performed better, with a CFRP diameter variation of only 0.05 mm compared to 0.15 mm with the uncoated drill bit. This is attributed to the TiAlN coating's ability to maintain sharp cutting edges and resist wear. While diameter variation in Ti panel holes were consistent for both drill bits, the uncoated drill bit produced larger CFRP holes, whereas the TiAlN-coated drill bit produced varying hole sizes in the CFRP panel [9]. Pardo et al. also discovered that while drilling CFRP/Al using TiAlCrN-coated drill bit, all of the holes created were substantially larger than the nominal diameter of the tool used (15 mm) [77]. Mathavan et al. reported that the average stack-up diameter error for holes drilled with ta-C + Ti, ta-C + Cr, ta-C, and uncoated tools are 20.58, 16.21, 17.24, and 13.28 μm, respectively. The increased error in coated tools is due to the added diameter from the coating and, specifically for ta-C + Ti, the high chemical affinity and adhesive tendency of titanium, which causes chip accumulation at the cutting edges. This issue is exacerbated as the Ti dopant is exposed due to wear, increasing the diameter error [135].

When considering the drilling progression, D'Orazio et al. measured the diameter difference in dry conditions after drilling the 170th hole, which approached a value of roughly 32 μm with the DLC-coated drill bit and around 58 μm with the TiAlN-coated drill bit when drilling CFRP/Al7075/CFRP stack panels [63]. Montoya et al. showed that uncoated and diamond-coated drill bits produced 9-μm tolerance holes even at the 250th hole, but TiAlCrN- and AlTiSiN-G-coated drill bits produced 18 μm tolerance range at the 75th hole when drilling CFRP/Al7010 stack panels [64]. Shyha et al. mentioned that diamond-coated drill generated the smallest diameter difference from start to finish, followed by C7-coated and uncoated drill bits that caused the greatest diameter difference while cutting Ti/CFRP/Al stack panels [68]. Kuo et al. found that TiAlN/TiN-coated drill bits produced more accurate hole diameters with a maximum variation of 0.02 mm from the nominal size when drilling Ti/CFRP/Al stacks, compared to uncoated drill bits (all up to 180 holes). This was due to a 33% reduction in wear at the coated drill bits' outer edges. They noted that coating did not affect hole diameter variation at low feed rates but did reduce variations at high feed rates. The primary factor influencing hole diameter in both CFRP and Ti layers was the drill bit coating, with PCRs of 64.5 and 57.5%, respectively [65]. D'Orazio et al. used a third-degree polynomial regression model to determine an inverse relationship between hole diameter and drill bit wear [63].

On the whole, the type of drill bit coating used has a significant impact on hole diameter control. Diamond-coated and various TiAlN-coated drill bits tend to produce more consistent hole diameters compared to uncoated drill bits. Coatings contribute to maintaining sharp cutting edges and reducing wear, which in turn improves diameter accuracy. Drill bit wear over the course of multiple holes can impact hole diameter accuracy. As drill bits wear down, hole diameters may deviate from the nominal size. Variations in drilling temperatures can influence hole diameters, with some materials expanding or contracting due to heat generated during the drilling process. Thermal effects can cause complex diameter changes, especially in composite materials.

4.5 Hole integrity errors

Hole circularity is the property of a surface where all of its points are intersected by planes perpendicular to axes that are equally spaced from those axes [186]. Circularity can be determined using the geometric tolerance that indicates how close a piece of a cylindrical part is to a true circle [187]. It is an important parameter for controlling the maximum allowed circularity error of the circular part. Although the number of researchers who study about circularity error when drilling stack-up panel is very limited and it has not received as much attention as surface integrity, the performance of machined items is greatly affected by the circularity of the drilled holes [188].

Kuo et al., when considering hole cylindricity, discovered that uncoated drills caused a maximum cylindricity error of 150 μm, whereas TiAlN/TiN-coated drill bits caused a maximum cylindricity error of 100 µm when drilling Ti/CFRP/Al stack [65]. Shyha et al. discovered that the CVD diamond-coated drill made better circularity at the end of the cutting process (156th hole) than the uncoated drill bit, whereas the C7-coated drill generated better circularity at the beginning of the cutting procedure [68]. Kuo et al. showed decreasing hole circularity with stack depth for Ti/CFRP/Al panel, with average circularity errors in Ti, CFRP, and Al layers ranging from 53 to 121 µm, 33 to 109 µm, and 25 to 78 µm, respectively [65]. They found that drill bit coating significantly impacted the Ti layer's hole diameter at 5% PCR level in ANOVA, but no factors significantly affected the out-of-roundness in the CFRP and Al layers. The trilobed hole shapes in the Ti layer were likely caused by drill's helical wander due to longer chisel edges or defects in drill geometry. According to Shyha et al., hole circularity variations in Ti, CFRP, and Al layers were up to 78, 39, and 53 µm, respectively, when drilling Ti/CFRP/Al under wet conditions [68]. They discovered that as the testing advanced, the circularity and cylindricity improved. According to Mathavan et al., the average circularity error values were attained when cutting CFRP/Al7075-T6 with uncoated, ta-C-coated, ta-C + Cr-coated, and ta-C + Ti-coated drill bits were 14.82, 16.16, 15.36, and 16.1 µm, respectively, on aluminum alloy panel and 15.16, 15.48, 15.1, and 13.96 µm, respectively, on CFRP panel [135]. The circularity was well within the statistical limits and was not affected much by the coating application in their case. According to Xu and Mansori, the circularity error produced by TiAlN-coated drill bit (6–14 µm) in Ti panel was greater than that produced by uncoated drill bit (4–8 µm) when drilling CFRP/Ti panel in CFRP → Ti sequence [9]. The circularity error generated during Ti → CFRP drilling with TiAlN coated drill bit was even greater (9–28 µm). Also, the circularity error in CFRP panel was greater than that in Ti panel irrespective of the drill bit used [9]. Xu et al. found that average cylindricity errors for holes in CFRP and titanium were higher with TiAlN-coated drills than with diamond-coated drills. Furthermore, MQL cooling reduced cylindricity errors in CFRP by 16.11% for TiAlN and 15.08% for diamond coatings. However, during titanium drilling, MQL increased cylindricity errors by 28.03% for TiAlN and 106.54% for diamond-coated drills, likely due to cooling shrinkage from MQL application [75]. Table 4 shows the summary of the work done so far by several researchers in terms of analyzed outputs under various coating conditions. This table can be used to compare the results on hole quality based on the application of different coatings based on various machining parameters.

Considering all these things, the type of drill bit coating has a notable impact on hole circularity. Coated drill bits, such as TiAlN/TiN or diamond-coated drills, tend to produce better circularity compared to uncoated ones. Circularity errors can vary between different materials within the stack-up panel and the choice of drilling sequence can also influence the results. In some cases, circularity errors may vary with the depth of the stack, indicating the need for careful consideration when drilling deep stacks. Some studies have shown that circularity and cylindricity tend to improve as the drilling process progresses. This suggests that initial deviations may be reduced through the course of drilling, possibly due to tool stabilization.

5 Conclusion

The use of hybrid composite/metal stack panels in aircraft manufacturing addresses limitations of traditional materials, with coated drill bits offering essential solutions for effective drilling. Coatings reduce friction, lower temperatures, and enhance hole quality, supporting manufacturing efficiency and reliability. Ti-based (e.g., TiN, TiAlN) and diamond coatings improve drill bit durability by increasing wear resistance and heat tolerance. Diamond coatings, notably CVD diamond, are optimal for hard materials like CFRPs, while DLC coatings with Ti or Cr layers add wear resistance and low friction.

When drilling CFRP/Ti or CFRP/Al stacks, varying wear mechanisms emerge: CFRP phases cause abrasion and chipping, while metal phases lead to adhesion, diffusion, and fracture due to metal properties. Coatings like DLC and nanocomposite TiAlN help mitigate these issues, though their effectiveness depends on drilling conditions. Diamond coatings manage heat efficiently but may face failure at high temperatures. Proper coating selection and process optimization are critical for extending drill bit life, ensuring hole quality, and reducing costs in CFRP/metal stack drilling operations. Thrust force in drilling is influenced by factors like drill geometry, material, coating, and cutting parameters. In composite/metal stacks, such as Ti6Al4V and CFRP, thrust force is higher in titanium due to elastoplastic chip formation, while CFRP chips break through brittle fracture. Coated drill bits—like diamond, TiAlN, and DLC—generally reduce thrust forces by enhancing hardness and reducing friction, though increased cutting-edge radius from coatings can occasionally raise forces. Proper coating selection and wear management are essential for minimizing thrust force in composite/metal stacks. Coatings like PVD TiAlN and AlTiN have minor impacts on torque, which is more affected by feed rate and speed. Coated drills can reduce torque, particularly in titanium, though it rises with wear and chip buildup. Minimum quantity lubrication (MQL) can stabilize torque, with diamond-coated drills performing well due to low friction. Temperature management is

Table 4 Detail of outputs examined in the past using coated tools for stack material drilling

Workpiece	Drill bit	Coating	Parameters	Analyzed outputs	Author
Ti-6Al–4 V/CFRP/AA7050	WC twist drills	PVD-coated TiAlN/TiN, uncoated	0.05 and 0.08 mm/rev	1. Drill bit life 2. Hole diameter accuracy	[65]
Ti-6Al-4 V/CFRP/AA-7050	WC twist drills	DLC and CVD coated diamond	0.08 and 0.15 mm/rev	1. Diameter of holes 2. Surface roughness 3. Burr height 4. Drill bit wear	[78]
Ti-6Al–4 V/CFRP/AA7050	WC drills	CVD diamond coated, C7 coated, uncoated	Feed (mm/rev)—0.05, 0.1, and 0.15 Speed—rev/min (1000/2000) (2000/4000) (3000/6000)	1. Drill bit life 2. Thrust force	[66]
CFRP/Al 7010 stack	Standard twist drill	Diamond, TiAlCrN, AlTiSiN-G coated and uncoated	Speed—55 m/min (3000 rev/min) Feed—0.04 mm/rev Feed rate—120 mm/min MQL—16 mm/min	1. Flank wear 2. Thrust forces 3. Drill bit failure 4. Hole diameter 5. Hole surface roughness	[64]
CFRP/Al 2024	Micrograin carbide	PVD coated nc-CrAlN/a-Si_3N_4 (Tripple Alwin)	Spindle speed (rev/min) 1050, 2020, 2750 Feed—0.05, 0.1, 0.15 mm/rev	1. Surface roughness 2. Thrust force	[70]
CFRP/Al 2024/CFRP	Standard twist drill	Uncoated and TiAlN coated	Speed 15, 30, 45, 60 m/min Spindle speed 752, 1504, 2256, 3009 rev/min Feed—0.025, 0.05, 0.075, 0.01 mm/rev	1. Hardness of the coating 2. Adhesion of Al 3. Delamination factors 4. Thrust forces 5. Surface cavities	[69]
CFRP/Al7075/CFRP	Standard twist drill	TiAlN, DLC coated	Different cutting speed and feed for both coatings	1. Drill bit wear 2. The delamination factor	[63]
T800/X850 CFRP and 7075-T651 Al	Drill with double point angle	Diamond coated	Spindle speed—1000, 2000, 3000 rev/min Feed rate—0.02, 0.04, 0.06, 0.08 mm/rev	1. Thrust forces 2. Drilling temperature 3. Diameter of the hole 4. Hole surface roughness	[67]
CFRP/Al7075-T6	Twist drill	Uncoated, ta-C, ta-C + Ti, ta-C + Cr coated	Spindle speed—2600 rev/min Feed rate—0.05 mm/rev	1. Delamination 2. Burr height	[163]
CFRP/Al7075-T6	Twist drill	Uncoated, ta-C, ta-C + Ti, ta-C + Cr coated	Spindle speed—2600 rev/min Feed rate—0.05 mm/rev	1. Hole diameter error 2. Hole surface roughness 3. Circularity error	[135]
CFRP/Al7075-T6	Twist drill	Uncoated and ta-C coated	Spindle speed (rev/min) = 2600 Feed rate (mm/rev) = 0.05	1. Hole diameter error 2. Hole surface roughness 3. Circularity error	[189]

critical, especially for CFRP, where excessive heat can degrade resin and cause fiber debonding. Diamond-coated drills help control temperatures by reducing friction and enhancing heat dissipation, improving overall performance and quality in drilling CFRP/metal stack assemblies.

Delamination in CFRP/Ti stack drilling is a critical failure mode that impacts component quality, fatigue life, and performance, often leading to high rejection rates. It occurs at both entrance and exit holes due to bending strains and chip evacuation. Drill bit coatings affect delamination, with DLC-coated drills typically showing lower delamination factors

Table 5 Comparison of coatings under different experimental parameters

Flank wear	Thrust force	Torque	DF %	Hole diameter variation	Roughness	Entrance Bur	Exit bur	Roundness	Temperature	
TiAlN > DLC	TiAlN > DLC (in CFRP and Al)		TiAlN > DLC	TiAlN > DLC (CFRP in, out and Al)						[63]
Diamond < uncoated = AlTiSiN-G < TiAlCrN	Diamond < uncoated < TiAlCrN < AlTiSiN-G (in CFRP and Al)			Diamond < uncoated < TiAlCrN < AlTiSiN-G	Diamond < uncoated (in CFRP and Al)					[64]
Uncoated < TiAlN/TiN	Uncoated < TiAlN/TiN (in Ti, CFRP, and Al)	Uncoated > TiAlN/TiN (in Ti, CFRP, and Al)		Uncoated > TiAlN/TiN (in Ti, CFRP, and Al)	Varying patterns depend on feed rate	Uncoated > TiAlN/TiN (in Ti)	Uncoated > TiAlN/TiN (in Al)	Uncoated > TiAlN/TiN (in Ti, CFRP, and Al)		[65]
Diamond > uncoated (low speed low feed, flood cool) Diamond < uncoated (medium, high speed, and feed flood cool) C7 > uncoated (low speed, high feed spray mist)	Diamond > uncoated (CFRP and Ti) Diamond < uncoated (Al)			Diamond < uncoated (Al, CFRP, Ti)	Diamond < uncoated (CFRP, Ti)	Diamond > uncoated (Ti 1st hole, Al last hole) Diamond < uncoated (Al 1st hole, Ti last hole)	Diamond > uncoated (Ti) Diamond < uncoated (Al)	Diamond < uncoated (Al, CFRP, Ti)		[66] [68]
	Uncoated > TiAlN		Uncoated > TiAlN							[68]
	Uncoated > Tripple Alwin (CFRP and Al)				Uncoated > Tripple Alwin (CFRP and Al)					[70]
	TiAlN > uncoated	Uncoated > TiAlN	TiAlN > uncoated	TiAlN > uncoated (Ti) TiAlN < uncoated (CFRP)			TiAlN > uncoated	TiAlN < uncoated (Ti, CFRP)		[9]
AlTiN > nano > uncoated	Varying with hole number									[71]
	TiAlN > diamond (CFRP) Ti varying based on feed	TiAlN < diamond (CFRP, Ti)	TiAlN < diamond							[41]
	Uncoated > diamond (CFRP, Ti)						Uncoated > diamond (Ti)		Uncoated > diamond (Ti)	[74]
		Diamond < TiAlN (dry CFRP) TiAlN < diamond (MQL CFRRP) Diamond < TiAlN (dry Ti) TiAlN < diamond (MQL Ti)		TiAlN < diamond (dry, low speed) TiAlN > diamond (dry, high speed)			TiAlN > diamond (dry) TiAlN < diamond (MQL)	TiAlN > diamond		[75]
TiAlN < TiAlCr/TiSi	TiAlN > TiAlCr/TiSi (Ti) TiAlN < TiAlCr/TiSi (CFRP)	TiAlN < TiAlCr/TiSi (Ti) TiAlN > TiAlCr/TiSi (CFRP)		TiAlN > TiAlCr/TiSi (CFRP) TiAlN < TiAlCr/TiSi (Ti)						[76]
	DLC > diamond	DLC > diamond		DLC > diamond		DLC < diamond	DLC > diamond	DLC > diamond		[78]
			Ta-C < ta-C + Ti < uncoated < ta-C + Cr	Uncoated < ta-C + Cr < ta-C < ta-C + Ti	Uncoated < ta-C < ta-C + Cr < ta-C + Ti (Al) Ta-C + Ti < ta-C + Cr < ta-C < uncoated (CFRP)		Ta-C + Cr < uncoated < ta-C + Ti < ta-C			[163] [135]

Table 6 Summary of positive and negative outcomes of each coating used in CFRP/metal stack up drilling

	Positive effects	Negative effects
DLC	• Exhibit less flank wear compared to TiAlN-coated drills • Results in minimal aluminum adhesion wear on the rake face, providing a good surface finish • Smooth surface after coating leads to superior hole quality compared to other coatings • Shows a lesser increase in thrust force in both metal and composite panel over time compared to TiAlN-coated drills • Generate the lowest torque in CFRP, followed by aluminum and titanium panels • Torque levels show minor increases after initial drilling but stabilize, indicating consistent performance with wear • Produce lower initial DF values compared to other coatings, likely due to their high hardness and resistance to wear, leading to reduced thrust forces • Contribute to improved drill bit guiding, leading to increased hole accuracy and reduced diameter variation • Help in maintaining sharp cutting edges for a longer duration • Show less thermal expansion, leading to smaller entry and exit hole diameter variations	• Suffer from abrasion, edge rounding, and localized chipping at the cutting edge due to high mechanical stresses • Coating failure occurs after drilling a certain number of holes due to high cutting temperatures and mechanical stress • May generate higher initial thrust forces compared to uncoated drills, especially in titanium and CFRP panels • May experience premature chipping and adherence of workpiece material • Initial torque in titanium panels may be slightly higher compared to uncoated drills • May result in a higher DF in MQL conditions compared to TiAlN coatings • With continuous drilling, the entrance hole diameter in CFRP layers tends to reduce more noticeably compared to other coatings
TiAlN	• Demonstrate higher wear resistance and reduced chip adherence compared to TiSiN • Encourage flank wear width but reduce adhesive wear by transferring heat to the chips • Reduce friction between the machined surface and the drill body, leading to lower thrust forces compared to uncoated drills • Produce lower torque magnitudes in Ti panels compared to uncoated drills, enhancing wear resistance • Under MQL conditions, show lower torque for all cutting parameters compared to dry conditions, indicating effective lubrication and reduced friction • Tend to produce lower and consistent exit delamination compared to uncoated drills due to increased hardness • Maintain burr height below 80 μm in dry condition and 40–75 μm in MQL condition, eliminating the need for deburring processes • Result in less surface cavities on CFRP hole walls, leading to improved surface roughness • Provide good thermal stability, maintaining sharp cutting edges and reducing the impact of heat during drilling, thus contributing to more accurate hole diameters • Offer excellent wear resistance, maintaining hole diameter accuracy better than uncoated drills	• Show adhesion of aluminum particles on the rake face, leading to wear and coating fracture • Exhibit higher flank wear compared to DLC-coated drills, leading to increased wear rates • Exhibit an increase in thrust force over time, compared to DLC and diamond coated drills • Over time, torque in CFRP and aluminum sections increases compared to uncoated drills due to wear • As the cutting edge wears, the shearing plastic temperature of titanium rises, increasing the risk of exceeding the glass transition temperature (T_g) of the resin and degrading drilling quality over time • May have a higher initial DF compared to DLC-coated drills due to slightly less hardness and wear resistance • Initially create holes that are larger than the nominal diameter, which then reduces to smaller diameters as the drill wears down • Exhibit greater deviation in the diameters between the entrance and exit holes in CFRP layers compared to DLC-coated drills
TiAlCrN	• Outperforms TiAlN and TiSiN due to higher wear resistance and coating strength • Demonstrates lower adhesion wear, providing a longer lifespan for the drill bit • Can provide a moderate reduction in thrust force compared to uncoated drills, especially in aluminum panels • Show improved diameter accuracy with reduced variations, especially at high feed rates • These coatings maintain hole size stability over a larger number of drilled holes compared to uncoated drills	• Experiences coating failure on the cutting edge, followed by adhesion wear • Shows similar flank wear to uncoated drills • Can exhibit an increase in thrust force over time compared to DLC-coated drills • Compared to other coatings like diamond, TiAlN, and TiAlCrN, it is less effective in reducing initial thrust forces, particularly in titanium panels • Produce holes with slightly larger diameter variations compared to diamond-coated drills which may later reduce in size due to wear

Table 6 (continued)

	Positive effects	Negative effects
AlTiSiN-G	• Provides some reduction in wear compared to uncoated drills but less effective than diamond coatings • Provide some reduction in thrust force compared to uncoated drills, especially in aluminum panels	• Shows adhesion wear with aluminum particles causing coating failure • Shows similar flank wear to uncoated drills • Exhibit higher initial thrust forces compared to uncoated drills • Similar to TiAlN, AlTiSiN-G-coated drills, it may not manage thrust force increases as effectively as DLC or diamond-coated drills do
Diamond	• High thermal conductivity minimizes titanium fusion on edges, reducing wear • Exhibit lower flank wear compared to uncoated drills, effectively reducing overall wear rates • Significantly reduce thrust forces in both CFRP and aluminum • Produce significantly lower torque under dry and MQL conditions in CFRP panels due to low friction coefficient and robustness against lubrication • Generate comparatively lower cutting temperatures than uncoated drills, enhancing drilling quality by reducing thermal damage and resin deterioration • Lower friction coefficient, high hardness, and higher thermal conductivity reduce temperature growth during drilling, resulting in lower burr heights (33–130 µm) under dry conditions • Produce more consistent hole diameters, even after multiple holes, compared to uncoated and some other coated drill bits especially in high-temperature applications, contributing to prolonged tool life due to reduced wear	• High cutting temperatures can cause oxidation and graphitization of the diamond, leading to coating failure after drilling a certain number of holes • Generate higher initial thrust forces due to the increased cutting-edge radius by the coating thickness • Experience higher thrust forces due to increased humidity under MQL, affecting the tribological properties of the diamond coating • Generate higher torque in titanium panels due to severe chip congestion at certain cutting speeds under MQL conditions • The coating may wear over time, potentially leading to increased temperatures and reduced performance in long-term use • Can be expensive compared to other coatings
AlTiN	• Show slightly lower torque in Ti panels compared to uncoated drills due to enhanced wear resistance • There is no appreciable variation in torque throughout the testing	• May not be as effective in reducing torque in CFRP panels compared to other coatings like TiAlN
TiAlCr/TiSi	• Produce less torque in titanium panels compared to TiAlN-coated drills under dry and mist-cooled environments • Produce lower torque in CFRP panels compared to titanium alloy parts • Enhance wear resistance, maintaining hole diameter consistency, especially in metal layers	• Torque nearly doubles in size with wear, indicating significant friction increase with prolonged use • The hole size remained stable in the Ti panel but increased in the CFRP panel as the number of holes increased
Uncoated	• Serve as a baseline for comparing the performance of coated drills, highlighting the benefits of coatings in reducing temperature and improving drilling quality • Some studies suggest that uncoated drills can produce a slightly better delamination quality compared to TiAlN-coated drills in specific conditions	• Produce higher drilling temperatures in Ti panels compared to coated drills, leading to thermal damage and resin deterioration in CFRP panels • Less efficient heat conduction and higher friction at the tool–work interface, exacerbating thermal issues • Tend to produce significantly higher exit delamination compared to coated drill bits as the number of drilled holes increases, often exceeding acceptable industrial limits • Produce larger burrs and higher drilling temperatures, leading to greater burr formation and surface roughness • Exhibit rapid wear, resulting in increased roughness and reduced performance over time
ta-C	• Show high hardness and strong bond strength with the tool • Can drill a high number of holes with lower delamination below industrial tolerance levels and better drilling quality over a greater number of holes	
ta-C + Cr	• Produce minimal burr height due to the lower coefficient of friction, resulting in less temperature generation, better diameter accuracy, and reduced ductility at the hole edge	• Has lower bond strength and hardness compared to ta-C coated tool shows faster wear, with increasing delamination limiting its effectiveness

Table 6 (continued)

	Positive effects	Negative effects
nc-CrAlN/a-Si_3N_4	• Yield lower roughness values in Al and CFRP holes compared to uncoated drill bits, due to better nanocrystalline layer bonding, contribute to better surface quality	
AlTiCrN	• Produce consistent interface diameters for aluminum and CFRP holes generally • Perform well in dry drilling conditions, maintaining more stable hole diameters compared to uncoated drills	• While better than uncoated drills, they may not perform as well as diamond or TiAlN-coated drills in terms of wear resistance over a large number of holes

(DF) than TiAlN due to DLC's high hardness, which reduces thrust forces. Drilling from CFRP to metal minimizes exit delamination by providing support from the metal layer. Burr formation in titanium panels also presents significant challenges, increasing cutting time by up to 40% and assembly costs by 30%. Coated drills like TiAlN and diamond reduce burr height compared to uncoated drills, with TiAlN-coated drills showing reduced aluminum adhesion and diamond-coated drills benefiting from high thermal conductivity. Minimum quantity lubrication (MQL) further aids TiAlN drills in reducing burrs, though diamond-coated drills may see increased burrs due to chip congestion. Drilling from metal to CFRP generally minimizes burr formation. Thus, coating selection, drilling sequence, and lubrication are key to optimizing drill performance and reducing defects in CFRP/metal stacks. The surface roughness of holes in composite/metal stacks is heavily influenced by material properties, machining conditions, and drill bit type. Coated drills, like nc-CrAlN/a-Si_3N_4 nano and diamond coatings, generally produce smoother surfaces than uncoated drills by reducing wear and enhancing finish. Diamond-coated drills, with their low friction, high hardness, and thermal conductivity, provide smoother surfaces and less thermal damage, especially in CFRP and aluminum. Roughness tends to increase with drill wear, and uncoated drills typically show higher roughness over time. Drilling from metal to composite also raises surface roughness due to chip evacuation challenges. Cooling methods, such as spray mist, help manage temperature and reduce roughness. In stack-up drilling, coated drills generally maintain better hole diameter control and circularity than uncoated bits, thanks to wear resistance and reduced thermal impact. However, drill wear, temperature variations, and material expansion affect diameter accuracy. Circularity can improve over time as drill stability increases, though factors like material type, stack depth, and cooling conditions (e.g., MQL) may also impact circularity. Optimal drill coatings and controlled conditions are essential for minimizing errors and ensuring quality in stack-up drilling operations. In summary, integrating hybrid composite/metal stack panels in aircraft manufacturing requires precise drilling to ensure quality and performance. Coated drill bits, like Ti-based and diamond coatings, enhance wear resistance, reduce friction, and manage heat, addressing challenges in drilling CFRP/metal stacks. These coatings help control drilling temperatures, reduce delamination and burr formation, and improve surface roughness and circularity. The direct comparison of different coatings under various conditions are shown in Table 5. Also, the advantages and disadvantages of each coating type used by researchers in the past for coating drill bits for composite/metal stack up drilling are tabulated in Table 6. While challenges remain in drill wear, temperature effects, and diameter consistency, selecting the right coatings and optimizing conditions are essential for advancing efficiency, reliability, and sustainability in aerospace manufacturing.

To address the challenges identified in this review paper, certain recommendations can be considered in the future. Research into the optimal thickness of coatings to balance the benefits of reduced wear and friction with potential drawbacks like increased cutting-edge radius and initial thrust forces may help to achieve better drill quality and to keep that parameter a constant one. Additionally, quantifying the bond strength of coating with tool and adding a dopant layer based on it may improve the bond strength. Development of new cost-effective, environmentally friendly coating with enhanced wear resistance, thermal stability, and reduced friction such as novel nanocomposite coatings, and multilayer coatings may also help to improve the drilling quality. Development of hybrid coatings that combine the benefits of different materials, such as the hardness of diamond with the lubricity of DLC or incorporating multiple layers with different properties, can also be tried. Integration of advanced lubrication and cooling techniques, to work synergistically with coated drill bits and further reduce temperatures and wear, can also be experimented. By focusing on these trends, the aerospace industry can continue to advance the performance and reliability of drilling operations in hybrid composite/metal stack panels, ultimately leading to more efficient manufacturing processes and higher-quality end products.

Author contribution J. Joy Mathavan was involved in conceptualization; methodology; resources; validation; writing—original draft and editing.

Funding This research did not receive any specific grant from funding agencies in the public, commercial, or not-for-profit sectors.

Data availability Data sharing is not applicable to this article as no datasets were generated or analyzed during the current study.

Declarations

Conflict of interest The authors declare no competing interests.

References

1. Ramulu M, Branson T, Kim D (2001) A study on the drilling of composite and titanium stacks. Compos Struct 54(1):67–77. https://doi.org/10.1016/S0263-8223(01)00071-X
2. Brinksmeier E, Janssen R (2002) Drilling of multi-layer composite materials consisting of carbon fiber reinforced plastics (CFRP), titanium and aluminum alloys. CIRP Ann 51(1):87–90. https://doi.org/10.1016/S0007-8506(07)61472-3
3. Kim D, Ramulu M (2007) Study on the drilling of titanium/graphite hybrid composites. J Eng Mater Technol 129(3):390–396. https://doi.org/10.1115/1.2744397
4. Xu J, Mkaddem A, El Mansori M (2016) Recent advances in drilling hybrid FRP/Ti composite: a state-of-the-art review. Compos Struct 135(C):316–338. https://doi.org/10.1016/j.compstruct.2015.09.028
5. Pawar OA, Gaikhe YS, Tewari A, Sundaram R, Joshi SS (2015) Analysis of hole quality in drilling GLARE fiber metal laminates. Compos Struct 123:350–365. https://doi.org/10.1016/J.COMPSTRUCT.2014.12.056
6. Starke EA, Staley JT (1996) Application of modern aluminum alloys to aircraft. Prog Aerosp Sci 32(2):131–172. https://doi.org/10.1016/0376-0421(95)00004-6
7. Giasin K (2016) Machining fibre metal laminates and Al2024-T3 aluminium alloy. PhD thesis. Department of Mechanical Engineering, University of Sheffield
8. Joy Mathavan J, Hassan MH, Xu J, Franz G (2022) Hole quality observation in single-shot drilling of CFRP/Al7075-T6 composite metal stacks using customized twist drill design. J Composites Sci 6(12):378. https://doi.org/10.3390/jcs6120378
9. Xu J, El Mansori M (2016) Experimental study on drilling mechanisms and strategies of hybrid CFRP/Ti stacks. Compos Struct 157:461–482. https://doi.org/10.1016/j.compstruct.2016.07.025
10. Ad Vlot JWG, Ed (2001) Fibre metal laminates: an introduction. 1st ed. Springer Dordrecht. https://doi.org/10.1007/978-94-010-0995-9.
11. Giasin K, Hawxwell J, Sinke J, Dhakal H, Köklü U, Brousseau E (2020) The effect of cutting tool coating on the form and dimensional errors of machined holes in GLARE® fibre metal laminates. Int J Adv Manuf Technol 107(5–6):2817–2832. https://doi.org/10.1007/s00170-020-05211-2
12. Ghassemieh E (2012) Performance and wear of coated carbide drill in machining of carbon fibre reinforced composite/titanium stack. Int J Mater Prod Technol 43(1–4):165–183. https://doi.org/10.1504/12.47682
13. Isbilir O, Ghassemieh E (2013) Comparative study of tool life and hole quality in drilling of CFRP/titanium stack using coated carbide drill. Mach Sci Technol 17(3):380–409. https://doi.org/10.1080/10910344.2013.806098
14. Che D, Saxena I, Han P, Guo P, Ehmann KF (2014) Machining of carbon fiber reinforced plastics/polymers: a literature review. J Manuf Sci Eng 136(3):034001. https://doi.org/10.1115/1.4026526
15. Liu DF, Tang YJ, Cong WL (2012) A review of mechanical drilling for composite laminates. Compos Struct 94(4):1265–1279. https://doi.org/10.1016/J.COMPSTRUCT.2011.11.024
16. Tong L, Yu Q, Zhao XL (2020) Experimental study on fatigue behavior of butt-welded thin-walled steel plates strengthened using CFRP sheets. Thin-Walled Structures 147:106471. https://doi.org/10.1016/j.tws.2019.106471
17. Altin Karataş M, Gökkaya H (2018) A review on machinability of carbon fiber reinforced polymer (CFRP) and glass fiber reinforced polymer (GFRP) composite materials. Defence Technol 14(4):318–326. https://doi.org/10.1016/J.DT.2018.02.001
18. Xu W, Zhang L (2018) Tool wear and its effect on the surface integrity in the machining of fibre-reinforced polymer composites. Compos Struct 188:257–265. https://doi.org/10.1016/J.COMPSTRUCT.2018.01.018
19. Sorrentino L, Turchetta S, Bellini C (2018) A new method to reduce delaminations during drilling of FRP laminates by feed rate control. Compos Struct 186:154–164. https://doi.org/10.1016/j.compstruct.2017.12.005
20. Aamir M, Tolouei-Rad M, Giasin K, Nosrati A (2019) Recent advances in drilling of carbon fiber–reinforced polymers for aerospace applications: a review. Int J Adv Manuf Technol 105(5):2289–2308. https://doi.org/10.1007/s00170-019-04348-z
21. Xu J et al (2022) A critical review addressing the drilling-induced damage issues for CFRP composites. Compos Struct 294:115594. https://doi.org/10.1016/j.compstruct.2022.115594

22. Ezugwu EO, Wang ZM (1997) Titanium alloys and their machinability—a review. J Mater Process Technol 68(3):262–274. https://doi.org/10.1016/S0924-0136(96)00030-1
23. Liu Z, An Q, Xu J, Chen M, Han S (2013) Wear performance of (nc-AlTiN)/(a-Si3N4) coating and (nc-AlCrN)/(a-Si3N4) coating in high-speed machining of titanium alloys under dry and minimum quantity lubrication (MQL) conditions. Wear 305(1–2):249–259. https://doi.org/10.1016/j.wear.2013.02.001
24. Prisco U, Impero F, Rubino F (2019) Peck drilling of CFRP/titanium stacks: effect of tool wear on hole dimensional and geometrical accuracy. Prod Eng Res Devel 13(5):529–538. https://doi.org/10.1007/s11740-019-00915-1
25. Impero F, Dix M, Squillace A, Prisco U, Palumbo B, Tagliaferri F (2018) A comparison between wet and cryogenic drilling of CFRP/Ti stacks. Mater Manuf Processes 33(12):1354–1360. https://doi.org/10.1080/10426914.2018.1453162
26. Yaşar N, Korkmaz ME, Gupta MK, Boy M, Günay M (2021) A novel method for improving drilling performance of CFRP/Ti6AL4V stacked materials. Int J Adv Manuf Technol 117(1):653–673. https://doi.org/10.1007/s00170-021-07758-0
27. Xu J, Lin T, Davim J, Chen M, EL Mansori M (2021) Wear behavior of special tools in the drilling of CFRP composite laminates. Wear 476:203738. https://doi.org/10.1016/j.wear.2021.203738
28. Xu J, Li C, Chen M, El Mansori M, Ren F (2019) An investigation of drilling high-strength CFRP composites using specialized drills. Int J Adv Manuf Technol 103(9):3425–3442. https://doi.org/10.1007/s00170-019-03753-8
29. Faraz A, Biermann D, Weinert K (2009) Cutting edge rounding: an innovative tool wear criterion in drilling CFRP composite laminates. Int J Mach Tools Manuf 49(15):1185–1196. https://doi.org/10.1016/J.IJMACHTOOLS.2009.08.002
30. Rawat S, Attia H (2009) Wear mechanisms and tool life management of WC–Co drills during dry high speed drilling of woven carbon fibre composites. Wear 267:1022–1030. https://doi.org/10.1016/j.wear.2009.01.031
31. Lin SC, Chen IK (1996) Drilling carbon fiber-reinforced composite material at high speed. Wear 194(1–2):156–162. https://doi.org/10.1016/0043-1648(95)06831-7
32. Chen WC (1997) Some experimental investigations in the drilling of carbon fiber-reinforced plastic (CFRP) composite laminates. Int J Mach Tools Manuf 37(8):1097–1108. https://doi.org/10.1016/S0890-6955(96)00095-8
33. Anand RS, Patra K (2017) Mechanistic cutting force modelling for micro-drilling of CFRP composite laminates. CIRP J Manuf Sci Technol 16:55–63. https://doi.org/10.1016/J.CIRPJ.2016.07.002
34. Seeholzer L, Scheuner D, Wegener K (2020) Analytical force model for drilling out unidirectional carbon fibre reinforced polymers (CFRP). J Mater Process Technol 278:116489. https://doi.org/10.1016/j.jmatprotec.2019.116489
35. Zitoune R, Krishnaraj V, Collombet F, Le Roux S (2016) Experimental and numerical analysis on drilling of carbon fibre reinforced plastic and aluminium stacks. Compos Struct 146:148–158
36. Caggiano A, Centobelli P, Nele L, Teti R (2017) Multiple sensor monitoring in drilling of CFRP/CFRP stacks for cognitive tool wear prediction and product quality assessment. Procedia CIRP 62:3–8. https://doi.org/10.1016/j.procir.2017.03.047
37. Angelone R, Caggiano A, Improta I, Nele L, Teti R (2018) Temperature measurements for the tool wear and hole quality assessment during drilling of CFRP/CFRP stacks. Procedia CIRP 67:416–421. https://doi.org/10.1016/j.procir.2017.12.235
38. Caggiano A, Rimpault X, Teti R, Balazinski M, Chatelain J-F, Nele L (2018) Machine learning approach based on fractal analysis for optimal tool life exploitation in CFRP composite drilling for aeronautical assembly. CIRP Ann 67(1):483–486. https://doi.org/10.1016/j.cirp.2018.04.035
39. Xia T, Kaynak Y, Arvin C, Jawahir IS (2016) Cryogenic cooling-induced process performance and surface integrity in drilling CFRP composite material. Int J Adv Manuf Technol 82(1):605–616. https://doi.org/10.1007/s00170-015-7284-y
40. Li R, Shih AJ (2007) Tool temperature in titanium drilling. J Manuf Sci Eng 129(4):740–749. https://doi.org/10.1115/1.2738120
41. Xu J, Ji M, Davim JP, Chen M, El Mansori M, Krishnaraj V (2020) Comparative study of minimum quantity lubrication and dry drilling of CFRP/titanium stacks using TiAlN and diamond coated drills. Compos Struct 234:111727. https://doi.org/10.1016/j.compstruct.2019.111727
42. Cantero JL, Tardío MM, Canteli JA, Marcos M, Miguélez MH (2005) Dry drilling of alloy Ti–6Al–4V. Int J Mach Tools Manuf 45(11):1246–1255. https://doi.org/10.1016/j.ijmachtools.2005.01.010
43. Mouritz AP (2012) Introduction to aerospace materials. 1st edn. Woodhead Publishing Limited
44. Giasin K, Ayvar-Soberanis S (2017) An investigation of burrs, chip formation, hole size, circularity and delamination during drilling operation of GLARE using ANOVA. Compos Struct 159:745–760. https://doi.org/10.1016/j.compstruct.2016.10.015
45. Giasin K (2018) The effect of drilling parameters, cooling technology, and fiber orientation on hole perpendicularity error in fiber metal laminates. Int J Adv Manuf Technol 97(9–12):4081–4099. https://doi.org/10.1007/s00170-018-2241-1
46. El-Sonbaty I, Khashaba UA, Machaly T (2004) Factors affecting the machinability of GFR/epoxy composites. Compos Struct 63(3):329–338. https://doi.org/10.1016/S0263-8223(03)00181-8
47. Abrão AM, Rubio JCC, Faria PE, Davim JP (2008) The effect of cutting tool geometry on thrust force and delamination when drilling glass fibre reinforced plastic composite. Mater Des 29(2):508–513. https://doi.org/10.1016/J.MATDES.2007.01.016
48. Giasin K, Hodzic A, Phadnis V, Ayvar-Soberanis S (2016) Assessment of cutting forces and hole quality in drilling Al2024 aluminium alloy: experimental and finite element study. Int J Adv Manuf Technol 87(5–8):2041–2061. https://doi.org/10.1007/s00170-016-8563-y
49. Giasin K, Ayvar-Soberanis S, French T, Phadnis V (2017) 3D Finite element modelling of cutting forces in drilling fibre metal laminates and experimental hole quality analysis. Appl Compos Mater 24(1):113–137. https://doi.org/10.1007/s10443-016-9517-0
50. Ben Soussia A, Mkaddem A, El Mansori M (2014) Rigorous treatment of dry cutting of FRP – interface consumption concept: a review. Int J Mech Sci 83:1–29. https://doi.org/10.1016/j.ijmecsci.2014.03.017
51. Khashaba UA (2012) Drilling of polymer matrix composites: a review. J Compos Mater 47(15):1817–1832. https://doi.org/10.1177/0021998312451609
52. Singh AP, Sharma M, Singh I (2013) A review of modeling and control during drilling of fiber reinforced plastic composites. Compos B Eng 47:118–125. https://doi.org/10.1016/j.compositesb.2012.10.038
53. Hocheng H (2012) Machining technology for composite materials: principles and practice. 1st edn. Woodhead Publishing Limited
54. Giasin K, Ayvar-Soberanis S, Hodzic A (2015) An experimental study on drilling of unidirectional GLARE fibre metal laminates. Compos Struct 133:794–808. https://doi.org/10.1016/j.compstruct.2015.08.007

55. Komanduri R (1997) Machining of fiber-reinforced composites. Mach Sci Technol 1(1):113–152. https://doi.org/10.1080/10940349708945641
56. Giasin K, Gorey G, Byrne C, Sinke J, Brousseau E (2019) Effect of machining parameters and cutting tool coating on hole quality in dry drilling of fibre metal laminates. Compos Struct 212:159–174. https://doi.org/10.1016/j.compstruct.2019.01.023
57. Kumar BS, Vijayan V, Baskar N (2016) Comparison of coated and uncoated carbide drill bits for drilling titanium grade 2 material. Mechanika 22(6):571–575. https://doi.org/10.5755/j01.mech.22.6.13467
58. Alphonse M, Raja B, Logesh KVK, Murugu Nachippan N (2017) Evolution and recent trends in friction drilling technique and the application of thermography. IOP Conf Ser Mater Sci Eng 197:012058. https://doi.org/10.1088/1757-899X/197/1/012058
59. Hari Nath Reddy R, Alphonse M, Raja Bupesh K, Palanikumar VK, Sai Krishna Sanjay KV, Madhu Sudhan DR (2020) Evaluating the wear studies and tool characteristics of coated and uncoated HSS drill bit - a review. Mater Today Proc 46:3779–3785. https://doi.org/10.1016/j.matpr.2021.02.022
60. Byakod R, Gopalakrishna DH, Prasanna S (2014) Effect of thin film coatings on drill bit. Int J Adv Res Eng Sci Technol 6–10. https://www.google.com/url?sa=i&url=https%3A%2F%2Fijarest.org%2Findex.php%2Fijarest%2Farticle%2Fdownload%2F3%2F3&psig=AOvVaw3LUVcK2IzAMZrEtXAdg_Zc&ust=1737014086380000&source=imag
61. Alphonse M, Bupesh Raja VK, Gupta M (2019) Optimization of plasma nitrided, liquid nitrided & PVD TiN coated H13–D2 friction drilling tool on AZ31B magnesium alloy. Mater Today Proc 46:9520–9528. https://doi.org/10.1016/j.matpr.2020.03.791
62. Chan Kwon B, Gil Ahn D, Yong Hwang J, Sung KD, Koo J, Ko S (2022) Performance enhancement of diamond-coating on step drill for machining CFRPs. J Manuf Process 75:527–537. https://doi.org/10.1016/j.jmapro.2021.12.060
63. D'Orazio A, El Mehtedi M, Forcellese A, Nardinocchi A, Simoncini M (2017) Tool wear and hole quality in drilling of CFRP/AA7075 stacks with DLC and nanocomposite TiAlN coated tools. J Manuf Process 30:582–592. https://doi.org/10.1016/j.jmapro.2017.10.019
64. Montoya M, Calamaz M, Gehin D, Girot F (2013) Evaluation of the performance of coated and uncoated carbide tools in drilling thick CFRP/aluminium alloy stacks. Int J Adv Manuf Technol 68(9):2111–2120. https://doi.org/10.1007/s00170-013-4817-0
65. Kuo CL et al (2018) Development of single step drilling technology for multilayer metallic-composite stacks using uncoated and PVD coated carbide tools. J Manuf Process 31:286–300. https://doi.org/10.1016/j.jmapro.2017.11.026
66. Shyha I, Soo SL, Aspinwall DK, Bradley S, Dawson S, Pretorius CJ (2010) Drilling of titanium/CFRP/aluminium stacks. Key Eng Mater 447:624–633. https://doi.org/10.4028/www.scientific.net/KEM.447-448.624
67. Wang C-Y, Chen Y-H, An Q-L, Cai X-J, Ming W-W, Chen M (2015) Drilling temperature and hole quality in drilling of CFRP/aluminum stacks using diamond coated drill. Int J Precis Eng Manuf 16(8):1689–1697. https://doi.org/10.1007/s12541-015-0222-y
68. Shyha IS et al (2011) Hole quality assessment following drilling of metallic-composite stacks. Int J Mach Tools Manuf 51(7–8):569–578. https://doi.org/10.1016/j.ijmachtools.2011.04.007
69. Zhong B, Zou F, An Q, Chen M, Zhang H, Xie C (2022) Experimental study on drilling process of a newly developed CFRP/Al/CFRP co-cured material. J Manuf Process 75(January):476–484. https://doi.org/10.1016/j.jmapro.2021.12.062
70. Zitoune R, Krishnaraj V, Almabouacif BS, Collombet F, Sima M, Jolin A (2012) Influence of machining parameters and new nano-coated tool on drilling performance of CFRP/aluminium sandwich. Composites Part B: Eng 43(3):1480–1488. https://doi.org/10.1016/j.compositesb.2011.08.054
71. Wang X, Kwon PY, Sturtevant C, Kim DDW, Lantrip J (2014) Comparative tool wear study based on drilling experiments on CFRp/Ti stack and its individual layers. Wear 317(1–2):265–276. https://doi.org/10.1016/j.wear.2014.05.007
72. Bayraktar Ş, Turgut Y (2020) Determination of delamination in drilling of carbon fiber reinforced carbon matrix composites/Al 6013–T651 stacks. Measurement 154:107493. https://doi.org/10.1016/j.measurement.2020.107493
73. Cao S, Li Y, Zhang K, Hou G, Luo B, Liu S, Liu P (2023) Investigation of CFRP damages induced by the interface high temperature and mixed tool wear mechanism in drilling of thin-walled CFRP/Ti stacks. Composite Structures 323:117438. https://doi.org/10.1016/j.compstruct.2023.117438
74. Xu J, Li C, Chen M, El Mansori M, Davim JP (2020) On the analysis of temperatures, surface morphologies and tool wear in drilling CFRP/Ti6Al4V stacks under different cutting sequence strategies. Compos Struct 234:111708
75. Xu J, Ji M, Chen M, El Mansori M (2020) Experimental investigation on drilling machinability and hole quality of CFRP/Ti6Al4V stacks under different cooling conditions. Int J Adv Manuf Technol 109(5–6):1527–1539. https://doi.org/10.1007/s00170-020-05742-8
76. Tashiro T, Fujiwara J, Inada K (2011) Drilling of CFRP/Ti-6Al-4V Stacks. Adv Mat Res 325:369–374. https://doi.org/10.4028/www.scientific.net/AMR.325.369
77. Pardo A, Heinemann R, Chen CC (2020) The effect of cutting parameter changeover position on interface borehole quality in drilling of aerospace CFRP/Al stacks. Procedia CIRP 101:314–317. https://doi.org/10.1016/j.procir.2020.11.014
78. Kuo C et al (2014) Tool wear and hole quality when single-shot drilling of metallic-composite stacks with diamond-coated tools. Proc Inst Mech Eng B J Eng Manuf 228(10):1314–1322. https://doi.org/10.1177/0954405413517388
79. Stephenson DA, Agapiou JS (2018) Metal cutting theory and practice. 3rd edn. Boca Raton: CRC Press. https://doi.org/10.1201/9781315373119
80. Liew WY, Jie JLL, Yan LY, Dayou J, Sipaut CS, Madlan MFB (2013) Frictional and wear behaviour of AlCrN, TiN, TiAlN single-layer coatings, and TiAlN/AlCrN, AlN/TiN nano-multilayer coatings in dry sliding. Procedia Eng 68:512–517. https://doi.org/10.1016/j.proeng.2013.12.214
81. Kurt M, Kaynak Y, Bagci E (2008) Evaluation of drilled hole quality in Al 2024 alloy. Int J Adv Manuf Technol 37(11):1051–1060. https://doi.org/10.1007/s00170-007-1049-1
82. Shunmugesh K, Kavan P (2017) Investigation and optimization of machining parameters in drilling of carbon fiber reinforced polymer (CFRP) composites. Pigm Resin Technol 46(1):21–30. https://doi.org/10.1108/PRT-03-2016-0029
83. Heinemann R, Hinduja S, Barrow G, Petuelli G (2006) Effect of MQL on the tool life of small twist drills in deep-hole drilling. Int J Mach Tools Manuf 46(1):1–6. https://doi.org/10.1016/j.ijmachtools.2005.04.003
84. Chim YC, Ding XZ, Zeng XT, Zhang S (2009) Oxidation resistance of TiN, CrN, TiAlN and CrAlN coatings deposited by lateral rotating cathode arc. Thin Solid Films 517(17):4845–4849. https://doi.org/10.1016/j.tsf.2009.03.038
85. Danişman Ş, Savaş S, Topal ES (2008) Cathodic arc TiN, TiAlN coated and uncoated twist drills under aggressive machining conditions. Tribology Industry 30(1–2):17–22
86. Puneeth HV, Smitha BS (2017) Studies on tool life and cutting forces for drilling operation using uncoated and coated HSS tool. Int Res J Eng Technol 4:1949–1954

87. Prajapati JP, Bhatt PM, Patel NS (2015) 'Force and wear analysis of PVD coated cutting tool' - a review. Int J Adv Res Innov Ideas Educ 1(1):9–16
88. Chen WC, Liu XD (2000) Study on the various coated twist drills for stainless steels drilling. J Mater Process Technol 99(1):226–230. https://doi.org/10.1016/S0924-0136(99)00428-8
89. Braic V et al (2010) TiAlN/TiAlZrN multilayered hard coatings for enhanced performance of HSS drilling tools. Surf Coat Technol 204(12–13):1925–1928. https://doi.org/10.1016/j.surfcoat.2009.08.011
90. Wang X, Kwon PY, Sturtevant C, Lantrip J (2013) Tool wear of coated drills in drilling CFRP. J Manuf Processes 15(1):127–135. https://doi.org/10.1016/j.jmapro.2012.09.019
91. Iliescu D, Gehin D, Gutierrez ME, Girot F (2010) Modeling and tool wear in drilling of CFRP. Int J Mach Tools Manuf 50(2):204–213. https://doi.org/10.1016/j.ijmachtools.2009.10.004
92. Hrechuk A, Bushlya V, M'Saoubi R, Ståhl JE (2018) Experimental investigations into tool wear of drilling CFRP. Procedia Manuf 25:294–301. https://doi.org/10.1016/j.promfg.2018.06.086
93. Ramirez C, Poulachon G, Rossi F, M'Saoubi R (2014) Tool wear monitoring and hole surface quality during CFRP drilling. Procedia CIRP 13:163–168. https://doi.org/10.1016/j.procir.2014.04.028
94. Sheikh-Ahmad JY (2015) Machining of polymer composites. Abu Dhabi, UAE. https://doi.org/10.1007/978-0-387-68619-6.
95. Wang X, Shen X, Yang G, Sun F (2017) Evaluation of boron-doped-microcrystalline/nanocrystalline diamond composite coatings in drilling of CFRP. Surf Coat Technol 330(September):149–162. https://doi.org/10.1016/j.surfcoat.2017.10.002
96. Wang X, Shen X, Zeng C, Sun F (2018) Combined influences of tool shape and as-deposited diamond film on cutting performance of drills for CFRP machining. Surf Coat Technol 347(May):390–397. https://doi.org/10.1016/j.surfcoat.2018.05.024
97. Xu J, An Q, Chen M (2014) A comparative evaluation of polycrystalline diamond drills in drilling high-strength T800S/250F CFRP. Compos Struct 117(1):71–82. https://doi.org/10.1016/j.compstruct.2014.06.034
98. Kuo C, Wang C, Ko S (2018) Wear behaviour of CVD diamond-coated tools in the drilling of woven CFRP composites. Wear 398–399:1–12. https://doi.org/10.1016/j.wear.2017.11.015
99. Dumpala R, Chandran M, Kumar N, Dash S, Ramamoorthy B, Rao MSR (2013) Growth and characterization of integrated nano- and microcrystalline dual layer composite diamond coatings on WC-Co substrates. Int J Refract Metals Hard Mater 37:127–133. https://doi.org/10.1016/j.ijrmhm.2012.11.007
100. Polini R, Bravi F, Casadei F, D'Antonio P, Traversa E (2002) Effect of substrate grain size and surface treatments on the cutting properties of diamond coated Co-cemented tungsten carbide tools. Diam Relat Mater 11(3):726–730. https://doi.org/10.1016/S0925-9635(02)00020-1
101. Xiang D, Guo Z, Zhang L, Feng H (2018) Preparation and cutting performance of ultra-smooth CVD composite diamond coated ladder-shape drilling tools. Diam Relat Mater 81:54–60. https://doi.org/10.1016/j.diamond.2017.11.008
102. Sheikh-Ahmad J, Sridhar G (2002) Edge trimming of CFRP composites with diamond coated tools: edge wear and surface characteristics, in General Aviation Technology Conference & Exhibition, SAE International. https://doi.org/10.4271/2002-01-1526.
103. Thompson JMT, May PW (2000) Diamond thin films: a 21st-century material, Philosophical Transactions of the Royal Society of London. Series A: Math, Phys Eng Sci 358(1766):473–495. https://doi.org/10.1098/rsta.2000.0542
104. Henerichs M, Voß R, Harsch D, Kuster F, Wegener K (2014) New production technologies in aerospace industry - 5th Machining Innovations Conference (MIC 2014) tool life time extension with nano-crystalline diamond coatings for drilling carbon-fibre reinforced plastics (CFRP). Procedia CIRP 24:125–129. https://doi.org/10.1016/j.procir.2014.07.144
105. Dumpala R, Chandran M, Madhavan S, Ramamoorthy B, Rao MSR (2015) High wear performance of the dual-layer graded composite diamond coated cutting tools. Int J Refract Metals Hard Mater 48:24–30. https://doi.org/10.1016/j.ijrmhm.2014.07.023
106. Srinivasan B, Rao MR, Rao BC (2016) On the development of a dual-layered diamond-coated tool for the effective machining of titanium Ti-6Al-4V alloy. J Phys D: Appl Phys 50(1):015302. https://doi.org/10.1088/1361-6463/50/1/015302
107. Najar KA, Sheikh NA, Butt MM, Mushtaq S, Shah MA (2019) Engineered synthetic diamond film as a protective layer for tribological and machining applications: a review. J Bio Tribocorros 5(3):59. https://doi.org/10.1007/s40735-019-0252-6
108. Sun FH, Zhang ZM, Chen M, Shen HS (2002) Fabrication and application of high quality diamond-coated tools. J Mater Process Technol 129(1–3):435–440. https://doi.org/10.1016/S0924-0136(02)00635-0
109. Wiora M et al (2009) Grain size dependent mechanical properties of nanocrystalline diamond films grown by hot-filament CVD. Diam Relat Mater 18(5):927–930. https://doi.org/10.1016/j.diamond.2008.11.026
110. Zhang J, Yuan Y, Zhang J (2018) Cutting performance of microcrystalline, nanocrystalline and dual-layer composite diamond coated tools in drilling carbon fiber reinforced plastics. Appl Sci 8(9):1642. https://doi.org/10.3390/app8091642
111. Lu FX et al (2006) Novel pretreatment of hard metal substrate for better performance of diamond coated cutting tools. Diam Relat Mater 15(11):2039–2045. https://doi.org/10.1016/j.diamond.2006.06.013
112. Wang H, Yang J, Sun F (2020) Cutting performances of MCD, SMCD, NCD and MCD/NCD coated tools in high-speed milling of hot bending graphite molds. J Mater Process Technol 276:116401. https://doi.org/10.1016/j.jmatprotec.2019.116401
113. Shabani M, Sacramento J, Oliveira FJ, Silva RF (2017) Multilayer CVD diamond coatings in the machining of an Al6061-15 Vol% Al2O3 composite. Coatings 7(10):165. https://doi.org/10.3390/coatings7100165
114. Takeuchi S, Oda S, Murakawa M (2001) Synthesis of multilayer diamond film and evaluation of its mechanical properties. Thin Solid Films 398(399):238–243. https://doi.org/10.1016/S0040-6090(01)01499-7
115. Salgueiredo E, Amaral M, Almeida FA, Fernandes AJS, Oliveira FJ, Silva RF (2013) Mechanical performance upgrading of CVD diamond using the multilayer strategy. Surf Coat Technol 236:380–387. https://doi.org/10.1016/j.surfcoat.2013.10.017
116. Vieira J, Contin A, Fraga MA, Corat EJ, Airoldi VT (2019) Growth and characterization of multilayer hot-filament chemical vapor deposition diamond coatings on WC–Co substrates. Surf Innov 7(1):36–43. https://doi.org/10.1680/jsuin.18.00020
117. Wang C, Wang X, Sun F (2018) Tribological behavior and cutting performance of monolayer, bilayer and multilayer diamond coated milling tools in machining of zirconia ceramics. Surf Coat Technol 353(August):49–57. https://doi.org/10.1016/j.surfcoat.2018.08.074
118. Fiaschi G, Rota A, Ballestrazzi A, Marchetto D, Vezzalini E, Valeri S (2019) A chemical, mechanical, and tribological analysis of DLC coatings deposited by magnetron sputtering. Lubricants 7(4):38. https://doi.org/10.3390/lubricants7040038

119. Aisenberg S, Chabot R (1971) Ion-beam deposition of thin films of diamondlike carbon. J Appl Phys 42(7):2953–2958. https://doi.org/10.1063/1.1660654
120. Aisenberg S, Chabot RW (1973) Physics of ion plating and ion beam deposition. J Vac Sci Technol 10(1):104–107. https://doi.org/10.1116/1.1317915
121. Erdemir A, Martin JM (2018) Superior wear resistance of diamond and DLC coatings. Curr Opin Solid State Mater Sci 22(6):243–254. https://doi.org/10.1016/j.cossms.2018.11.003
122. Okamoto T, Umehara N, Murashima M, Saito K, Manabe K, Hayashi K (2021) The clarification of friction mechanism in oil lubrication for CN_x coating by *in-situ* observation of friction area with reflectance spectroscopy. Tribology Online 16(1):49–58. https://doi.org/10.2474/trol.16.49
123. Lee W-Y, Jang Y-J, Tokoroyama T, Murashima M, Umehara N (2020) Effect of defects on wear behavior in ta-C coating prepared by filtered cathodic vacuum arc deposition. Diam Relat Mater 105:107789. https://doi.org/10.1016/j.diamond.2020.107789
124. Murashima M, Deng X, Izuoka H, Umehara N, Kousaka H (2019) Effect of oxygen on degradation of defects on ta-C coatings deposited by filtered arc deposition. Surf Coat Technol 362:200–207. https://doi.org/10.1016/j.surfcoat.2019.01.115
125. Erdemir A (2001) The role of hydrogen in tribological properties of diamond-like carbon films. Surf Coat Technol 146–147:292–297. https://doi.org/10.1016/S0257-8972(01)01417-7
126. Erdemir A (2004) Genesis of superlow friction and wear in diamondlike carbon films. Tribol Int 37(11):1005–1012. https://doi.org/10.1016/j.triboint.2004.07.018
127. Donnet C et al (1999) Diamond-like carbon-based functionally gradient coatings for space tribology. Surf Coat Technol 120–121:548–554. https://doi.org/10.1016/S0257-8972(99)00432-6
128. Andersson J, Erck RA, Erdemir A (2003) Friction of diamond-like carbon films in different atmospheres. Wear 254(11):1070–1075. https://doi.org/10.1016/S0043-1648(03)00336-3
129. Li X, Deng X, Kousaka H, Umehara N (2017) Comparative study on effects of load and sliding distance on amorphous hydrogenated carbon (a-C:H) coating and tetrahedral amorphous carbon (ta-C) coating under base-oil lubrication condition. Wear 392–393:84–92. https://doi.org/10.1016/j.wear.2017.09.009
130. oerlikon balzers (2019) Hand book on Carbon-Based BALINIT coatings
131. Cho SJ, Lee KR, Eun KY, Hahn JH, Ko DH (1999) Determination of elastic modulus and Poisson's ratio of diamond-like carbon films. Thin Solid Films 341(1–2):207–210. https://doi.org/10.1016/S0040-6090(98)01512-0
132. Rajak DK, Kumar A, Behera A, Menezes PL (2021) Diamond-like carbon (DLC) coatings: classification, properties, and applications. Appl Sci 11(10):1–20. https://doi.org/10.3390/app11104445
133. Goh GD, Yap YL, Agarwala S, Yeong WY (2019) Recent progress in additive manufacturing of fiber reinforced polymer composite. Adv Mater Technol 4(1):1800271. https://doi.org/10.1002/admt.201800271
134. Wang Y et al (2020) Tribological properties of Ti-doped diamond-like carbon coatings under boundary lubrication with ZDDP. J Tribol 143:1–28. https://doi.org/10.1115/1.4049373
135. Mathavan JJ, Hassan MH, Mahmud AS (2024) A comparative study of hole integrity performance in composite-metal stacks using coated and uncoated tungsten carbide drill bits. Materwiss Werksttech 55(1):89–106. https://doi.org/10.1002/mawe.202300077
136. Outka DA, Hsu WL, Boehme DR, Yang NYC, Ottesen DK, Johnsen HA, Clift WM, Headley TJ (1994) Compilation of diamond-like carbon properties for barriers and hard coatings. Livermore. https://digital.library.unt.edu/ark:/67531/metadc1311391/m1/19/
137. Murakawa M, Watanabe S (1990) The possibility of coating cubic BN films on various substrates. Surf Coat Technol 43–44:145–153. https://doi.org/10.1016/0257-8972(90)90069-O
138. Voevodin AA, Donley MS (1996) Preparation of amorphous diamond-like carbon by pulsed laser deposition: a critical review. Surf Coat Technol 82(3):199–213. https://doi.org/10.1016/0257-8972(95)02734-3
139. Savvides N, Window B (1985) Diamondlike amorphous carbon films prepared by magnetron sputtering of graphite. J Vac Sci Technol, A: Vac, Surf Films 3(6):2386–2390. https://doi.org/10.1116/1.572887
140. Guo Y et al (2019) Tribological properties of Ti-doped diamond-like carbon coatings under dry friction and PAO oil lubrication. Surf Interface Anal 51(3):361–370. https://doi.org/10.1002/sia.6588
141. Zhang S, Bui XL, Zeng XT, Li X (2005) Towards high adherent and tough aC coatings. Thin Solid Films 482(1–2):138–144. https://doi.org/10.1016/j.tsf.2004.11.165
142. Konca E, Cheng YT, Alpas AT (2006) Dry sliding behaviour of non-hydrogenated DLC coatings against Al, Cu and Ti in ambient air and argon. Diam Relat Mater 15(4–8):939–943. https://doi.org/10.1016/j.diamond.2005.11.030
143. Jebaratnam JM, Hassan MH, Mahmud AS, Gérald F (n.d.) Characterization of nanocomposite tetrahedral amorphous carbon coated drill bits for improved drilled-hole quality in carbon fiber-reinforced polymer/Al7075-T6 stacks. J Compos Mater p. 00219983231207988, https://doi.org/10.1177/00219983231207988.
144. Fujiwara J, Nagaura R, Tashiro T (2013) Drilling of CFRP/Ti6Al4V stack board. Int J Automation Technol 7(4):426–32
145. Müller-Hummel P, Lahres M (1995) Quantitative measurement of temperatures on diamond-coated tools during machining. Diam Relat Mater 4(10):1216–1221. https://doi.org/10.1016/0925-9635(95)00299-5
146. Pu J-C, Wang S-F, Sung JC (2009) High-temperature oxidation behaviors of CVD diamond films. Appl Surf Sci 256(3):668–673. https://doi.org/10.1016/j.apsusc.2009.08.042
147. Kuo C, Li Z, Wang C (2017) Multi-objective optimisation in vibration-assisted drilling of CFRP/Al stacks. Compos Struct 173:196–209. https://doi.org/10.1016/j.compstruct.2017.04.026
148. Luo B, Li Y, Zhang K, Cheng H, Liu S (2015) A novel prediction model for thrust force and torque in drilling interface region of CFRP/Ti stacks. Int J Adv Manuf Technol 81(9–12):1497–1508. https://doi.org/10.1007/s00170-015-7294-9
149. Zitoune R, Krishnaraj V, Collombet F (2010) Study of drilling of composite material and aluminium stack. Compos Struct 92(5):1246–1255. https://doi.org/10.1016/J.COMPSTRUCT.2009.10.010
150. Xu J, El Mansori M, Voisin J, Chen M, Ren F (2019) On the interpretation of drilling CFRP/Ti6Al4V stacks using the orthogonal cutting method: chip removal mode and subsurface damage formation. J Manuf Process 44:435–447. https://doi.org/10.1016/j.jmapro.2019.05.052
151. Xu J, El Mansori M, Chen M, Ren F (2019) Orthogonal cutting mechanisms of CFRP/Ti6Al4V stacks. Int J Adv Manuf Technol 103(9):3831–3851. https://doi.org/10.1007/s00170-019-03734-x
152. Brinksmeier E, Fangmann S, Rentsch R (2011) Drilling of composites and resulting surface integrity. CIRP Ann Manuf Technol 60(1):57–60. https://doi.org/10.1016/j.cirp.2011.03.077
153. Abrão AM, Faria PE, Rubio JCC, Reis P, Davim JP (2007) Drilling of fiber reinforced plastics: a review. J Mater Process Technol 186(1–3):1–7. https://doi.org/10.1016/j.jmatprotec.2006.11.146
154. Skopp A, Klaffke D (1998) Aspects of tribological testing of diamond coatings. Surf Coat Technol 98(1):1027–1037. https://doi.org/10.1016/S0257-8972(97)00224-7

155. Kim D, Beal A, Kwon P (2016) Effect of tool wear on hole quality in drilling of carbon fiber reinforced plastic–titanium alloy stacks using tungsten carbide and polycrystalline diamond tools. J Manuf Sci Eng 138(3):031006. https://doi.org/10.1115/1.4031052
156. Pecat O, Brinksmeier E (2014) Tool wear analyses in low frequency vibration assisted drilling of CFRP/Ti6Al4V stack material. Procedia CIRP 14:142–147. https://doi.org/10.1016/j.procir.2014.03.050
157. Li C, Xu J, Chen M, An Q, El Mansori M, Ren F (2019) Tool wear processes in low frequency vibration assisted drilling of CFRP/Ti6Al4V stacks with forced air-cooling. Wear 426–427:1616–1623. https://doi.org/10.1016/j.wear.2019.01.005
158. Keizo S, Masafumi S, Masaki T, Yoshimichi Y (1985) Tool wear in cutting carbon-fiber-reinforced plastics: the effect of physical properties of tool materials. Bull JSME 28(245):2781–2788. https://doi.org/10.1299/jsme1958.28.2781
159. Kuo CL et al (2014) The effect of cutting speed and feed rate on hole surface integrity in single-shot drilling of metallic-composite stacks. Procedia CIRP 13:405–410. https://doi.org/10.1016/j.procir.2014.04.069
160. Geng D et al (2019) Delamination formation, evaluation and suppression during drilling of composite laminates: a review. Compos Struct 216:168–186. https://doi.org/10.1016/J.COMPSTRUCT.2019.02.099
161. Erturk AT, Vatansever F, Yarar E, Karabay S (2019) Machining behavior of multiple layer polymer composite bearing with using different drill bits. Compos B Eng 176:107318. https://doi.org/10.1016/j.compositesb.2019.107318
162. Ho-Cheng H, Dharan CKH (1990) Delamination during drilling in composite laminates. J Eng Industry 112(3):236–239. https://doi.org/10.1115/1.2899580
163. Jebaratnam JM, Hassan MH, Mahmud AS, Gérald F (2023) Characterization of nanocomposite tetrahedral amorphous carbon coated drill bits for improved drilled-hole quality in carbon fiber-reinforced polymer/Al7075-T6 stacks. J Compos Mater 57(27):4255–4274. https://doi.org/10.1177/00219983231207988
164. Li Y, Jiao F, Zhang Z, Feng Z, Niu Y (2022) Research on entrance delamination characteristics and damage suppression strategy in drilling CFRP/Ti6Al4V stacks. J Manuf Processes 76:518–531. https://doi.org/10.1016/j.jmapro.2022.02.018
165. An Q, Zhong B, Wang X, Zhang H, Sun X, Chen M (2021) Effects of drilling strategies for CFRP/Ti stacks on static mechanical property and fatigue behavior of open-hole CFRP laminates. J Manuf Processes 64:409–420. https://doi.org/10.1016/j.jmapro.2021.01.036
166. Sui S, Song G, Sun C, Zhu Z, Guo K, Sun J (2020) Experimental investigation on the performance of novel double cone integrated tool in one-shot drilling of metal stacks. Int J Adv Manuf Technol 109(1):523–534. https://doi.org/10.1007/s00170-020-05474-9
167. Niknam SA, Zedan Y, Songmene V (2014) Machining burrs formation & deburring of aluminium alloys. Light metal alloys applications 99-122. https://doi.org/10.5772/58361.
168. Hassan MH, Razali MF (2020) Comparison of coated and uncoated drill bit on the drilling quality of CFRP/AL7075-T6 stacked materials. Proc Mechanical Eng Res Day 16:336–338
169. Hazarika M, Dixit US (2015) Setup planning for machining. 1st edn. Springer International Publishing. https://doi.org/10.1007/978-3-319-13320-1
170. Batzer SA, Haan DM, Rao PD, Olson WW, Sutherland JW (1998) Chip morphology and hole surface texture in the drilling of cast aluminum alloys. J Mater Process Technol 79(1–3):72–78. https://doi.org/10.1016/S0924-0136(97)00324-5
171. Mahdi A, Turki Y, Habak M, Salem M, Bouaziz Z (2020) Experimental study of thrust force and surface quality when drilling hybrid stacks. Int J Adv Manuf Technol 107(9):3981–3994. https://doi.org/10.1007/s00170-020-05252-7
172. Krishnaraj V et al (2012) Optimization of machining parameters at high speed drilling of carbon fiber reinforced plastic (CFRP) laminates. Compos B Eng 43(4):1791–1799. https://doi.org/10.1016/j.compositesb.2012.01.007
173. Azmi AI, Lin RJT, Bhattacharyya D (2013) Machinability study of glass fibre-reinforced polymer composites during end milling. Int J Adv Manuf Technol 64(1):247–261. https://doi.org/10.1007/s00170-012-4006-6
174. Rawat S, Attia H (2009) Characterization of the dry high speed drilling process of woven composites using Machinability Maps approach. CIRP Ann 58(1):105–108. https://doi.org/10.1016/j.cirp.2009.03.100
175. Kim D, Ramulu M (2004) Drilling process optimization for graphite/bismaleimide–titanium alloy stacks. Compos Struct 63(1):101–114. https://doi.org/10.1016/S0263-8223(03)00137-5
176. Li MJ, Soo SL, Aspinwall DK, Pearson D, Leahy W (2014) Influence of lay-up configuration and feed rate on surface integrity when drilling carbon fibre reinforced plastic (CFRP) composites. Procedia CIRP 13:399–404. https://doi.org/10.1016/j.procir.2014.04.068
177. Kalidas S, Devor RE, Kapoor SG (2001) Experimental investigation of the effect of drill coatings on hole quality under dry and wet drilling conditions. Surf Coat Technol 148(2):117–128. https://doi.org/10.1016/S0257-8972(01)01349-4
178. Ekici E, Motorcu AR, Yıldırım E (2021) An experimental study on hole quality and different delamination approaches in the drilling of CARALL, a new FML composite. FME Transactions 49(4):950–961. https://doi.org/10.5937/FME2104950E
179. Kim D, Beal A, Kang K, Kim SY (2017) Hole quality assessment of drilled CFRP and CFRP-TI stacks holes using polycrystalline diamond (PCD) tools. Carbon Lett 23(3):1–8. https://doi.org/10.5714/CL.2017.23.001
180. Dahnel AN, Ascroft H, Barnes S, Gloger M (2015) Analysis of tool wear and hole quality during ultrasonic assisted drilling (UAD) of carbon fibre composite (CFC) / titanium alloy (Ti6Al4V) stacks. in Proceedings of the ASME 2015 International Mechanical Engineering Congress and Exposition, Houston, Texas, USA. https://doi.org/10.1115/IMECE2015-50416.
181. Ashrafi SA, Sharif S, Farid AA, Yahya MY (2013) Performance evaluation of carbide tools in drilling CFRP-Al stacks. J Compos Mater 48(17):1–14. https://doi.org/10.1177/0021998313494429
182. Fernández-Pérez J, Cantero JL, Díaz-Álvarez J, Miguélez MH (2019) Hybrid Composite-metal stack drilling with different minimum quantity lubrication levels. Materials 12(3):448. https://doi.org/10.3390/ma12030448
183. Hassan MH, Abdullah J, Mahmud AS, Supran A (2018) Effect of drill geometry and drilling parameters on the formation of adhesion layer in drilling composite-metal stack-up material. J Mech Eng (JMechE) 2:90–98
184. Jebaratnam JM, Hassan MH (2024) Process enhancement and performance evaluation of single-shot drilling of CFRP/aluminum stacks: a review. Int J Adv Manuf Technol 135:3015–3050. https://doi.org/10.1007/s00170-024-14610-8
185. Hassan MH, Abdullah J, Franz G, Shen CY, Mahmoodian R (2021) Effect of twist drill geometry and drilling parameters on hole quality in single-shot drilling of CFRP/Al7075-T6 Composite Stack. J Composites Sci 5(7):189
186. Dimensioning and tolerancing (1994) In ASME Y14.5M -1994. New York: The American Society of Mechanical Engineers p. 144.
187. Hoffman P, Hopewell E, Brian Janes, KS Jr (2011) Precision machining technology. 2nd edn. Cengage Learning
188. Paolo Davim (2013) Machining composites materials. John Wiley & Sons, Ltd.

189. Mathavan JJ, Bin Hassan MH, Bin Mahmud AS (2023) Comparative study of hole quality performance in drilling of CFRP/Al7075-T6 stack using tetrahedral amorphous carbon coated drill. In AIP Conference Proceedings, American Institute of Physics Inc. https://doi.org/10.1063/5.0178378.